



Norwegian University of
Science and Technology

Electrochemical oxidation of salicylic acid using BDD as electrode material

Linda Bottesi

Civil and Environmental Engineering (2 year)

Submission date: March 2016

Supervisor: Thomas Meyn, IVM

Norwegian University of Science and Technology
Department of Hydraulic and Environmental Engineering



UNIVERSITÀ DEGLI STUDI DI TRENTO



NTNU

Norwegian University of
Science and Technology

Department of Civil, Environmental and Mechanical Engineering

MASTER THESIS
in Environmental Engineering

**ELECTROCHEMICAL OXIDATION OF
SALICYLIC ACID USING BDD/Si AS
ELECTRODE MATERIAL**

Supervisors:

Thomas Meyn

Student:

Bottesi Linda

Academic year 2014/2015

Contents

1	Introduction	1
1.1	Objectives of the work	2
2	Description of the Landfill Leachate	3
2.1	SHMIL Åremma landfill	4
2.2	Background about the legal situation	6
2.3	Characteristics of leachate by water quality data	6
3	Theoretical background	9
3.1	Advanced Oxidation Processes (AOPs)	9
3.2	Electrochemical Process	11
3.3	Electrochemical Oxidation	12
3.4	Direct Oxidation	14
3.5	Indirect Oxidation	15
3.6	Electrodes Material	16
3.7	Boron-doped Diamond (BDD)	16
3.8	Salicylic acid	17
3.9	Limiting current density	19
4	Experimental part	25
4.1	Chemicals	25
4.2	DiaClean Lab Unit	26
4.3	UV/VIS spectrophotometer PerkinElmer LAMBDA 650	32
4.4	Apollo 9000 Total Organic Carbon (TOC) Analyzer	33
4.5	Experiment with potassium indigo trisulfonate dye	34
4.6	Calibration curve	36
5	Results and discussion of the results	39
5.1	Determination of the salicylic acid degradation kinetic	39
5.2	Calibration	40
5.3	Evaluation of the pH and temperature variation	45
5.4	Istantaneous Current Efficiency (ICE)	52
6	Conclusions and further studies	55
6.1	Total organic carbon analyze	65
6.2	Absorbance spectrum	68
6.3	Comparison pH and temperature	71

List of Figures

2.1	Position of SHMIL Åremma	4
2.2	Location of the landfill close to Mosjøen	4
2.3	Average temperature and average precipitation for Mosjøen (1961-1990)	5
3.1	scheme of direct and indirect oxidation of pollutants [1]	13
3.2	Mechanism of direct anodic oxidation [2]	14
3.3	Comparison between cyclic voltammogram of platinum and BDD [3] . .	17
3.4	Process of mineralization of salicylic acid with possible intermediates creation [4]	18
3.5	Schematic curves showing the different trends of the limiting [5]	20
3.6	Profile of the throughflow area inside the cell	21
4.1	Structural formula of salicylic acid [6]	25
4.2	Structural formula of potassium Indigo trisulfonate [7]	26
4.3	DiaClean Lab unit	27
4.4	Flux scheme of the compartment of DiaClean Lab unit [3]	27
4.5	Detail of the double loop inside the tank	28
4.6	Detail of the remote control of the refrigerator Julabo FP 50	28
4.7	Characteristics of the pump DAB KVC 20/50 M	29
4.8	Details of the flowmeter	29
4.9	Detail of the power supply DiaClean PS-1000	30
4.10	Detail of the electrolytic cell DiaClean	30
4.11	Balance Sartorius Analytic A200S	31
4.12	HACH sensION+ PH31 pHmeter	31
4.13	ODEON Classic conductimeter	31
4.14	Scheme of the UV/VIS spectrophotometer [8]	33
4.15	Apollo 9000 Total Organic Carbon (TOC) Analyzer TM Tekmar	34
4.16	Sample of indigo solution at t=0	35
4.17	Detail of the indigo solution inside the tank at t=0	35
4.18	Sample of indigo solution at t=70 minutes	36
4.19	Detail of the indigo solution inside the tank at t=70 minutes	36
4.20	Dilution of the salicylic acid standards	37
4.21	Calibration curve with standards of salicylic acid at 298 nm	37
5.1	Evaluation of the electrolyte influence with experimental results of ab- sorbance at 298 nm - $NaSO_4$ and $NaCl$	41
5.2	Evaluation of the electrolyte influence with trend extrapolation - $NaSO_4$ and $NaCl$	41
5.3	Detail of the oscillative behavior in the experiment with $NaSO_4$	42

5.4	Evaluation of the influence of the reversal of the current with experimental results of absorbance at 298 nm - $NaSO_4$ and $NaCl$	42
5.5	Evaluation of the influence of the reversal of the current with trend extrapolation - $NaSO_4$ and $NaCl$	43
5.6	Evaluation of the influence of the electrolyte molarity with experimental results of absorbance at 298 nm - $NaSO_4$ and $NaCl$	43
5.7	Evaluation of the influence of the electrolyte molarity with trend extrapolation - $NaSO_4$ and $NaCl$	43
5.8	Evaluation of the influence of the current applied with experimental results of absorbance at 298 nm - $NaSO_4$ and $NaCl$	44
5.9	Evaluation of the influence of the current applied with trend extrapolation - $NaSO_4$ and $NaCl$	45
5.10	Expertmental details of the experiment carried out the 4 th February 2016	46
5.11	Absorbance spectrum for pH 12 at 27°C	47
5.12	Total organic carbon for pH 12 at 27°C	47
5.13	Absorbance at wavelenght of 298 nm for pH 12 at 27°C	47
5.14	Comparison of degradation rate at different pHs at a given temperature with $NaSO_4$ as supporting electrolyte	49
5.15	Comparison of degradation rate at different temperatures at a given pH with $NaSO_4$ as supporting electrolyte	49
5.16	Details of the samples for TOC analyze of the experiment at 27°C and pH 12	50
5.17	TOC measuraments at 27°C for different pH	50
5.18	Absorbance values at 298 nm at 27°C for different pH	51
5.19	Absorbance spectrum for the experiment at 27°C and 3 pH	51
5.20	Absorbance spectrum for the experiment at 27°C and 12 pH	51
5.21	Comparison between of the temperature and pH influence on istantaneous current efficiency normalized	53
5.22	Istantaneous current efficiency percentage: comparison for different temperatures at pH 3	53
6.1	Total organic carbon at pH 3 - 13°C	65
6.2	Total organic carbon at pH 3 - 20°C	65
6.3	Total organic carbon at pH 3 - 27°C	65
6.4	Total organic carbon at pH 7 - 13°C	66
6.5	Total organic carbon at pH 7 - 20°C	66
6.6	Total organic carbon at pH 7 - 27°C	66
6.7	Total organic carbon at pH 12 - 13°C	67
6.8	Total organic carbon at pH 12 - 20°C	67
6.9	Total organic carbon at pH 12 - 27°C	67
6.10	Absorbance spectrum at pH 3 - 13°C	68
6.11	Absorbance spectrum at pH 3 - 20°C	68
6.12	Absorbance spectrum at pH 3 - 27°C	68
6.13	Absorbance spectrum at pH 7 - 13°C	69
6.14	Absorbance spectrum at pH 7 - 20°C	69
6.15	Absorbance spectrum at pH 7 - 27°C	69
6.16	Absorbance spectrum at pH 12 - 13°C	70
6.17	Absorbance spectrum at pH 12 - 20°C	70
6.18	Absorbance spectrum at pH 12 - 27°C	70

6.19	Comparison of different temperature at pH 3	71
6.20	Comparison of different temperature at pH 7	71
6.21	Comparison of different temperature at pH 12	71
6.22	Comparison of different temperature at pH 3	72
6.23	Comparison of different temperature at pH 7	72
6.24	Comparison of different temperature at pH 12	72
6.25	Comparison of different pH at 13°C	73
6.26	Comparison of different pH at 20°C	73
6.27	Comparison of different pH at 27°C	73
6.28	Comparison of different pH at 13°C	74
6.29	Comparison of different pH at 20°C	74
6.30	Comparison of different pH at 27°C	74

List of Tables

2.1	Average monthly temperature and precipitation (1961-1990)	5
2.2	Concentrations of the characterising parameters (2006-2015)	7
2.3	Loads of the characterising parameters (2006-2015)	7
2.4	Priority substances in the leachate (2006-2015)	8
3.1	Electrochemical oxidation potential for different oxidizing agents (table chapter 11-10 [9])	10
3.2	Solubility of salicylic acid in water	19
3.3	Characteristics of the DiaClean Lab Unit system	21
4.1	Characteristics of BDD/Si electrodes	30
4.2	Constant parameters of the experiments	32
4.3	Results of the experiment with potassium indigo trisulfonate at 298 nm	35
5.1	Summary of the kinetics for calibration experiments	40
5.2	Summary of the kinetics for pH and temperature experiments	45
6.1	List of Norwegian hazardous substances ([10])	63
6.2	European list of priority substances (European Parliament and of the Council EU 2013)	64

Abstract

The major project of SHMIL landfill's leachate aims at finding a complete treatment scheme that leads to stay below the limits of the polluted compounds defined by legislation before 2020. The presented work is part of the initial phase and it focuses on an advanced oxidation process, which uses radicals to oxidize pollutants, in particular the organic matter. The process is called electrochemical oxidation and it uses electrodes that generate radicals on the anode surface which oxidize hazardous compounds.

The Chemical Oxygen Demand (COD) has not been reduced at all by the same redox reactions, as some organic substances are more persistent and must be treated with more advanced techniques. Oxidation by radicals is the most efficient and quickest way that leads to the increment of BOD_5/COD , meanwhile the concentration of the pollutants decreases, because the radicals react with both, biodegradable and non biodegradable organic matter. Furthermore, other studies prove a good removal ratio for heavy metals and ammonia nitrogen using electrochemical oxidation. Because of this, it can be argued the treatment can reach good results for the application on the complex matrix of landfill leachate.

From a theoretical perspective, the treatment is challenging because the specific aspect of the radical oxidation are not completely known and the techniques are not developed enough to test it. Also from a practical considerations, the setup is new and finding the methodology to carry out an experiment requires a creative effort.

In the reported work, different configurations of the setup are analyzed. In the electrolytic cell, the electrodes are made of a cover of BDD (boron-doped diamond) on a silicon support. The evaluated aspects are the following: the electrolyte nature of NaCl and $NaSO_4$, the concentration of it in the solution (0,05 M and 0,1 M), the application of reversal mode or not, the applied current (1 A, 3,5 A and 7 A), the pH of the solution (3, 7 and 12) and the temperature ($13^\circ C$, $20^\circ C$ and $27^\circ C$).

The collected data for every experiment are temperature, conductivity, applied current, voltage, pH of the solution, absorbance spectrum and TOC concentration.

The experiments carried out with NaCl demonstrates a higher removal rate compared to the ones with other electrolyte. Moreover, the comparison between the different applied currents, indicates a better efficiency for the higher current. For the second round of experiments, it can be argued that at higher temperature, as well as higher pH, the absorbance value at the peak of 298 nm, decreases faster than the other configurations. The results of the TOC analysis, instead, shown the removal ratio is basically the same for all the configurations with a slightly higher carbon concentration of the last sample for the experiments at $13^\circ C$. The final result of the carbon concentration together with the ones of the absorbance, indicate the generation of the intermediates is influenced by different parameters, but the final carbon concentration does not change. It seems

that the carbon content is removed with a lower rate than the compounds responsible for the absorbance at 298 nm.

Keywords: advanced oxidation processes, BDD, wastewater treatment, landfill's leachate, salicylic acid

Sommario

Lo scopo del progetto riguardante il percolato prodotto dalla discarica SHMIL è quello di trovare una catena di trattamenti che permettano il soddisfacimento dei limiti per tutte le varie sostanze specificate dalle normative prima del 2020.

Il qui presente lavoro di tesi va ad introdursi nella fase iniziale di tale di progetto e focalizza l'attenzione su un processo di ossidazione chimica avanzata, il quale si serve di radicali liberi per ossidare gli inquinanti, principalmente la sostanza organica. Tale trattamento è chiamato ossidazione elettrochimica e utilizza due elettrodi che fungono da anodo e catodo per generare radicali sulla superficie dell'anodo che successivamente vanno ad ossidare gli inquinanti in soluzione.

L'ossidazione mediante radicali è la più efficace e veloce se paragonata ai classici meccanismi redox e permette di aumentare il rapporto BOD_5/COD , nello stesso tempo in cui la concentrazione di inquinanti diminuisce, poichè i radicali nel loro processo di ossidazione reagiscono sia con la sostanza organica biologicamente degradabile che non. Inoltre, altri studi dimostrano che tale AOP ha la capacità di ossidare altri composti quali i metalli pesanti e l'ammoniaca, prospettando esiti positivi per l'applicazione di tale trattamento su di una matrice complessa come il percolato da discarica.

E' un trattamento innovativo e stimolante sia dal punto di vista teorico, perchè esistono ancora molti aspetti poco conosciuti sul processo di degradazione da parte dei radicali e poche tecniche per indagarli, sia dal punto di vista pratico, poichè l'impianto utilizzato è un recente acquisto del dipartimento e comporta un certo sforzo creativo identificare la metodologia dell'esperimento.

Nel lavoro presentato in questa tesi sono state analizzate e confrontate possibili configurazioni dell'impianto. La reazione di ossidazione avviene nella cella elettrolitica, nella quale sono presenti due elettrodi di silicio ricoperti di BDD di forma circolare. Sono stati valutati diversi aspetti: la natura dell'elettrolita paragonando NaCl e $NaSO_4$, la sua concentrazione in soluzione analizzando 0,05 M e 0,1 M, l'applicazione o meno della modalità *reversal*, la corrente applicata di 1 A, 3,5 A e 7 A, il pH della soluzione confrontando 3, 7 e 12 ed infine la temperatura analizzata per 13°C, 20°C e 27°C.

Per le differenti configurazioni sono stati collezionati dati di temperatura, conduttività, corrente, voltaggio, pH, istante temporale, spettro di assorbimento e TOC.

Gli esperimenti effettuati con NaCl dimostrano un tasso di rimozione superiore a quelli con $NaSO_4$; inoltre il confronto tra i risultati ottenuti con diverse correnti applicate indicano un'efficacia maggiore quando la corrente applicata è di 7 A. Per quanto riguarda gli altri parametri di temperatura e pH, si può notare che a temperature superiori, così come a pH maggiori, l'assorbanza al picco a 298 nm, si abbassa più velocemente, indicando una trasformazione più repentina dell'acido salicilico nei suoi composti intermedi a peso inferiore. Osservando i risultati dell'analisi del TOC le differenze nel

decadimento di concentrazione di carbonio non sottolineano particolari discrepanze, anche se per gli esperimenti condotti a $13^{\circ}C$ si nota un decadimento leggermente inferiore nell'ultimo campione analizzato. Concludendo, i risultati ottenuti dall'analisi del TOC e dello spettro di assorbimento, provano che la generazione di prodotti intermedi è influenzata dai parametri applicati, mentre il decadimento di concentrazione di carbonio non cambia in funzione di questi.

Parole chiave: processo di ossidazione avanzata, BDD, acque reflue, percolato da discarica, acido salicilico

Abbreviation

A	absorbance
AOPs	advance oxidative processes
BDD	boron doped diamond
BOD_5	biologic oxygen demand after 5 days
BTEX	acronym for benzene, toluene, ethylbenzene and xylenes
CAS NO.	chemical abstracts service number
CH_4	methane gas
COD	chemical oxygen demand
D_{SA}	molecular diffusivity of salicylic acid
EO	electro oxidation
F	Faraday's constant
HPLC	high performance liquid chromatography
$HO\cdot$	hydroxyl radical
i	applied current density
i_{lim}	limiting current density
ICE	instantaneous current efficiency
IUPAC	International Union of Pure and Applied Chemistry
k	reaction rate constant
k_m	mass transport coefficient
LC-MS	liquid chromatography – mass spectrometry
MQ	Mili-Q water
MSW	municipal solid waste
MW_{O_2}	molar weight oxygen
MW_{SA}	molar weight salicylic acid
NDIR	non dispersive infra red
$NH_4 - N$	nitrogen amount in Ammonia species
PAH	polycyclic aromatic hydrocarbons
PBDE	polybrominated diphenyl ethers
PFOS	perfluorooctanesulfonic acid or perfluorooctane sulfonate
PNEC values	predicted non effective concentrations values
r_i	residual of the function
R^2	correlation factor
Re	Reynold's number
Sc	Schmidt's number
Sh	Sherwood's number
SHMIL	Sondre Helgeland Miljøverk
T	transmittance
ThOD	theoretical oxygen demand
TOC	total organic carbon

UV/VIS	ultraviolet-visible light
VFA	volatile fatty acid
2,3-DHBA	2,3-Dihydroxybenzoic acid
2,5-DHBA	2,5-Dihydroxybenzoic acid
α	rate of applied current density on limiting current density
μ	dynamic viscosity of water
ρ	density of water
σ^2	standard deviation

Chapter 1

Introduction

Nowadays one of the most applied choice for the end of life cycle of municipal solid waste (MSW) is land filling. The storage of different materials in combination with the rainwater percolation cause spillage of leachate, that is a potentially polluting liquid. It may cause harmful effects on the environment: especially if it comes in contact with the groundwater and surface water surrounding the landfill site [11].

Landfill leachate has different composition and concentration of pollutants depending on several factors: the kind of waste, the compaction of the stored wastes, the amount of precipitation, the design cover, interaction with outer environment and the age of the landfill. All these aspects are interconnected and their combination determines quality and composition of the leachate [12].

The AOPs are a widely accepted treatment used for the landfill leachate for their capability of these processes to remove complex, recalcitrant and organic substances not easily degradable by biological mechanisms. The organic substances can be oxidized completely to carbon dioxide and water, but in most cases a partial oxidation results sufficient to reduce the toxicity of the leachate [9].

Electrochemical oxidation is an advanced oxidative process that uses hydroxyl radicals and other powerful oxidative agents to oxidize pollutants into an electrolytic cell. It is based on two different mechanisms: direct oxidation and indirect oxidation. The first one can directly form radicals that attacks the harmful substances and lead them to mineralization, instead the second one uses mediators to oxidize the pollutants. Important mediators are chloride-ions or sulphate-ions.

In this master thesis, the main goal is the examination and the determination of the removal efficiency for different configurations of the electrochemical oxidation for a model substance (salicylic acid) and the relative kinetics. The setup used for the experiment part is a lab unit which comprehensives of tank, flowmeter, pump and electrolytic cell. The experimental part has been carried out in the laboratory of *Institutt for vann og miljøteknikk* at the department of Hydraulic and Environmental Engineering at NTNU.

The work is presented in the further chapters. The initial focus is on the description of the Åremma landfill and its leachate in the chapter 2, together with a short background about the legal situation in Norway. Afterwards there is a theoretical part in

chapter 3, in which the advanced oxidative processes are reported and the electrochemical oxidation is widely described. A particular section is dedicated to the importance of the electrodes material, instead another section is occupied by the presentation of the chosen model compound and the last one is for the calculation of the limiting current density. With chapter 4, the attention moves to the experimental part and to the description of the setup used, the materials and applied methodology. In chapter 5 the results and the respective discussion are presented. Finally the chapter 6 presents the conclusions and a proposal for further research.

1.1 Objectives of the work

This thesis is collocated in a wider project related to the definition of a treatment scheme with the goal of treating the leachate of the Åremma landfill near Mosjøen.

The first part of the work aims to develop a possible treatment, which could be used as first step in the plant. Moreover it focuses on testing the optimized parameters to use in a laboratory plant and further in situ.

According to the leachate data and the list of European priority hazardous substances (6.2) and other legal regulations, the significant substances to treat are *COD*, *NH₃*, heavy metals and micropollutants.

The low *BOD/COD* ratio, the possibility to use energy directly provided by the landfill and the low temperature are aspects that make interesting an AOPs instead a conventional biological sector; in particular an electrochemical oxidation for different reasons explained in the chapter 3.

The second part of the thesis is an experimental work in which the degradation of salicylic acid is tested in a setup under certain conditions. The density current applied and the electrolyte nature and molarity have been investigated to find a stable and significant system, instead the pH and the temperature are well evaluated with UV/VIS spectrum and TOC measurement.

Chapter 2

Description of the Landfill Leachate

The landfill leachate is the spillage caused principally by precipitation percolating through stored waste. The percolating water that comes in contact with solid waste gets contaminated and the result is termed as leachate.

Usually leachate has high values of COD, pH, ammonia nitrogen and heavy metals as well as strong color and odor. The composition varies according to different parameters of the landfill including: age, degree of compaction, waste composition, climate and moisture content in waste [13].

Generally it is characterised with the age of landfill: young landfills (1-2 years) have BOD_5/COD ratio > 0.6 , while old landfills (more than 10 years) have a lower biodegradability with a ratio < 0.3 . These characterizations underline the biodegradability of the system that is higher in the first years because of the amount of organic compounds, easily biodegradable.

During the storage in the landfill, there are 3 important processes going on: hydrolysis, fermentation and methanogenesis [14]. The hydrolysis of organic matter leads to a lower molecular weight compound and afterwards a rapid anaerobic fermentation generates volatile fatty acids (VFA). This phase is the step of young landfills and is called acidogenic phase, which releases large quantities of VFA [15]. The phase of the older landfill is the methanogenic phase and it is characterized by the conversion of VFAs into biogas (CH_4), that can be used to generate energy. The leachate in this last phase contains high concentration of ammonia nitrogen, several harmful compounds for the environment and slower biodegradable organic compounds like recalcitrant compounds, heavy metals and other micropollutants.

In addition to the organic load, ammonia nitrogen is released from the wastes mainly by decomposition of proteins and its concentration does not have a linear decrease trend with age of the landfill, like the BOD_5/COD ratio. The dilution effect can help in the reduction of ammonia nitrogen concentration.

Usually the investigated parameters regarding leachate are: COD, BOD_5 , BOD_5/COD ratio, ammonia nitrogen, color, pH, alkalinity, oxidation-reduction potential and heavy metals [16].

Depending mainly on the composition of sanitary landfill leachate, different mecha-

nisms can be indicated as suitable treatments. Different treatments have been investigated, such as flocculation-precipitation [17], activated adsorption carbon [18], membrane technologies [19] and chemical oxidation [11]. Advanced technologies have received increasing attention in the last years and they are described in chapter (3).

2.1 SHMIL Åremma landfill

The Søndre Helgeland Miljøverk (SHMIL) Åremma is located close to the town of Mosjøen in the central part of Norway. Mosjøen is situated in the municipality of Vefsn in the southern part of Nordland County (Fig. 2.1). The Figure (2.2) focuses on the SHMIL Åremma location near Mosjøen.

The landfill is owned by eleven municipalities and ensures the disposal of waste from



Figure 2.1: Position of SHMIL Åremma



Figure 2.2: Location of the landfill close to Mosjøen

41000 inhabitants. It was founded in the year 1995 and it collects non-hazardous waste. So far no treatments for the landfill leachate are expected. The leachate flows out in a collector and discharges directly into the fjord by a pump. A treatment plant for SHMIL is planned to be operative from 2017.

The location of the landfill is an important aspect to keep in consideration during the decisional process part. In fact the low temperature is a parameter that can influence the efficiency of the treatment plant, especially the biological sector, if expected. The landfill is approximately 70-80 m above sea level. The average monthly temperature and precipitation are shown in Table (2.1) and they are evaluated between 1961 and 1990, a time frame long enough to argue a monthly trend.

Month	T [$^{\circ}C$]	Precipitation [mm]
Jan	-5,7	186
Feb	-4,5	135
Mar	-1,6	150
Apr	2,4	99
May	7,6	79
Jun	11,6	80
Jul	13,4	100
Aug	12,8	116
Sept	8,6	191
Oct	4,6	230
Nov	-1,4	181
Dec	-4,2	198
Year	3,6	1745

Table 2.1: Average monthly temperature and precipitation (1961-1990)

The average temperature of the year is $3,6^{\circ}C$ and the total average precipitation is 1745 mm.

It can be easily inferred from the Figure (2.3) the fact that the precipitation is higher in winter time than during summer with a peak in October. The precipitation influences the amount of leachate formed in the landfill and also its dilution index.

Aiming to develop a optimized treatment scheme for this case study, there are these

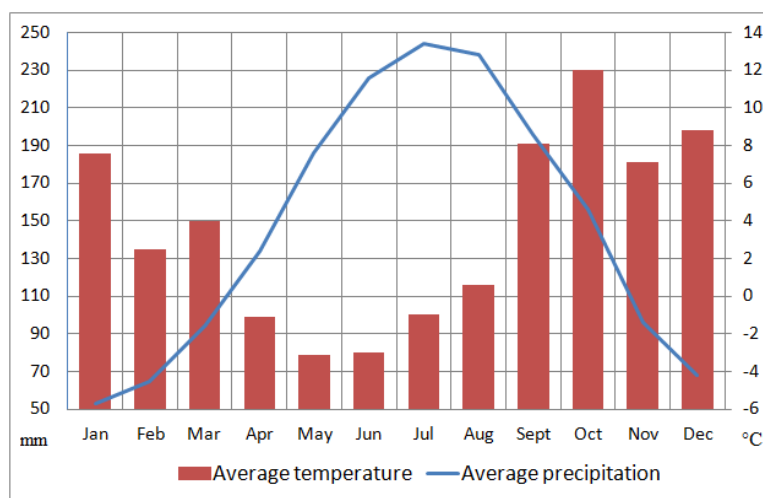


Figure 2.3: Average temperature and average precipitation for Mosjøen (1961-1990)

three characteristics to focus on:

- low temperature;
- restrictive amount of space (approximately $50 m^2$) available to build a treatment plant;
- available energy derivated by methane gas generated inside the landfill.

2.2 Background about the legal situation

The legal situation in Norway regarding leachate treatment is rather complicated. There are some guidelines with some requirements that the leachate has to fulfill, but a complete list of parameter limits are not defined up to now.

The guidelines in consideration are given by the European Union (see Table 6) and also by the *Deponidirektivet and Rammedirektivet for avfall*, that are applicable even in Norway. There are threshold values tabulated for the following parameters: total organic carbon, total nitrogen, total phosphorous, iron, zinc, copper, lead, nickel, chromium, manganese, arsenic, mercury, tin-organic compounds, volatile chlorinated compounds phthalate, polycyclic aromatic hydrocarbon (PAH), chlorobenzene, chlorophenol, herbicides.

For those parameters that do not have regulation, there is a supplementary "list of priority substances" available, which summarize the substances to reduce and reduced to zero by 2020. The list is presented in Appendix (2.4).

2.3 Characteristics of leachate by water quality data

For Åremma landfill leachate, several parameters have been investigated over the years with the goal of understanding in a clear way the data, a summary is necessary.

The parameters can be split in different categories, which are [20]:

- Characterising parameters (pH, conductivity, suspended solid concentration, COD, BOD, TOC, Total-P, Total-N and $NH_4 - N$)
- Alkaline earth metals (Ca, K, Mg, Na)
- Heavy metals (Fe, Al, As, Ba, Cd, Co, Cr, Cu, Hg, Mn, Mo, Ni, Pb, Zn, V)
- Polycyclic aromatic hydrocarbons (Naphthalene, Acenaphthylene, Acenaphthene, Fluorene, Phenanthrene, Anthracene, Fluoranthene, Pyrene, Benzanthracene, Chrysene, Benzofluoranthene, Benzopyrene, Dibenzanthracene, Benzoperylene, Indenopyrene, PAH cancerogenic)
- BTEX (Benzene, Toluene, Ethylbenzene, O/M/P/xylene)
- Herbicides (2,4-D, MCPA, MCPP, 2,4,5-T, 2,4,5-TP, MCPB, 2,4-DB, 2,4-DP)
- Hydrocarbons.

The data is recorded every three months for a interval of 9 years, from 2006 up to now. In total there are 51 measurements and the complete list can be found as attachment in Appendix (6.2). Figure (2.2) and (2.3) shows the basic parameters measured.

The unclear legal situation causes problems on how individuate the compounds to treat and what is the threshold value. For most of the parameters, the thresholds are not overcome from european requirements, but they exceed for PNEC-values (Predicted Non Effective Concentrations), that are an index which determine the possible hazards on the environment, due to the exceeded concentrations. PNEC values are often below legal threshold values and they are not a mandatory limitation for the norwegian landfills, but they are useful to get an overview of which substances are more toxic and how

they could be treated.

Comparing the data and the literature values [21], inferences can be drawn. COD, BOD_5 and TOC are consistently low, which suggests a small organic pollution. Even if the leachate contains only a small amount of COD, the BOD/COD ratio is less than 0,1: hence it can be argued that the landfill is old and some biological treatment may not be the preferable solution.

The pH is nearly neutral and the suspended solids concentration shows values in the same range as per literature. Total nitrogen is quite high compared to the organic parameters and it is present mostly in ammonia nitrogen form; only a small fraction of it, is in nitrate form, that is the one which creates problem of eutrophication. Instead the total phosphorous has low values. Furthermore the conductivity is in the same range of literature values.

The load of these parameters is not stable in time and it is not straight forward to find a correlation between cause and effect. There are more than one reason for the variability of loads: precipitation amount, saturation of the ground, season of the year and so on. All the combinations of these factors provokes a variable load of pollutants.

From the analysis of the characterising parameters and of the others from the dif-

Parameter	Average	Standard Deviation	Max	Min	Unit
pH	6,8	0,3	7,4	6,4	-
COD	211,5	108,8	643	72	mg/L
BOD_5	20,7	28,6	160	4	mg/L
TOC	59,5	29,8	135	3	mg/L
Total P	0,55	0,40	2,3	0,1	mg/L
Total N	102,2	41,3	200	22	mg/L
$NH_4 - N$	95,2	39,4	210	20	mg/L
Suspended solids	86,6	56,3	360	27	mg/L
Conductivity	257,1	70,4	420	122	mS/m

Table 2.2: Concentrations of the characterising parameters (2006-2015)

Parameter	Average	Standard Deviation	Max	Min	Unit
COD	40,98	57,62	320,0	2,6	kg/d
BOD_5	3,36	4,02	16,9	0,2	kg/d
TOC	10,43	11,63	47,7	0,9	kg/d
Total P	0,08	0,09	0,35	0,01	kg/d
Total N	15,94	16,66	79,6	2,2	kg/d
$NH_4 - N$	14,99	15,67	74,7	2,1	kg/d
Suspended solids	11,64	8,92	49,8	1,5	kg/d

Table 2.3: Loads of the characterising parameters (2006-2015)

ferent categories, it can be argued that the leachate of Åremma is principally not strongly polluted and most of the parameters undergo the threshold value for its case. On the other hand, this consideration does not permits the underestimation of problem at hand. Some parameters exceed the limit anyway and a specific treatment must be

studied. The final list with the focus on the priority substances to treat before 2020 for the case in question is reported in Table (2.4).

For most of the parameters of the characterising list and even of the other categories,

Priority Substance	Median	Unit
Anthracene	0,031	$\mu g/L$
PBDE-99	0,001	$\mu g/L$
PBDE-203	0,002	$\mu g/L$
Naphtalene	1,735	$\mu g/L$
Octylphenole	0,318	$\mu g/L$
Trichlorobenzene	0,020	$\mu g/L$
Cadmium and Organic Cadmium compounds	0,092	$\mu g/L$
Lead and Organic Lead compounds	1,380	$\mu g/L$
Mercury and Organic Mercury compounds	0,026	$\mu g/L$
Nickel and Organic Nickel compounds	16,100	$\mu g/L$
Tributyltin	0,002	$\mu g/L$
Benzene	0,200	$\mu g/L$
Terbutryn	0,237	$\mu g/L$
PFOS	0,090	$\mu g/L$
Nonylphenol	1,050	$\mu g/L$
PAH	0,060	$\mu g/L$
Arsenic	3,790	$\mu g/L$
Bisphenol A	15	$\mu g/L$
Chromium	11,700	$\mu g/L$

Table 2.4: Priority substances in the leachate (2006-2015)

the standard deviation has a high value, which indicates a large variability in the pollutant outlet. In particular, the deviation standard is higher for those substances having a higher measured value. When the detected value is low, even the variability of it is not consistent.

The unpredictability of the pollution adds a difficulty grade for identifying an adequate treatment.

As shown, the substances in the list belong to different categories and this makes it harder to define a specific treatment type for any particular pollutant. This is an added reason as to why the AOPs is a good solution for treating different pollutant compounds as organic matter, ammonia nitrogen and micropollutants at the same time.

Chapter 3

Theoretical background

3.1 Advanced Oxidation Processes (AOPs)

Since the 1970s advanced oxidation processes (AOPs) have received attention as a possible approach to oxidize compounds that are resistant to biological oxidation processes. These chemicals include agricultural pesticides, herbicides, fuel, solvents, human drugs and endocrine disruptors.

The fulfillment of new quality standards refers especially to those substances with a toxic effect on the biological sphere, preventing the well working of the biological degradation process. Obviously must be guarantee destruction of toxic pollutants as well as of recalcitrant compounds.

Usually AOPs are applied at ambient temperature and pressure and have a versatile capability, because of the different ways for hydroxyl radicals ($HO\cdot$) production, thus allowing a wide possibility of applications. They can be used as an integration of the biological compartment, to degradate toxic and refractory substances. Furthermore AOP application is suitable when wastewater have a low COD concentration otherwise the application of these reactants is not economical sustainable [22].

AOPs aim at the complete mineralization of the contaminants or at least, at their transformation into less harmful products. In many cases a complete oxidation to CO_2 , water and inorganics is not necessary, because after the first oxidation step the new compounds lose their harmful characteristic and are more amenable to a subsequent biological treatment. AOPs are preferential over other processes because contaminants can be destroyed completely and thus avoiding the mass transfer in a different phase. Consequently there is no need for an additional treatment like stripping or adsorption [23].

AOPs are often used in combination with other processes, either as a pretreatment for a biological compartment for increasing the biodegradability of the matters or as a post-treatment for oxidizing the remaining toxic and refractory compounds after a conventional biological treatment.

AOPs generate $HO\cdot$ at room temperature and pressures.

Radicals are molecules containing an orbital with a single unpaired electron; usually the notation is an abbreviated version of Lewis structure with only one dot that symbolizes the electron in the outer orbital. The reactions with hydroxyl radicals are efficient and non selective due to the high reaction rate (on the order of $10^8 - 10^9 L/mol \cdot s$) with the most part of organic compounds in water.

As shown in Table (3.1), hydroxyl radical is one of the most reactive oxidants, only

fluorine is more reactive.

Oxidizing agent	Electrochemical oxidation potential, E° [V]
Fluorine	3.06
Hydroxyl radical	2.8
Oxygen (atomic)	2.42
Ozone	2.08
Hydrogen peroxide	1.78
Hypochlorite	1.49
Chlorine	1.36
Chlorine dioxide	1.27
Oxygen (molecular)	1.23

Table 3.1: Electrochemical oxidation potential for different oxidizing agents (table chapter 11-10 [9])

The pollutants react with the hydroxyl radicals, as shown in (3.1), generating byproducts. $\cdot OH$ -radicals destroy refractory organic compounds in a non-selectively way.



The hydroxyl radical can degrade organic molecules by radical addition, hydrogen abstraction, electron transfer and radical combination [9].

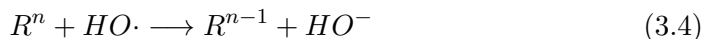
- Radical addition: it is the reaction of an unsaturated aliphatic or aromatic organic compound with a hydroxyl radical. The product of this reaction is a radical organic compound, reactive for further oxidation to a stable end product;



- Hydrogen abstraction: a hydrogen atom is removed from the organic compound by the hydroxyl radical. This newly formed radical initiates a chain reaction with oxygen;



- Electron transfer: it is used to form ions of higher valence;



- Radical combination: two radicals combine together to generate a stable product.



The efficacy of an AOP depends primarily on the capability of the system to generate radicals. Each process has a different mechanism to form radicals, but once $HO\cdot$ are generated, the following reactions are the same in all AOPs. In the subsequent sections ozonation and Fenton process are reported: both methods are applied for the waste water as well as for landfill leachate treatment.

Ozonation

Ozone (O_3) can oxidize by conventional oxidation or advanced oxidation processes. The difference between two methods are the target compounds to degrade and the operational condition, especially the pH value. Considering ozonation an AOP, the hydroxyl radicals are formed according to reaction (3.6), which is effective at an alkalyne pH. Usually the pH of the solution is increased (pH>8) before the treatment by ozonation to enhance the process. If the raw water contains a moderate concentration of carbonate ion (CO_3^{2-}), another treatment is chosen because the pH is spontaneously kept low [24]. The higher the pH, the faster is the reaction, with a optimum at pH 11.

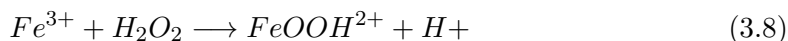
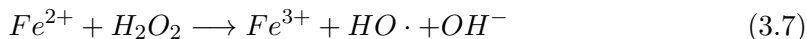


Organic compounds can be oxidated directly by O_3 molecules or by indirect reactions with $HO \cdot$. Consequently the oxidation rate is given by both reactions: direct oxidation and AOP.

Ozone can be combined with UV light irradiation at 254 nm or by adding hydroxyl peroxide (H_2O_2) to increase its performance in terms of time and reaction products [23].

Fenton process

Fenton process was discovered by Henry J.H. Fenton in 1894 and it is nowadays considered a promising application for wastewater treatment [25]. It includes ferrous or ferric ions which react with hydrogen peroxide to generate hydroxyl radicals and other highly reactive radical compounds, by reaction (3.7) and by the so-called "Fenton-like" reaction (3.8) [22].



It is a method widely investigated for wastewater treatment and it has been demonstrated that it is effective in destroying toxic compounds such as phenols and herbicides. The Fenton process is efficient when pH of the solution is in a acid condition (between 2 and 3.5) in order to increase the kinetic of the reaction (3.8). The low pH requirement is the main drawback of this method, because most of the treated solutions have an initial pH in the range of 5-9 and thus require a preliminar acidification before the treatment.

The Fenton processes can be divided in two different categories: homogeneous Fenton, which requires the addition of the reagent in liquid form and heterogeneous Fenton which uses iron in the solid phase. Iron can be added as salt or by generation at the sacrificial anode while hydrogen peroxide is a molecule easy to handle and environmentally friendly.

3.2 Electrochemical Process

Electrochemistry is already widely applied for environmental problems as a technique of monitoring and trace level detection of pollutants in the air, water and soil, on thus help to prevent pollution caused by industrial processes. There are applications also in the field of drinking water, waste water treatment for tannery, electroplanting, dairy, textile processing, oil industries etc [22]. This particular application is also investigated

for the treatment of landfill leachate.

The technologies are based on electron transfer between electrodes and electrolytic solution, due to an applied current between the anode and the cathode. The difference of potential promotes oxidation/reduction reactions of the pollutant compounds [26]. There are several advantages related to an electrochemical treatment applications [27]:

- **Environmental compatibility:** the electron is a clean reagent, because the production of unwanted sideproducts is avoided.
- **Versatility:** it can involve direct or indirect oxidation and reduction, phase separation; it is applicable to a variety of media and pollutants in different phases and treat large or small volumes with high or low concentration of pollutants.
- **Energy efficiency:** electrodes and electrolytic cells can be designed to minimize power losses and to allow experiments at lower temperature compared to their equivalent non-electrochemical counterparts.
- **Amenability to automation:** the electrical variables are particularly suitable for automatized processes and data acquisition.
- **Cost effectiveness:** the required equipment is simple to construct and if correctly designed, inexpensive.

The high effectiveness in the elimination of persistent pollutants led to an increased number of experiments in the field of water and wastewater treatment; particularly focused on electro-Fenton and electrochemical oxidation methods [26].

Electro-Fenton process

The electro-Fenton process involves the mixture of H_2O_2 and ferrous ion (Fe^{2+}) to generate hydroxyl radicals, very strong oxidizing species.

The main advantages of this process are its efficiency in COD removal and BOD_5/COD ratio increment, furthermore only a short operating time is needed and the volume of sludge produced is lower than regular Fenton process [28].

The electro-Fenton process is based on an electro-catalytically generated, hydroxyl radicals in an acidic solution containing a suitable amount of dissolved oxygen and ferric/ferrous ions. This process starts with the generation of hydrogen peroxide from the reduction of oxygen and, if present, the simultaneous formation of ferrous ions from ferric ions on the cathode surface. After this first step, the Fenton reaction takes place between hydrogen peroxide and ferrous ions to generate hydroxyl radicals. The hydroxyl radicals produced in this way are used in the oxidation of harmful chemicals which can be hazardous for the environment.

3.3 Electrochemical Oxidation

Electrochemical oxidation is one of the most popular electrochemical procedure for removing organic pollutants from the wastewater [29].

The process is based on the effluent electrolysis and consists in an electrolytic cell, where the oxidation is carried out by two different mechanisms:

- *direct anodic oxidation*: pollutants exchange electrons directly on the electrodes surface and depending on the anode material, hydroxyl radicals can promote selective oxidation and also complete mineralization. The oxygen is transferred from the water, that is the source of oxygen atoms, to the reaction products.
- *indirect oxidation* using oxidants or mediators, such as chlorine, persulfate and so on, instead of hydrogen peroxide radicals. Usually to promote indirect oxidation, oxidants are added from outside. However, even without any external adding, the raw leachate already contains some of these promotors and the indirect mechanism can take place anyway.

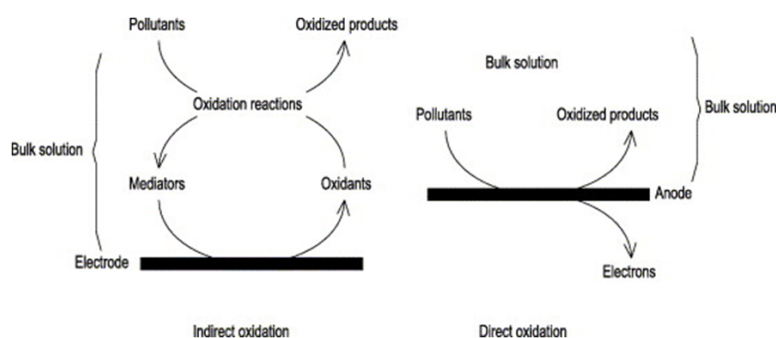


Figure 3.1: scheme of direct and indirect oxidation of pollutants [1]

These concepts are better explained in the further sections.

The choice of focusing on electro oxidation (EO) has been motivated by different reasons [26]:

- pH can be maintained at the same value as the raw leachate without conducting an acidification as required for the Fenton process. In the pH range of 6-9 the efficiency of EO increases, in particular for ammonia nitrogen removal, that is transformed into nitrogen gas at alkaline conditions;
- with EO, recalcitrant and toxic compounds are oxidized with a good removal efficiency as well as ammonia. By using other AOPs, ammonia is not significantly removed. There are studies ([30], [31] and [32]) that demonstrate effectiveness of EO in COD oxidation compared with other process for landfill leachate;
- the addition of reagents such as iron salts or ozone is not required;
- EO is also promising for the successful removal of heavy metals: Fernandes et al. [33] performed a system which combines in a first step EC with a iron consumable electrode and in a second step EO with boron-doped diamond (BDD) electrodes and they could prove a total removal of chromium and zinc. After the first step chromium is almost completely removed, instead zinc is only partially removed and it needs EO to be efficient.

Even after plenty experimental trials, no complete agreement has been attained on the nature of adsorbed intermediates and the details of the reaction mechanism are not completely elucidated so far. Inside the same process different mechanisms coexist and

contribute to the global degradation.

3.4 Direct Oxidation

In the direct oxidation, the generation of active oxygen occurs at the anode surface in a physical way, producing $HO\cdot$ or in a chemisorbed way, by the oxide lattice (MO_{x+1}).

The mechanism is schematically shown in Figure (3.2). The oxidation can follow

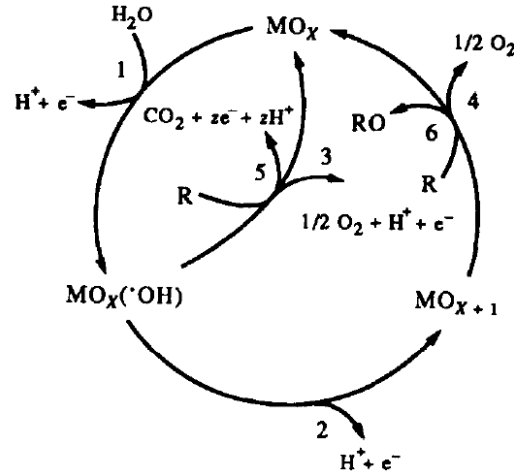
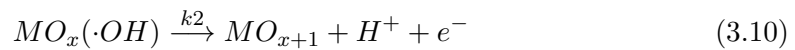
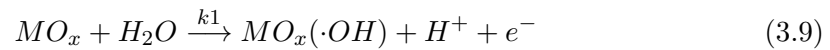


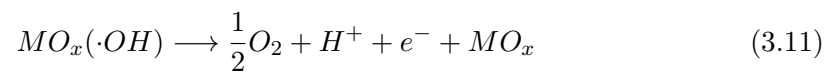
Figure 3.2: Mechanism of direct anodic oxidation [2]

two pathways: the complete combustion, thus the production of CO_2 and water or the conversion to other biological compounds, those need a further treatment. In particular, these processes coexist during the oxidation and the final products present in the solution, are a combination of both the ways.

Describing the scheme, the first step in Eq. (3.9) shows the water in an acidic media, produces hydroxyl radicals, at the anode surface (the same products can be formed in an alkaline condition with OH^-). The oxygen is given by the water, through the dissociative adsorption of it or through the electrolytic discharge of it at potentials above its thermodynamic stability [34]. The second step is the formation of the higher oxide MO_{x+1} , described in Eq. (3.10), in which the adsorbed hydroxyl radicals interact with the oxygen in the oxide anode.



To conclude the loop, there are reactions which are competitive with the organic matter oxidation. If there is any oxidable organics, the reactions lead to the production of dioxygen (3.11 and 3.12); otherwise the chemisorbed "activate oxygen" participate in the formation of selective oxidation.



Selective oxidation

The electrochemical conversion transforms mainly "non-biocompatible" organics into "biocompatible" organics, increasing the possibility of a further biological treatment, if the BOD/COD ratio reaches a higher value. Selective oxidation is enhanced when the condition (3.13) is satisfied.

$$k_2 \gg k_1 \quad (3.13)$$

If the second reaction is faster than the first one, the concentration of hydroxyl radicals is almost zero at the anode surface, infact they have been used for the generation of higher oxides. Efficient anodes for selective oxidation of organics are those with low concentration of active sites and high concentration of the so-called "oxygen vacancies" in the oxide lattice. MO_{x+1} is an example of an oxide having a high concentration of "oxygen vacancies".

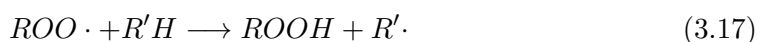
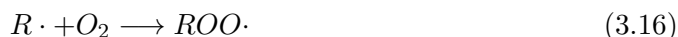
Complete combustion

The electrochemical combustion carries out the complete mineralization to CO_2 and water. High concentrations of hydroxyl radicals on the anode surface are involved in the oxidation of the organic matter. Thus, the second reaction is faster than the first one.

$$k_2 \ll k_1 \quad (3.14)$$

The condition (3.14) is satisfied with anodes having a large number of active sites for the adsorption of hydroxyl radicals and low concentration of "oxygen vacancies" in the oxide lattice. An example of this is an oxide with an excess oxygen in the oxide lattice, which can be an oxide doped with a metal oxide with a higher oxidation state.

To arrive at the complete combustion, there are other intermediate reactions but the specific mechanism is complex and not completely known. It can be simplified with the following formation of organic radicals (3.15), reaction with dioxygen (3.16), formation of hydroperoxide (3.17) and further decomposition of intermediates, due to the instable nature of hydroperoxide [2].



Depending on the anode material, conversion or combustion is increased. For this reason anode material is an important parameter to set and according with the literature, several materials have been investigated.

3.5 Indirect Oxidation

The electrochemical oxidation can be performed also in a indirect way. Organic pollutants exchange electrons through the mediation of some electroactive species, which act as an intermediary between the electrode and the organics [34]. Concerning the

indirect oxidation, the most used electrochemical oxidants are chlorine, hypochlorite or sulphate. In the presence of a high chloride concentration, inorganic and organic pollutants are mostly eliminated.

This technology has also two important drawbacks: the possible formation of chlorinated organic intermediates or final products and the need of salt addition, if the concentration of chlorine is low in the raw leachate.

Another kind of indirect oxidation is the one which uses mediators. Metal ions, called mediators are oxidized at the anode surface from a stable state to a more reactive and high-valence state. In this form the mediators can directly attack and oxidize organic pollutants. Typical mediators are Ag^{2+} , Co^{3+} , Fe^{3+} , Ce^{4+} and Ni^{2+} . The drawback of this method is the production of sludge polluted from heavy metals, which limits its application. Furthermore an acidic media is necessary to avoid precipitation of the metals before the reaction with the organic matter [22].

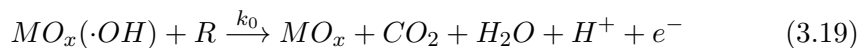
3.6 Electrodes Material

As already introduced, the nature of the electrodes material influences the selectivity and the efficiency of the electrochemical oxidation process. It is possible to distinguish between two classes of electrodes, defined as *active* and *non-active* [35].

- An active electrode has higher available oxidation states on the electrodes surface and this means the adsorbed hydroxyl radicals interact mainly with the anode to form higher oxide. The reaction is the (3.18) and it uses the so-called chemisorbed active oxygen as a mediator to form intermediary oxidated products. Active anodes have low oxygen evolution overpotential and consequently are good electrocatalysts for the oxygen evolution reaction.



- A non-active electrode avoids the formation of higher oxides and hydroxyl radicals oxidate in a nonselective way to the complete combustion, thus to CO_2 and water (3.19). Non-active anodes have high oxygen evolution overpotential and consequently are poor electrocatalysts for the oxygen evolution reaction.



According to the literature, many anodic materials have been tested to find those that are more efficient for different kinds of pollutants. Some active anode materials are carbon and graphite, platinum-based anodes, iridium-based oxides and ruthenium-based oxides. Instead the most used non-active anode materials are antimony-doped tin oxide, lead dioxide and boron-doped diamond [34].

3.7 Boron-doped Diamond (BDD)

Boron-doped diamond is one of the most widely studied materials for wastewater and water disinfection. It is also promising in the field of the organic pollutants removal

from leachate, in a lab scale [36] as well as pilot plant [37].

BDD has an inert surface with low adsorption properties, strong corrosion stability and high oxygen evolution overpotential. The large amount of $\cdot OH$ produced have high reactivity for organic oxidation, due to their weakly interaction with the anode surface.

In many papers BDD efficiency is demonstrated; several compounds reach complete mineralization, such as carboxylic acids [38], herbicides [39], benzoic acid [40], naphthol [41], phenol [42], cyanides [43] and others.

Compared to platinum, BDD has a wider working window, as shown in Fig. (3.3), that means it can reach cathodic and anodic potentials and it can generate a multitude of active elements. For these properties it is often applied for landfill leachate treatment.

However, diamond electrodes have some drawbacks as well, like their high cost and

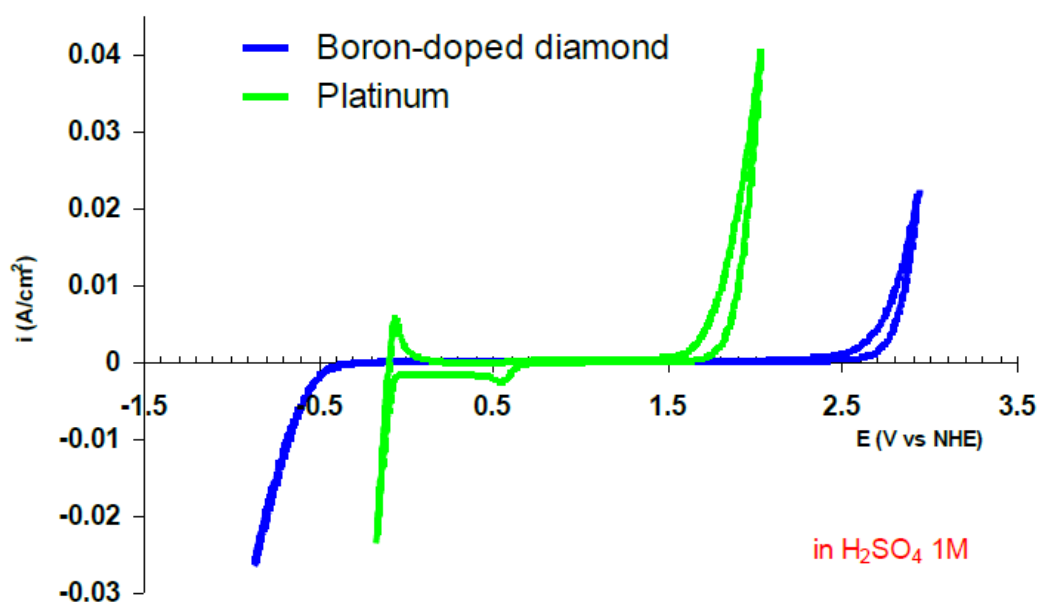


Figure 3.3: Comparison between cyclic voltammogram of platinum and BDD [3]

the difficulties in finding an appropriate substrate, where to deposit the thin diamond layer. Tantalum, Niobium and Tungsten are expensive, instead Silicon is brittle and poor conductive [34].

3.8 Salicylic acid

Aiming to the oxidation of organic matter, salicylic acid is chosen as a model organic molecule [44]. The choice of this compound has been made due to its ability to act as a spintrap for free hydroxyl radicals in the biological system and for its structure, containing an aromatic ring.

With these characteristics, it is a good model to prove that the system uses hydroxyl radicals to oxidize organic matter. Its rate constants with OH radicals is $2,2 \cdot 10^9 L/mol^{-1} s^{-1}$ [45].

The salicylic acid is a colorless crystalline organic acid. The IUPAC name is 2-hydroxy benzoic acid. It is widely used in organic synthesis and it is identified as a plant hor-

none. The molecular formula is $C_7H_6O_3$ and the OH group is ortho to the carboxyl group.

It is well known for its medical application: as a skin-care product and as an important active metabolite of aspirin. It has particular properties to ease aches and pains and reduce fever. Because of these abilities has been used since ancient time as an anti-inflammatory drug. It is used also to treat seborrhoeic dermatitis, acne, psoriasis, calluses, keratosis pilaris, acanthosis nigricans, ichthyosis and warts as other hydroxy acids.

It is even used as a bactericidal, as a food preservative, as an antiseptic and in some shampoo.

The mineralization process of the salicylic acid is a mechanism that can involve

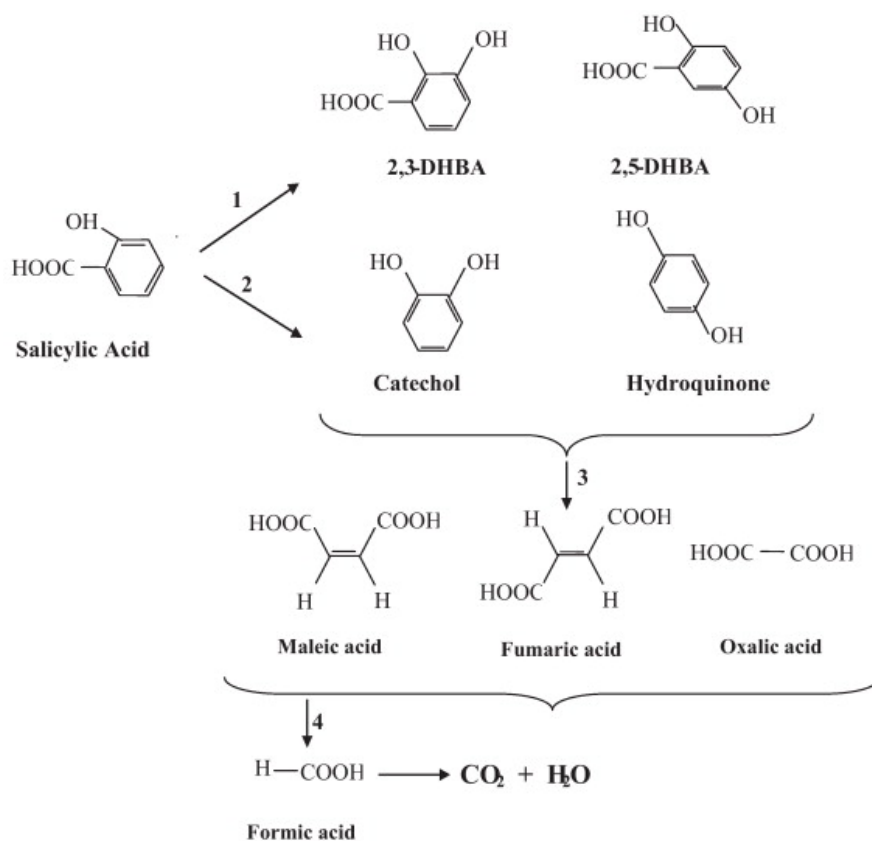


Figure 3.4: Process of mineralization of salicylic acid with possible intermediates creation [4]

different intermediates depending on the pathway the system enhances and on the electrode material used. A simple scheme of the oxidative reactions is presented by Rabaaoui and Allagui [4] and is described in Figure (3.4). It involves hydroxylation, decarboxylation, opening of the benzenic ring and further oxidation. A possible first step is the hydroxylation of the salicylic acid by hydroxyl radicals until the formation of dihydroxylated intermediates (1) and the decarboxylation with the formation of catechol and hydroquinone (2). The intermediates emit at a wavelength close to the peak at 298 nm of the salicylic acid, that can avoid an easy determination of them in the solution. It can be used a technique for identify the different present compounds [46].

Afterwards aliphatic carboxylic acid are formed with the cleavage of the benzenic ring (3), which are consequently oxidized to formic acid (4) and at the end mineralized to carbon dioxide and water.

Different aromatic intermediates and generated carboxylic acid, formed during the degradation of salicylic acid, can be detected by HPLC.

The solubility in water is reported in Table (3.2). Experimentally, the solution of salicylic acid in water is not easily soluble and it is advisable to stay below the limit of the table and shake strongly.

Temperature [$^{\circ}C$]	Solubility [g/L]
0	1,24
25	2,48
40	4,14
75	17,41
100	77,79

Table 3.2: Solubility of salicylic acid in water

3.9 Limiting current density

A further important parameter to keep in consideration is the applied current used. In particular the definition of limiting current density is necessary to understand the mechanism difference for both of the schemes.

Panizza et al. [5] developed a simple mathematical model that describes the direct oxidation and hydroxyl radicals oxidation mechanism. First of all, the limiting current density is expressed by the Eq. (3.20) and it is directly proportional to COD(t).

$$i_{lim} = nFk_mCOD(t) \quad (3.20)$$

where

i_{lim}	A/m^2	limiting current density
n	-	number of exchanged electrons involved in the reaction
F	$C \text{ mol}^{-1}$	Faraday's constant
k_m	$m \text{ s}^{-1}$	average mass transport coefficient in the electrochemical reactor
$COD(t)$	$molO_2m^{-3}$	chemical oxygen demand at a given time t

Depending on the applied current density, there are two possible operating regimes:

- $i < i_{lim}$
if the applied current density is below the limiting current density, the electrolysis is under current control. That means the organic intermediates are formed during the oxidation and COD decreases linearly with time, according to Eq. (3.21).

$$COD(t) = COD_0 \left(1 - \frac{\alpha A k_m}{V} \cdot t \right) \quad (3.21)$$

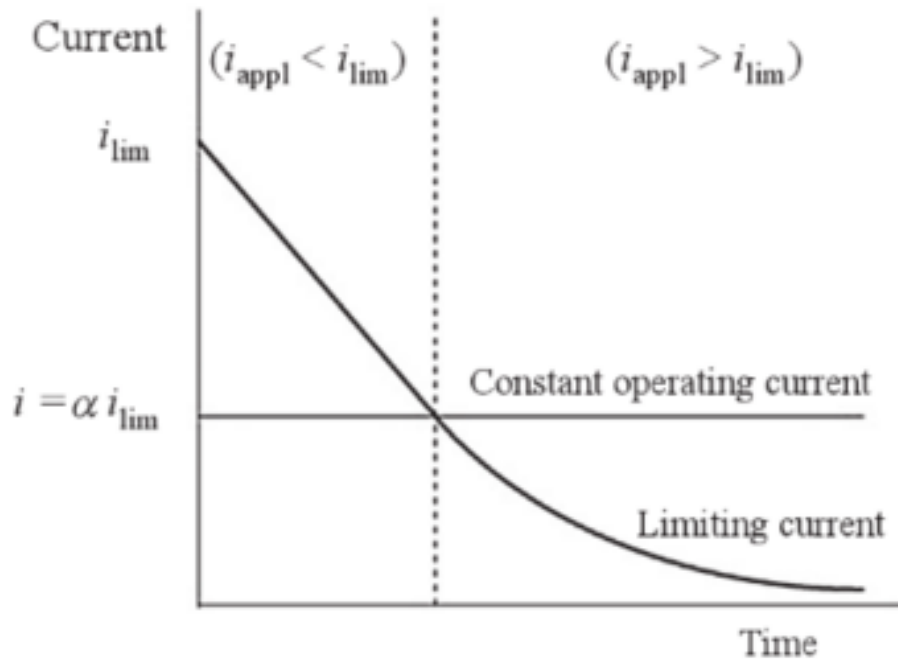


Figure 3.5: Schematic curves showing the different trends of the limiting [5]

where

α	[-]	$\frac{i}{i_{lim}}$
A	[m^2]	anodic area (surface of the electrode)
V	[m^3]	treated volume

- $i > i_{lim}$
if the applied current density is above the limiting current density, the electrolysis is under mass transport control. In this case, the organic compounds are completely combusted to CO_2 and the COD decay follows an exponential trend, showed in the Eq. (3.22).

$$COD(t) = COD_0 \cdot \exp\left(-\frac{Ak_m}{V} \cdot t\right) \quad (3.22)$$

When the intermediate situation happens, the applied current density is for a certain time above the limiting current density and then, when this one decreases, below it. For this situation, the $COD(t)$ can be calculated by the Eq. (3.23).

$$COD(t) = \alpha COD_0 \cdot \exp\left(-\frac{Ak_m}{V} \cdot t + \frac{1 - \alpha}{\alpha}\right) \quad (3.23)$$

The COD depends on time and it decreases with the passing of the minutes. In Figure (3.5), it is shown the possible situations, in the intermediate case. The curve is linear until the i_{lim} reaches the i_{appl} , when it becomes exponential.

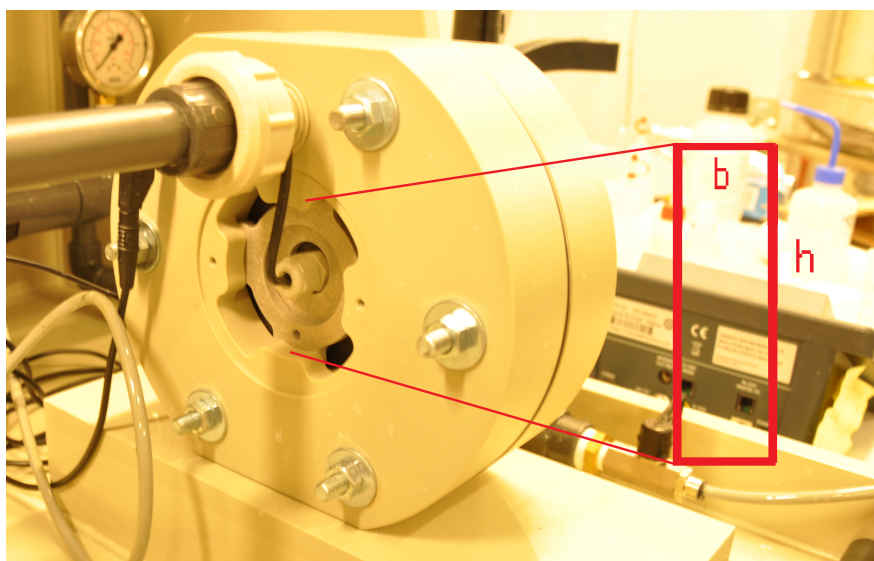


Figure 3.6: Profile of the throughflow area inside the cell

In the following sections, the calculations for the specific coefficients used in the Eq. (3.20) are reported.

All the parameters used are mentioned in the Table (3.3).

The throughflow area is the profile of the area between the electrode circular plates,

Parameter	Symbol	Unit	Value
molecular diffusivity of salicylic acid [47]	$D_{SA}(20^{\circ}C)$	$\frac{m^2}{s}$	$7,43 \cdot 10^{-10}$
dynamic viscosity of water	$\mu(20^{\circ}C)$	$\frac{kg}{ms}$	$1,002 \cdot 10^{-03}$
water density	$\rho(20^{\circ}C)$	$\frac{kg}{m^3}$	998,29
Faraday's constant	F	$\frac{C}{mol}$	96485,33
molar weight oxygen	MW_{O_2}	$\frac{g}{mol}$	32
exchanged electrones for salicylic acid	n	$\frac{e^-}{mol}$	4
molar weight salicylic acid	MW_{SA}	$\frac{g}{mol}$	138,12
inner-electrode gap	b	m	0,001
throughflow-area	A	m^2	$9,44 \cdot 10^{-05}$
flow	Q	$\frac{L}{h}$	300
hydraulic diameter for rectangular ducts	$D = \frac{4A}{P}$	m	$2 \cdot 10^{-03}$

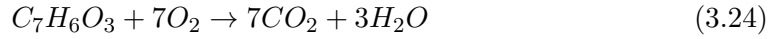
Table 3.3: Characteristics of the DiaClean Lab Unit system

as indicated in Fig (3.6).

Theoretical Oxygen Demand of salicylic acid

In a system where the only external organic addition is the amount of salicylic acid, it can be assumed that the ThOD is equivalent to the COD.

The ThOD is the theoretical demand of oxygen for oxidize the organic matter. To calculate it, the oxidation reaction of the salicylic acid is studied in Eq. (3.24): 7 moles of O_2 are necessary to oxidize 1 mole of salicylic acid.



The conversion factor from milligrams of salicylic acid to milligrams of oxygen is explained in the Eq. (3.25).

$$7 \frac{molO_2}{molSA} \frac{32 \frac{mgO_2}{molO_2}}{138,12 \frac{mgSA}{molSA}} = 1,62 \frac{mgO_2}{mgSA} \quad (3.25)$$

$$ThOD = 300 \frac{mgSA}{L} \frac{1,62 \frac{mgO_2}{mgSA}}{32 \frac{mgO_2}{L}} = 15,20 \frac{molO_2}{L} \quad (3.26)$$

For the experiment it has been hypotized the only organic addition is the salicylic acid, that means the ThOD is at the same time also the COD.

Average mass transport coefficient

The mass transport coefficient depends on the characteristics of the system as well as on the flow, if it is a laminar or a turbulent regime. Initially the Schmidt's number and the Reynolds's number are calculated, following the Eq. (3.27) and (3.28).

$$Sc = \frac{\mu}{\rho D_{SA}} = 1351 \quad (3.27)$$

$$Re = \frac{\rho DQ}{A\mu} = 1759 \quad (3.28)$$

D is the hydraulic diameter for a rectangular duct and is calculated by Eq. (3.29).

$$D = \frac{4A}{P} = \frac{4A}{2(h+b)} = \frac{2A}{h} = 0.002m \quad (3.29)$$

where P is the wetted perimeter. If the condition $b \ll h$ is satisfy, the hydraulic diameter can be calculated by the last part of the formula.

With the Schmidt's number and the Reynolds's number, it is possible to calculate the Sherwood's number by the Eq. (3.30).

$$Sh = 0.54Re^{0.385}Sc^{0.2} = 41 \quad (3.30)$$

At this point the average mass transport coefficient can be found with the Eq. (3.31). In particular, it has to be mentioned that the mass transport coefficient is in the same range of the one given by the setup supplier.

$$k_m = Sh \frac{D_{SA}}{L} = 1,51 \cdot 10^{-5} \quad (3.31)$$

Limiting current density

Once all the parameters have been determinated, the limiting current density is easily calculated by (3.32).

$$i_{lim} = nFk_mCOD(t) = 8,84 \frac{mA}{cm^2} \quad (3.32)$$

Considering the electrodes area is 70 cm^2 , the limiting current is 0,62 A.

Several authors tried to focus on different parameters, how they enhance direct oxidation or indirect oxidation. The electrode material is the most important factor, that influences mostly the hydroxylation mechanism. Other parameters can be changed to have an overview about the working of the setup: the inner electrodes gap, the electrolyte concentration and type, the applied density current. All these parameters have been already tested by different authors in a batch reactor experiment.

Chapter 4

Experimental part

In this chapter, the description of the laboratory experience is briefly reported. In the relative sections it can be found the chemicals used, a detailed description of the setup and the devices for the absorbance measurements and TOC analyze. Furthermore it is specified the experiment with potassium indigo trisulfonate and the calibration curve, which is useful for the transformation of absorbance value to effective concentration, contained in the system.

4.1 Chemicals

The following list contains all the chemicals used in the experiments.

- Milli-Q water (MQ) is the water prepared by a purification system. It has been used to dilute samples and prepare the solution. The purification processes involve successive steps of filtration and deionization to achieve a purity expediently characterised in terms of resistivity. The *ultrapure* water is of "Type 1", which is the grade required for critical laboratory applications such as HPLC mobile phase preparation, blanks and sample dilution in GC, HPLC, AA, ICP-MS and other advanced analytical techniques. The resistivity is $18.2\text{ M}\Omega\text{cm}$ at $20\text{ }^\circ\text{C}$ and the TOC is 0.04;
- Salicylic acid provided by VWR, 100% pure, CAS 69-72-7, molar mass of 138,12 g/mol ;

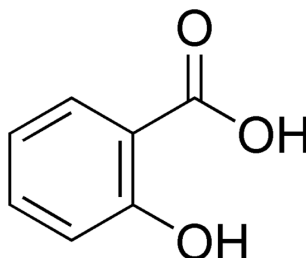


Figure 4.1: Structural formula of salicylic acid [6]

- Sodium chloride (NaCl) by SDS, CAS 764714-5, molar mass of 58.44 *g/mol*;
- Sodium sulfate (Na_2SO_4) by EMSURE, CAS 7757-82-6, molar mass of 142.04 *g/mol* (anhydrous);
- Potassium Indigo trisulfonate by Sigma-Aldrich, CAS 67627-18-3, molar mass of 616.72 *g/mol*;

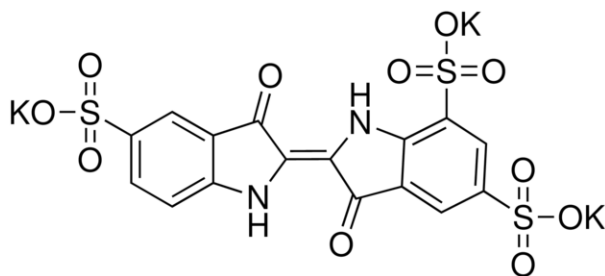


Figure 4.2: Structural formula of potassium Indigo trisulfonate [7]

- Chloride acid (HCl): a solution of 1 M as acidifier;
- Sodium hydroxide (NaOH): a solution of 2 M as basifier;
- Dihydrogen phosphate ($H_2PO_4^-$): concentrate as acidifier.

4.2 DiaClean Lab Unit

The WaterDiam Sarl developed a compact lab unit that aims to the generation of oxidants for disinfection, with a particular application for swimming pool and legionella inactivation and even for the destruction of organics for wastewater treatments.

The setup in Figure (4.3) is depicted in the scheme (4.4). The initial solution volume is inside the tank, where a cooling system with a double cooling loop maintains the temperature constant during the experiment. When the setup is in operation, the solution goes into the pump and then through the filter and then into the cell where two BDD electrodes on a silicon support are inserted. A flowmeter detector allows to check and modulate the transient flow.

In the following list, the different compartments of the setup and their specific characteristics are briefly described.

- **Tank:** it can store a volume up to 20 liters and it is made of polypropilene (PP), which is an inert material to avoid the contamination of the solution. This is where the initial solution is inserted and where the pH and the temperature are measured. From the tank, the solution goes into the pump through an opening valve and through another pipe the investigated solution flows back into the same tank.
Moreover when the experiment is finished and the setup needs to be cleaned, another opening valve is located at the bottom of the tank, that permits to empty it. At the top of the tank there is a hole for the evacuation of the gases produced during electrolysis.

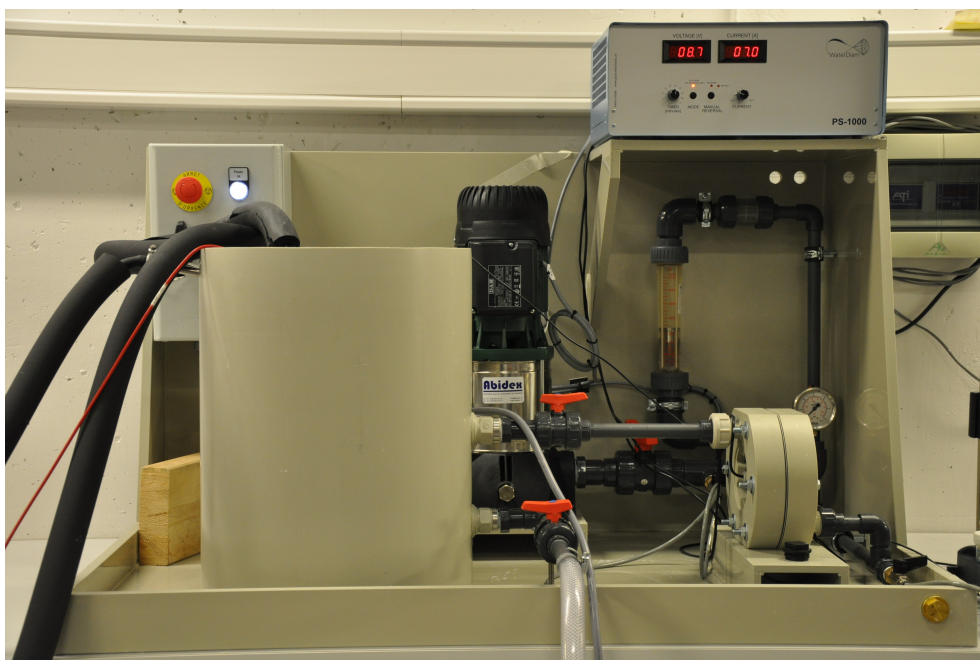


Figure 4.3: DiaClean Lab unit

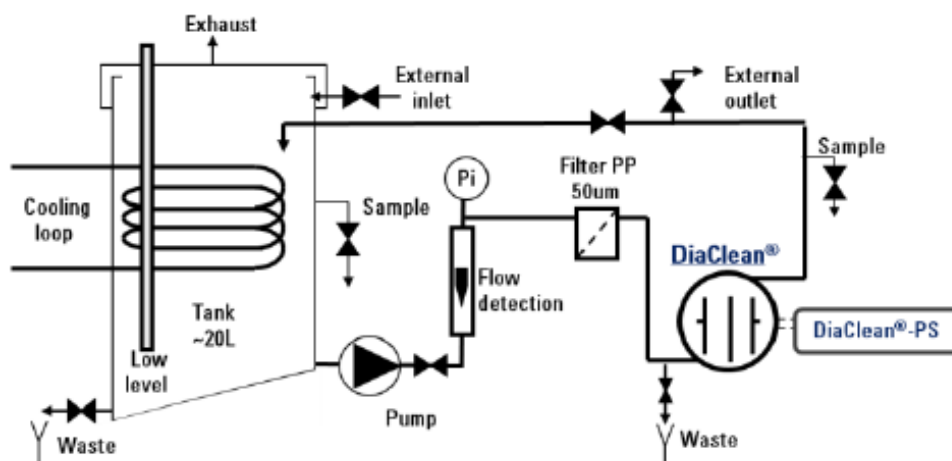


Figure 4.4: Flux scheme of the compartment of DiaClean Lab unit [3]

- **Refrigerator and heating circulator Julabo FP 50:** with the aim of maintaining the temperature constant during the experiment, it is necessary to use a refrigerator control device. The instrument uses an external pump to recirculate oil (8940114 H10) at low temperature into a system of a double cooling loop, lying inside the tank. There is an external sensor which measures the temperature inside the tank and in function of the variability of it, the main device changes the temperature of the oil bath, maintaining the fluctuations into the tank below a certain limit.

The refrigerator can reach the temperature of $-94\text{ }^{\circ}\text{C}$.

To insulate the system from the laboratory environment and to accelerate the cooling, a stable temperature a cover in neoprene is installed around the tubes. Different parameters can be changed to improve the efficiency of the cooling sys-

tem. The set values are reported below in the bracket.

- XP_{ext} range: $0,1\div 99,9$ (0,3) is the range below the setpoint, in which the control circuit reduces the heating capacity from 100 % to 0 in an energy safe mode.
- Tn_{ext} range: $3\div 9999$ (1350) is the reset time necessary at the system for a proportional regulation. If it is too low it may cause instabilities, otherwise if it is excessive, it may cause an unnecessary prolongation of the compensation.
- Tv_{ext} range: $0\div 999$ (3) is the differential component, that reduces the transient time. An insufficient value may cause a high overshooting during the running up and an excessive value may cause instabilities and oscillations.
- XPU range: $0,1\div 99,9$ (0,6) is necessary only for external control and it is paragonable to XP_{ext} .
- pump level (4) is the speed of the pump.

Even with this improvement, the pump as well as the electrolytic cell heats the solution into the system relatively fast and the control temperature device is not that effective to reach and maintain temperature lower than $12^{\circ}C$. For this reason the experiments have been carried out in a range of $13-27^{\circ}C$.

In Fig. (4.5) and (4.6) the details of the double cooling loop are reported together with the remote control of the refrigerator respectively.



Figure 4.5: Detail of the double loop inside the tank

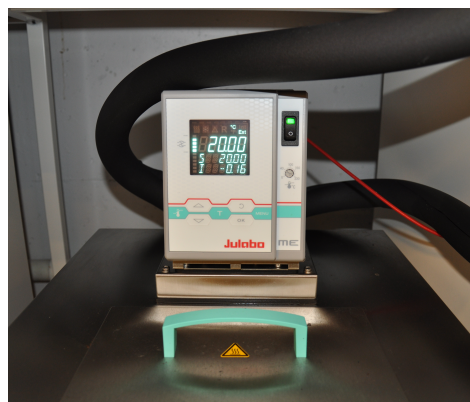


Figure 4.6: Detail of the remote control of the refrigerator Julabo FP 50

- **Pump:** it is made of inert materials. It is connected to the low contact switch (Li_{SL}), in function of stopping the system if the flow is below a certain limit. The pump is provided by DAB and it can work in the range $0.6-4.8 m^3/h$. For the specifics, the technical scheme is reported in Figure (4.7).
- **Flowmeter:** it is a transparent plexiglass cylinder where a metallic cone moves up and down in function of the transient discharge of the system. It can be adjusted by turning a valve in the range between 100 and $1000 L/h$. The security system to stop the running of the pump is a magnetic plate and it can be set in



Figure 4.7: Characteristics of the pump DAB KVC 20/50 M



Figure 4.8: Details of the flowmeter

a low position of the cylinder, corresponding to the minimum discharge. When the metallic cone reaches at the same level of the magnetic plate, the system is running with a low level of water in the tank and this may cause the backwash of air bubbles in the pump and damage it.

The cone indicates the transient discharge value, when the base matches with the level. As it can be seen in the Figure (4.8), the flowmeter shows 300 L/h .

- **Filter:** it avoids the entrance of particles or solid elements in the electrodes cell, the most delicated compartment of the system. The filter stoppes particles with a width more than 50 μm .

Considering the experiments carried out, the presence of the filter is not mandatory because the model compound is in the solution and there is no production of sludge or precipitate. From the other hand, it is an important instrument for the application of the real landfill leachate.

- **Sampling valves:** there are two different sampling valves. One is before the filter and the other is after it. As already mentioned, the system is completed mixed and there are no particles, which can be stopped by the filter, so there should not be differences between both samples taken from the sampling valves. Furthermore the system is running in a continous mode, hence the concentration should be the same in every compartment of the setup. The procedure used during the experiments, is to use the valve before the filter.

- **Power supply DiaClean PS-1000:** it is a power supply at low voltage, current tunable and polarity reversal function with tunable frequencies. The range of possible applied current is between 0.6 up to 20 A.

It is possible to use the polarity reversal function and switch the anode and cathode inside the cell according to a fixed time, that can be between 5 minutes up to 70 minutes. It is even possible to use the device without the reversal function in a manual mode. Reversing the polarity is important to protect the electrolytic cell and let the electrodes last longer.

By the power supply, applied current and relative voltage can be measured instantaneously.



Figure 4.9: Detail of the power supply DiaClean PS-1000

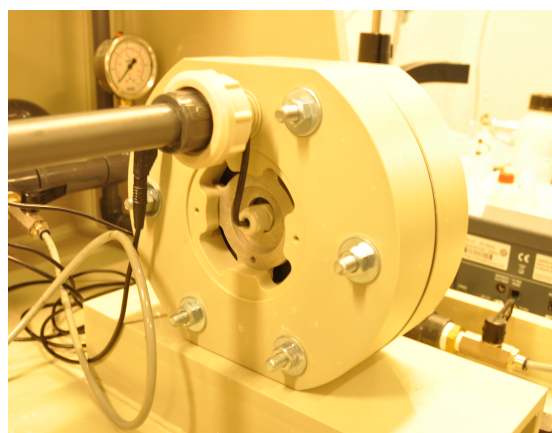


Figure 4.10: Detail of the electrolytic cell DiaClean

Parameter	Value	Unit
Thickness	2	mm
Resistivity	100	$m\Omega cm$
Film thickness	2÷3	μm
Boron concentration	500-1000	ppm

Table 4.1: Characteristics of BDD/Si electrodes

- **Electrodes cell DiaClean:** it is an electrolytic cell with a single compartment. It contains two circular BDD electrodes on a silicon support; their surface is 70 cm^2 . The BDD electrodes on silicon substrate are produced by NeoCoat SA based in La Chaux-de-Fonds, that optimize the properties of the electrodes in accordance to the geometry of the DiaClean. The characteristics of the electrodes are those reported in Table (4.1).

The gap between the electrodes is 1 mm and the current applied to both of the electrodes, permits to define an anode and a cathode, that are interchangeable, in function of the reversal role.

DiaClean enables oxidant production by direct electrolysis for diverse water treatment applications. The separating electrodes are floating bipolar diamond electrodes (patented concept).

In conclusion, it can be summarized the usual procedure during the laboratory experience with the flow chart of Figure (4.4) and the following short explanation.

The balance Sartorius Analytic A200S in Figure (4.11) has been used to weigh 3 grams of salicylic acid. The balance has a sensitivity of $\pm 0,0001\text{ g}$. The amount of acid is added into a flask and mixed in 2 liters of distilled water. To help the mixing of the solution, it is advisable to shake strongly and warm the flask, because, as already said, the solubility of salicylic acid in water increases with the temperature.

Once the solution of salicylic acid is at room temperature, the flask is filled up to the level of 2 liters with a disposal glass pasteur pipette and added to the tank in the

system. Afterwards the support electrolyte is added and the tank is filled up to 10 liters with distilled water.



Figure 4.11: Balance Sartorius Analytic A200S

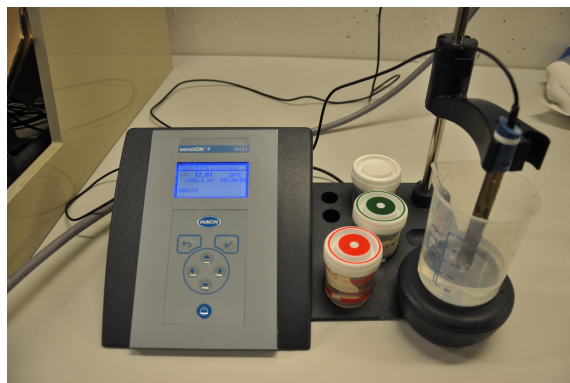


Figure 4.12: HACH sensION+ PH31 pHmeter



Figure 4.13: ODEON Classic conductimeter

The final solution is stirred before with a spoon for a raw mixing and consequently the system is switched on, let the pump helping it. In the meanwhile the temperature control system is set at the fixed temperature and it starts to cool down the oil bath as well as the cooling loop, modifying the entire solution temperature. It takes approximately one hour to reach the desired temperature.

Before applying the current, the pH is adjusted with a base (NaOH) or an acid (HCl) in function of the required pH. When the solution is at a stable temperature as well as stable pH, the DiaClean power supply is turned on and set on the fixed current. The chosen mode of the power supply is the automatic one and the reversal time is set on 30 minutes.

The first sample is taken directly before the application of the current and the conductivity, the absorbance with the UV/VIS spectrophotometer and TOC are analysed.

Parameter	Value	Unit
Flow	300	L/h
Volume	10	L
Salicylic acid concentration	300	mg/L
Electrode gap	1	mm
Reversal mode	30	min

Table 4.2: Constant parameters of the experiments

Prior the TOC analyses, the samples have been acidified with phosphoric acid and stored in a refrigerator.

For all the further samples, conductivity and absorbance measurements have been collected, instead every 60 minutes another sample is stored for the TOC analysis.

Some parameters have been set and maintained constant for each experiment. The other parameters instead will be specified for every experiment.

4.3 UV/VIS spectrophotometer PerkinElmer LAMBDA 650

Ultraviolet-visible spectrophotometry refers to absorption or reflectance spectroscopy in the ultraviolet-visible spectral region. It uses light in the visible range or adjacent as near-UV and near-infrared.

The UV/VIS spectrophotometer measures the intensity of the light passing through a sample. The intensity of the direct light is I_0 and the intensity of the light passing through the sample is called I . The ratio I/I_0 is the transmittance (T) and it is usually expressed as a percentage.

The absorbance instead, is a function of the percentage transmittance, that follows the Equation (4.1).

$$A = -\log\left(\frac{\%T}{100\%}\right) \tag{4.1}$$

In the scheme of Figure (4.14) it is depicted the function of the instruments inside the UV/VIS spectrophotometer. The basic parts are a light source, a holder for the sample cuvette, a prism to separate the different wavelengths of light and a detector. The radiation source is given by a tungsten lamp, which emits between 300 and 2500 nm and by a deuterium arc lamp, which emits instead in the ultraviolet region between 190 and 400 nm.

The detector is a photomultiplier tube, that is usually used with scanning monochromators. With these latter ones, the light is filtered and only a single wavelength can reach the detector. In this way, a single value of intensity is associate at a specific wavelength.

The spectrophotometer UV/VIS PerkinElmer LAMBDA 650 uses a single beam, in which all of the light passes through the same cell and the only possibility to measure the I_0 is by removing the sample, procedure mandatory before every round of experiments, through the button *Autozero*.

The absorbance spectrum has been taken from 220 nm up to 500 nm, that is a

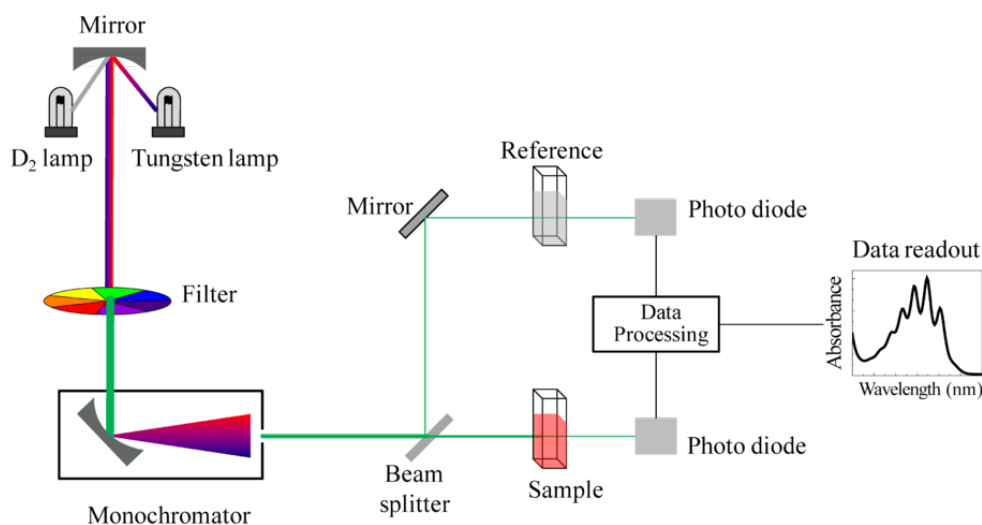


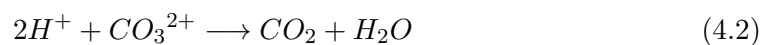
Figure 4.14: Scheme of the UV/VIS spectrophotometer [8]

wide range to contain all the oscillation of the salicylic acid samples.

4.4 Apollo 9000 Total Organic Carbon (TOC) Analyzer

The TOC analyzer measures the effective carbon inside every samples. It uses combustion at temperature in the range of 680-1000°C with a patented reusable platinum catalyst for the lowest detection limits.

In a combustion analyzer, the sample is splitted in two. Half of it is injected into a chamber where it is acidified with phosphoric acid, to turn all of the inorganic carbon into carbon dioxide as per the following reaction (4.2):



The other half of the sample is injected into a combustion chamber, where all the carbon, organic and inorganic, reacts with oxygen, forming carbon dioxide. Afterwards it's sent into a cooling chamber and finally both of the sample are put into the detector for measurement. The amount of organic carbon is determined by subtracting the total inorganic carbon to the total carbon content.

The detector is a Non-Dispersive Infra-Red (NDIR), which is sensitive for very low levels of TOC. Each sample is diluted 100 times and measured together with two standards s1 and s2, that correspond to the minimum level of the TOC expected into the sample and the maximum.

The sample has been taken every hour, acidified with the dihydrogen phosphate ion ($H_2PO_4^-$) and stored in a refrigerator. For each experiment there are a number of 6 samples for the TOC analyze.

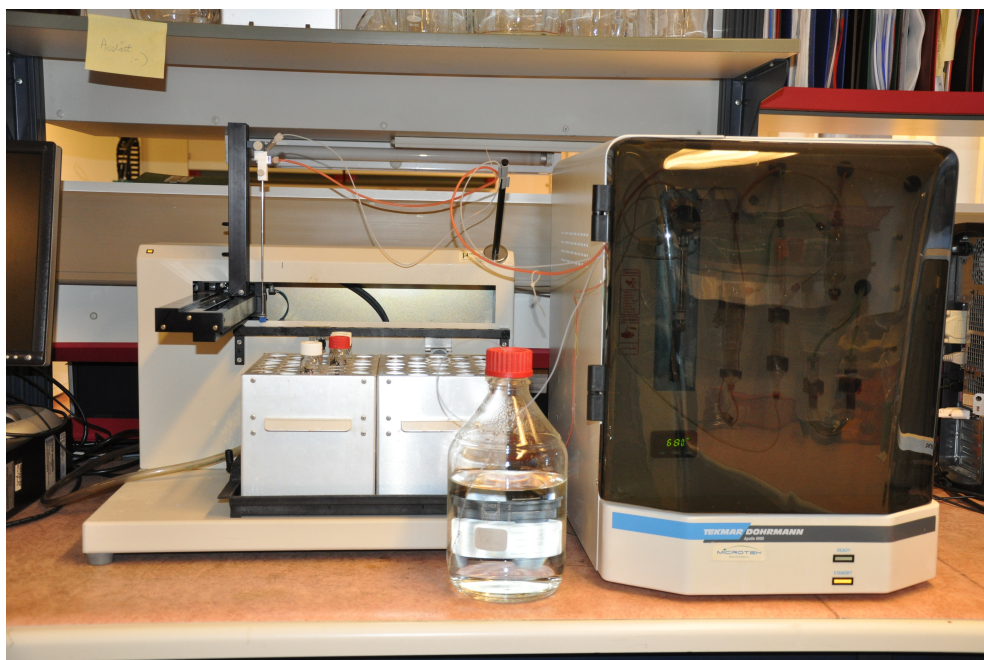


Figure 4.15: Apollo 9000 Total Organic Carbon (TOC) Analyzer™ Tekmar

4.5 Experiment with potassium indigo trisulfonate dye

As first trial, the setup has been tested with potassium Indigo trisulfonate, a dye supplied by SIGMA-ALDRICH. This experiment has been carried out mainly to have a visible evidence of the potential of the setup. Beside the color removal, the absorbance has been measured.

The potassium indigo trisulfonate has been chosen for two different reasons: its colored characteristic and also its organic nature. Because of this last property, it is possible to compare the kinetic of the indigo degradation with the one of salicylic acid.

The volume of the solution inside the system is 10 liters and the added mass of dye is 0,4626 g. The concentration of indigo into the water is not relevant, because the main goal is to see a gradual disappearance of the color. The initial concentration gives a strong and omogeneous coloration into the tank, as supporting electrolyte, 18 g of NaCl were added. The temperature during the experiment was around 24°C.

In 45 minutes the blue color was removed and regarding the adsorbance, the results are shown in the Table (4.3). The blank sample is Milli-Q water.

For each experiment a blank sample at the beginning of the measurement and another one at the end was taken.

The results in Table (4.3) are an average of three measurement with a set wavelength at 298 nm. In the Figures (4.16), (4.17), (4.18) and (4.19) there are respectively the details of the samples and the inner part of the tank for the first and the last sample. The effectiveness of the system for removing the dye has been proved.

Time [min]	Absorbance
blank	0.0374
0	6.66
5	10
10	2.58
15	2.00
20	1.51
25	0.91
30	0.44
35	0.16
40	0.053
45	0.045
50	0.046
55	0.047
60	0.047
65	0.045
70	0.048
blank	0.0371

Table 4.3: Results of the experiment with potassium indigo trisulfonate at 298 nm

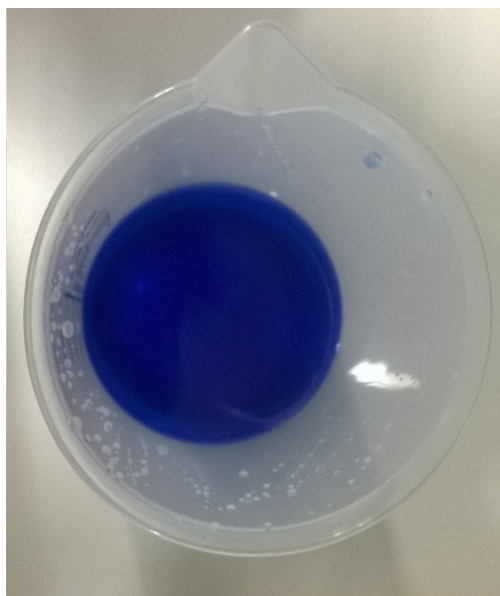


Figure 4.16: Sample of indigo solution at t=0



Figure 4.17: Detail of the indigo solution inside the tank at t=0



Figure 4.18: Sample of indigo solution at $t=70$ minutes



Figure 4.19: Detail of the indigo solution inside the tank at $t=70$ minutes

4.6 Calibration curve

In order to use the UV/VIS spectrophotometer for quantify the concentration inside the system, the calibration curve has to be determined.

The measured standards are 1 mg/L , 5 mg/L , 10 mg/L , 50 mg/L and 100 mg/L . Those standards are prepared by 1 liter of 500 mg/L of salicylic acid solution. From the stock solution, the dilutions used are prepared as shown in the Figure (4.20), where MQ is the Milli-Q water.

The calibration curve is shown in Figure (4.21). The standards absorbance fits perfectly with the linear equation, in fact the correlation factor R^2 is 1.

The inverse of the equation (4.3) allows to relate the real concentration into the sample from the measured absorbance at 298 nm .

The calculation of the concentration are reported in the final table for every experiment in the Appendix (6).

$$x = 40,486y - 1,798 \quad (4.3)$$

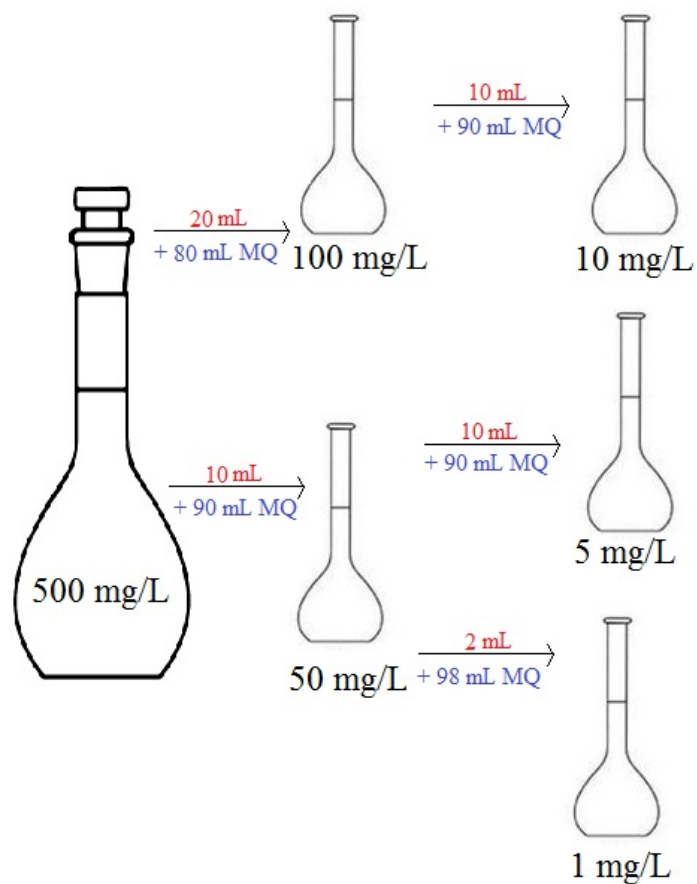


Figure 4.20: Dilution of the salicylic acid standards

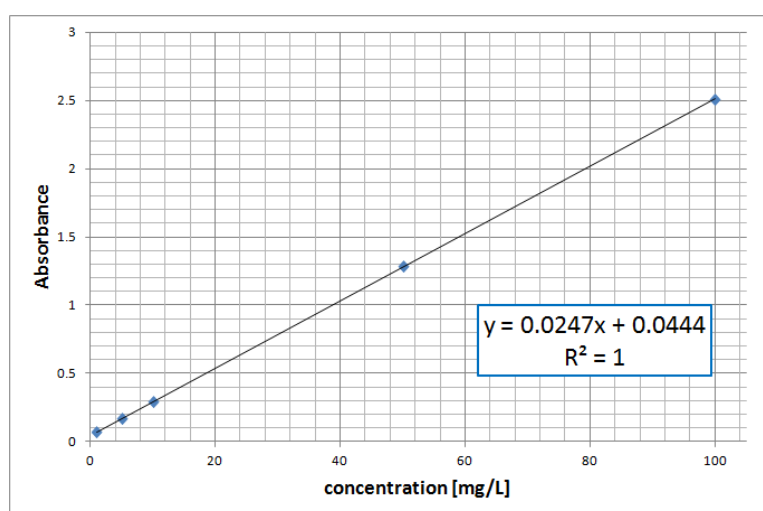


Figure 4.21: Calibration curve with standards of salicylic acid at 298 nm

Chapter 5

Results and discussion of the results

In this chapter, the results of the different experiments carried out in the laboratory of drinking water at NTNU (Department for Water and Environmental, S. P. Andersens veg 5, 7031 Trondheim, Norway) are reported.

For every single experiment, the sampling time (min), pH, temperature ($^{\circ}C$), conductivity ($\mu S/cm$), applied current (A), voltage (V), absorbance at 298 nm have been measured. The details of the experiments can be consulted in the Appendix (6).

5.1 Determination of the salicylic acid degradation kinetic

For each experiment the kinetic of salicylic acid degradation has been calculated. The kinetic order can be zero, first or second, depending if the extrapolated trend fits better with a linear, an exponential or a second order kinetic curve. As said in the theoretical chapter (3), the expectation of the decay is a first order kinetic (5.1), that means the trend of the experiments correspond to an exponential curve. The results prove a good fit with the first order kinetic for all the experiments. This is due to the applied current (7 A) that is above the limiting density current (0,62 A) for all the configuration analyzed.

For every time frame the k has been calculated and the final average has been used to plot the extrapolated curves. Furthermore the σ^2 has been found by the least squares method, that uses the technique of minimize the residual of the function. The residual is defined as Eq. (5.2), where $f(x_i)$ is the value of the fitting curve and y_i is the measured value. The least squares method is optimum when the sum is minimum (5.3).

$$\frac{1}{t_2 - t_1} \cdot \ln \left(\frac{c_1}{c_2} \right) = k \quad (\text{constant}) \quad (5.1)$$

$$r_i = y_i - f(x_i) \quad (5.2)$$

$$\sigma^2 = \sum_{i=1}^n r_i^2 \quad (5.3)$$

The related kinetic rate and σ^2 are reported in Table (5.1) and Table (5.2) in the respective following sections and also in the Appendix (6) with the partial calculation.

5.2 Calibration

The first part of the experiments, as already said, is the calibration of the system. The setup is a new instrument that needs a certain number of experiments for working in a proper way. It is important to identify its peculiarity and the aspects needing attention during the preparation and the running of every single experiment.

Many parameters have to be set before testing the influence of temperature and pH, like the initial concentration of salicylic acid in the system, the volume treated, the flow velocity passing through the cell, the applied current, the electrolyte nature and its molarity.

After several experiments some of the basic conditions have been set. It has been chosen 10 liters of a solution of salicylic acid at 300 mg/L in the system, processed at 300 L/h.

In particular, the range of the initial concentration and the discharge are parameters suggested by the setup provider to have a good working conditions for the system.

In the Table (5.1) a summary of the kinetic calculation for the different experiments are presented. For the detailed sheets, see Appendix (6).

electrolyte	molarity [M]	current [A]	equation	R^2	k [min^{-1}]	σ^2
NaCl	0,05	7	$e^{-0.00479}$	0.99117	0.005068	0.0000258
NaCl	0,05	7 (no rev.)	$e^{-0.00585}$	0.99107	0.005964	0.0000295
NaSO ₄	0,05	7	$e^{-0.00181}$	0.98854	0.001902	0.0000263
NaSO ₄	0,05	7 (no rev.)	$e^{-0.00191}$	0.99686	0.001877	0.0000049
NaCl	0,1	7	$e^{-0.00795}$	0.99405	0.007687	0.0000679
NaSO ₄	0,1	7	$e^{-0.00196}$	0.98610	0.001773	0.0000511
NaSO ₄	0,05	1	$e^{-0.00130}$	0.98593	0.001411	0.0000185
NaSO ₄	0,05	3,5	$e^{-0.00169}$	0.99748	0.001710	0.0000135

Table 5.1: Summary of the kinetics for calibration experiments

The first parameter investigated and evaluated is the influence of the electrolyte: NaCl and NaSO₄.

In an electrochemical oxidation process, an important rule is given by the electrolyte nature. The electrolyte enhances the movement of the charged ions in the system and promotes the indirect oxidation by mediators.

It has been added to the system, 0.05 M of sodium sulphate or sodium chloride. The results of the experiments are shown in Figure (5.1) with a graph of the results of the UV/VIS spectrophotometer measured at a wavelength of 298 nm and in Figure (5.2) with an extrapolation curve of the exponential decay of the salicylic acid degradation, calculated by k. The tests are carried out with 7 A as applied current and 20°C.

It is easily concluded that the NaCl as support electrolyte is more effective than

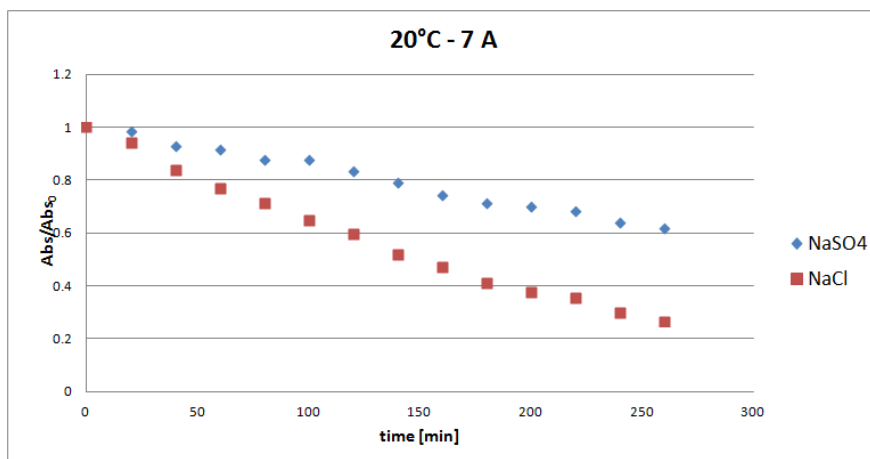


Figure 5.1: Evaluation of the electrolyte influence with experimental results of absorbance at 298 nm - $NaSO_4$ and $NaCl$

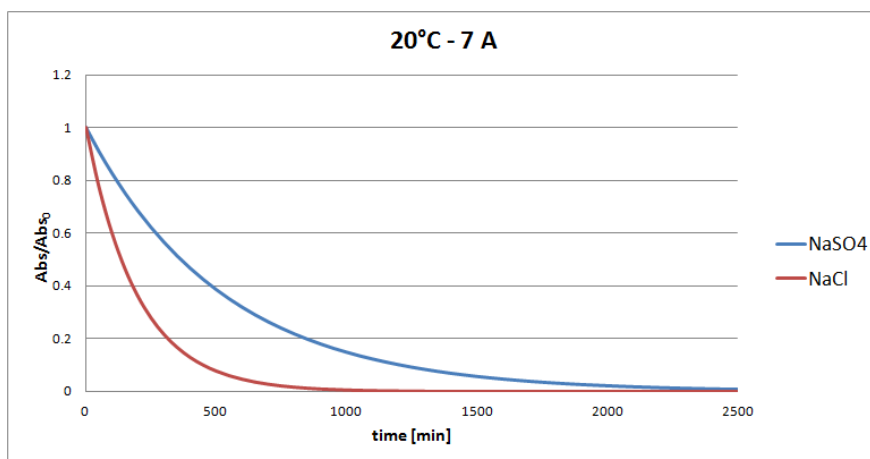


Figure 5.2: Evaluation of the electrolyte influence with trend extrapolation - $NaSO_4$ and $NaCl$

the $NaSO_4$. The kinetic values, that are the exponential coefficient, are respectively -0.005 and -0.002 . This means the solution with $NaCl$ reaches the complete mineralization after 1000 minutes, against the 2400 minutes, necessary time for the one with sodium sulphate.

From the results in Figure (5.3) it can be noted a slight oscillative behavior in the decay. This can be due to the mechanism of the degradation of the organic compound or to the influence of the switching in application of the current from one electrode to the other one. Aiming to check if this second hypothesis is the real cause of the oscillations, the same experiment has been carried out without the reversal of the applied current. As reported in the Appendix (6) and also explained in the chapter (4), the applied current changes its value switching between $+7$ A to $-6,4$ A every 30 minutes, the reversal mode is chosen to protect of the electrodes and to use both of them with the same frequency.

The next round of experiments compare the reversal mode to the ones with a fix cur-

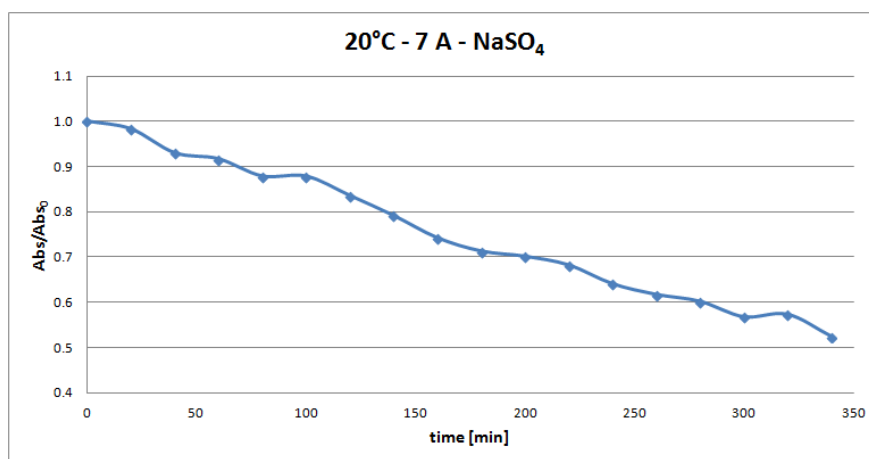


Figure 5.3: Detail of the oscillative behavior in the experiment with $NaSO_4$

rent, set at 7 A. The manual mode is used to avoid the switching of the electrodes. The results shown in Figure (5.4) and (5.5) demonstrate that the change of the current inside the system is not the cause of the oscillative behavior because this behavior is visible for both of them and the final trend of the experiments is not widely influenced. For the experiments with sodium chloride as support electrolyte, a small difference can be noticed, probably due to the application of a continuous current (7 A) that is higher for the whole time, compared to the one that switches between 7 and -6.4 A. With an effective higher current, the removal rate is enhanced. Instead for the experiments with $NaSO_4$, no differences can be mentioned.

It could be argued that the oscillative behavior is provoked by the creation of some intermediates during the mineralization that are more or less degradable and they produce a different peak in the absorbant spectrum. To verify this assumption, another technique should be involved, like for example the HPLC. This is also a natural further step for better understanding the oxidation mechanism.

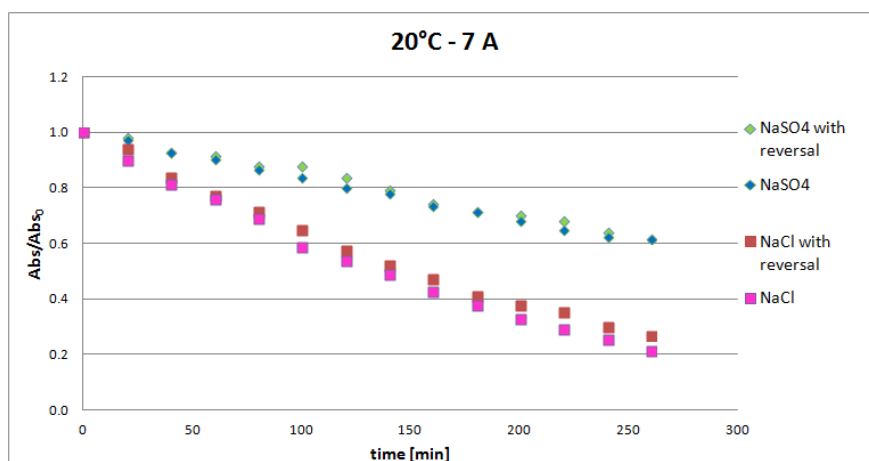


Figure 5.4: Evaluation of the influence of the reversal of the current with experimental results of absorbance at 298 nm - $NaSO_4$ and $NaCl$

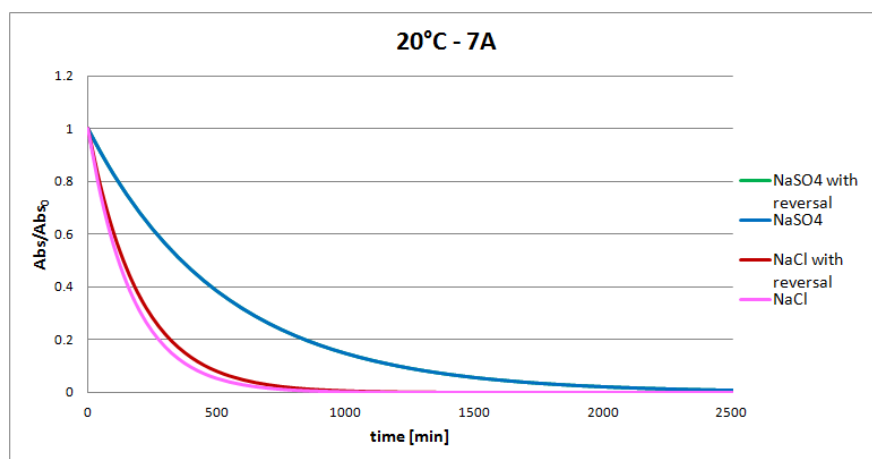


Figure 5.5: Evaluation of the influence of the reversal of the current with trend extrapolation - $NaSO_4$ and $NaCl$

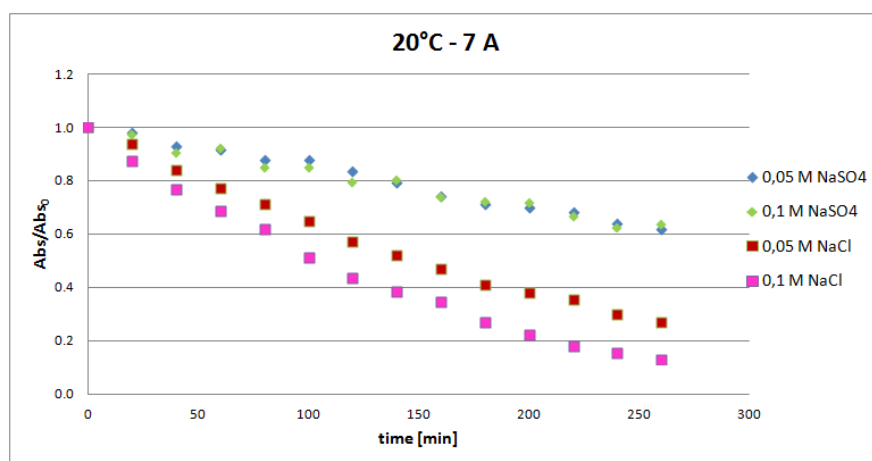


Figure 5.6: Evaluation of the influence of the electrolyte molarity with experimental results of absorbance at 298 nm - $NaSO_4$ and $NaCl$

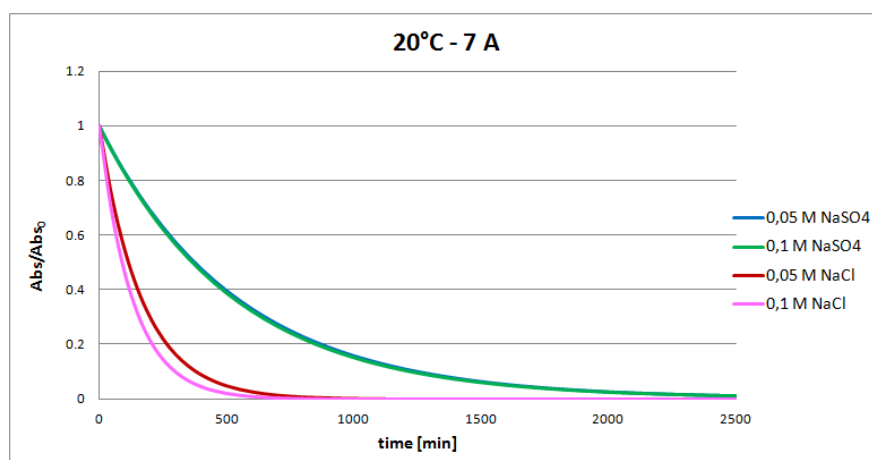


Figure 5.7: Evaluation of the influence of the electrolyte molarity with trend extrapolation - $NaSO_4$ and $NaCl$

Once it had been figure out that the reversal mode of the system does not influence the behavior of the decay, the further parameter to evaluate is the concentration of the electrolyte. It has been tested a molarity of 0.05 M and 0.1 M for sodium chloride as well as for sodium sulphate.

The results plotted in Figure (5.6) and (5.7), show the influence of the concentration of the salt. In particular it can be noticed that the difference in the model, obtained by the kinetic, is wider for results of the experiments with the sodium chloride than for the others with $NaSO_4$. The results of the kinetic coefficients are between -0.0051 and -0.0077 for $NaCl$ and from -0.0019 to -0.0018 for $NaSO_4$ (see Table 5.1). In the case of sodium sulphate, the kinetic value for the higher molarity is even smaller than the one at 0,05 M, but it can be considered of the same order.

In the end, the influence of the concentration of the electrolyte is well demonstrated for the experiments with $NaCl$ but it is not obvious for the ones with $NaSO_4$.

Despite of the experiments with sodium chloride as support electrolyte are promising, the electrolyte chosen for the following experiments has been the $NaSO_4$ for safety reasons. During the experiments using NaCl, chlorine gas was formed and could be smelled in the whole laboratory which represented a health issue. Due to the gas nature, these substances are difficult to hold inside the system without a proper insulation. In the future developments of the system, the setup can be modify and improved to make it completely insulated, also in a perspective way for the treatment of the real leachate. By the way for the present project, the chosen electrolyte is the $NaSO_4$.

Another important parameter to set is the applied current during the oxidation. The limiting current density calculated in the theoretical part is $8,8mA/cm^2$ (chapter 3), that corresponds to 0,62 A for 70 cm^2 . Currents with higher intensity had been tested with the aim of finding an exponential trend because the value is above the limit. The experiments in Figure (5.8) and Figure (5.9) have been carried out at $20^\circ C$, 0,05 M $NaSO_4$ and with an applied current of 1 A, 3,5 A and 7 A.

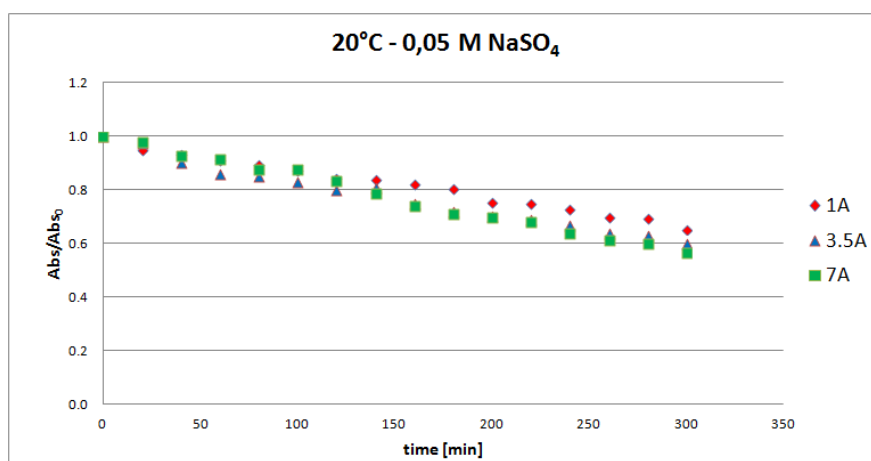


Figure 5.8: Evaluation of the influence of the current applied with experimental results of absorbance at 298 nm - $NaSO_4$ and $NaCl$

The results show a proportional increment of the degradation rate with the increment

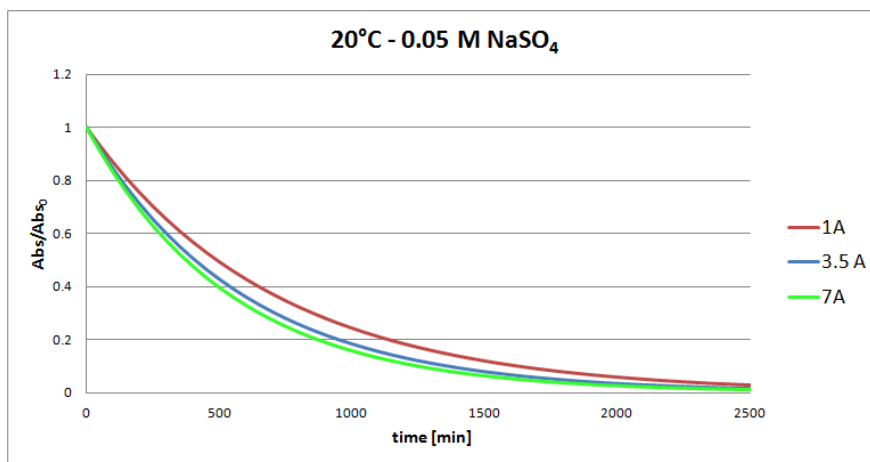


Figure 5.9: Evaluation of the influence of the current applied with trend extrapolation - $NaSO_4$ and $NaCl$

of the applied current and the most effective experiment is the one carried out at 7 A. It can be argued the kinetic rate is improved, when the applied current passes from 1 A to 3,5 A and up to 7 A. The current chosen for the following experiments is 7 A.

5.3 Evaluation of the pH and temperature variation

The second part of the experimental work is the comparison of the different decay for pH 3, 7 and 12 and in parallel at the temperature of 13, 20 and 27 °C.

As mentioned in the previous section, two type of graphs corresponding to different data, are reported. The graph described by points indicators is derivated by the values of the absorbance at the peak, instead the one with a continuous line is obtained by the model that uses the kinetic coefficient. Furthermore, the TOC analysis has been collected and reported as well as the complete absorbance spectrum has been reported in Appendix (6).

pH	T [°]	equation	R^2	k [min^{-1}]	σ^2
3	13	$1e^{-0.00158}$	0.99537	0.00161	0.00048
3	20	$1e^{-0.00179}$	0.99357	0.00178	0.00080
3	27	$1e^{-0.00218}$	0.99735	0.00218	0.00045
7	13	$1e^{-0.00140}$	0.99109	0.00133	0.00082
7	20	$1e^{-0.00196}$	0.99161	0.00204	0.00089
7	27	$1e^{-0.00245}$	0.99126	0.00250	0.00059
12	13	$1e^{-0.00186}$	0.99207	0.00182	0.00062
12	20	$1e^{-0.00224}$	0.99630	0.00222	0.00050
12	27	$1e^{-0.00295}$	0.99757	0.00297	0.00030

Table 5.2: Summary of the kinetics for pH and temperature experiments

In the Table (5.2) the extrapolate exponential equation and the relative correlation

04.02.2016 Dilution 1:3
 300 mg/L
 0.05 M
 10 L

Day
 Concentration of salicylic acid
 Concentration of NaSO₄

time	T (°C)	pH	Absorbance	conductivity (µS/cm)	current (A)	voltage (V)	time (min)	Abs/abs_0	$k=1/\Delta t \ln(c_1/c_2)$	$\sigma^2=\sum(k-k_m)^2$	concentration (mg/L)
11.20	27.34	11.88	7.3523	10.79	7.00	9.40	0	1	-	-	x=40.48y-1.797
11.40	26.85	11.85	6.8690	11.16	7.00	8.50	20	0.9343	0.003400	1.8296E-07	295.8644
12.00	27.03	11.82	6.4725	11.19	-6.40	-7.70	40	0.8803	0.002972	1.7856E-13	276.2976
12.20	26.88	11.78	6.0407	11.24	7.00	8.80	60	0.8216	0.003453	2.309E-07	260.2470
12.40	27.04	11.80	5.6156	11.71	7.00	8.50	80	0.7638	0.003649	4.5777E-07	242.7632
13.00	27.10	11.74	5.2623	11.68	-6.40	-7.70	100	0.7157	0.003249	7.6479E-08	225.5526
13.20	26.98	11.85	4.9376	12.63	7.00	8.90	120	0.6716	0.003185	4.5338E-08	211.2510
13.40	26.94	11.86	4.6730	12.70	7.00	8.50	140	0.6356	0.002754	4.7561E-08	198.1032
14.00	27.25	11.85	4.4475	12.56	-6.40	-7.70	160	0.6049	0.002472	2.496E-07	187.3907
14.20	26.87	11.84	4.1967	12.25	7.00	8.80	180	0.5708	0.002902	4.8772E-09	178.2632
14.40	27.04	11.87	3.9498	13.07	7.00	8.50	200	0.5372	0.003032	3.5592E-09	168.1093
15.00	27.01	11.81	3.7317	13.32	-6.40	-7.70	220	0.5076	0.002840	1.7415E-08	158.1134
15.20	26.94	11.80	3.5559	13.46	7.00	8.80	240	0.4836	0.002413	3.1274E-07	149.2834
15.40	27.02	11.86	3.3848	13.32	7.00	8.50	260	0.4604	0.002466	2.5564E-07	142.1660
16.00	27.06	11.81	3.1824	13.26	-6.40	-7.70	280	0.4328	0.003082	1.2145E-08	135.2368
16.20	26.97	11.84	3.0144	13.17	7.00	8.80	300	0.4100	0.002712	6.7744E-08	127.0445
Average									0.002972	Sum	120.2429
									0.002972	1.9647E-06	

 Figure 5.10: Experimental details of the experiment carried out the 4th February 2016

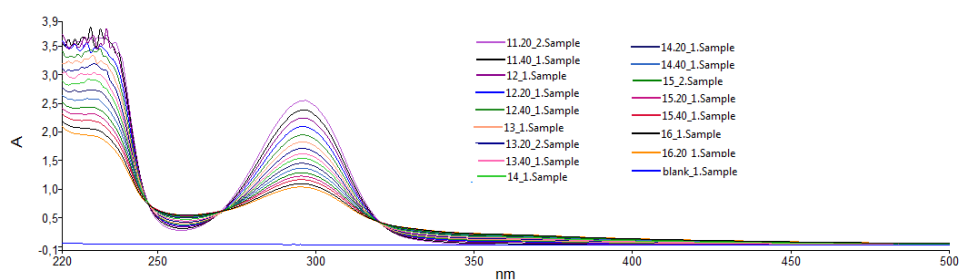


Figure 5.11: Absorbance spectrum for pH 12 at 27°C

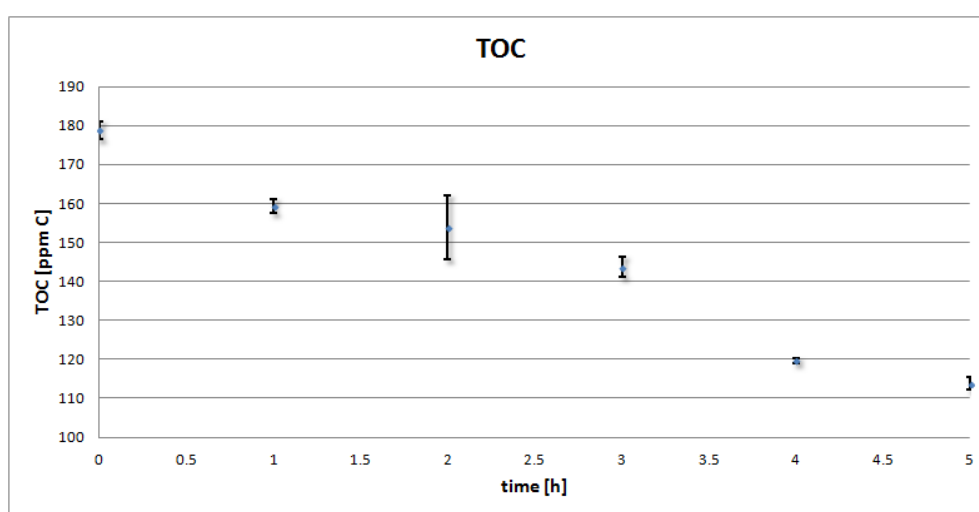


Figure 5.12: Total organic carbon for pH 12 at 27°C

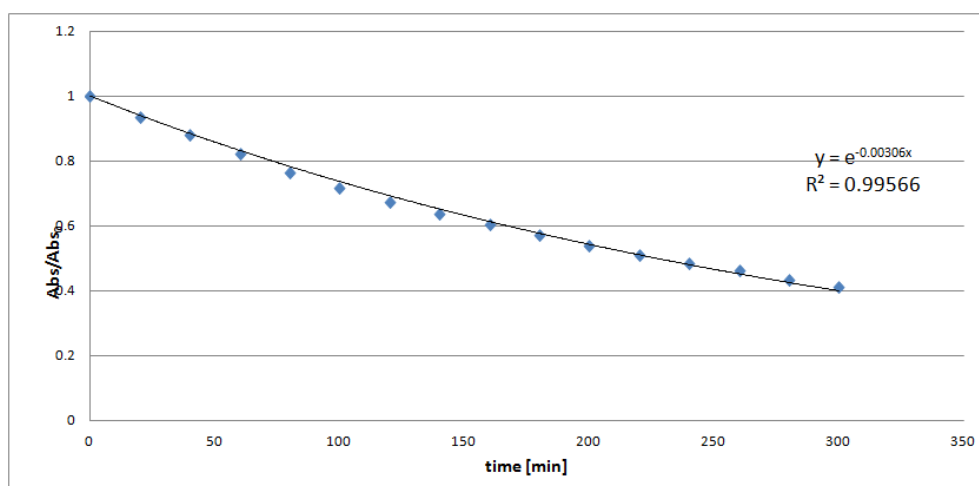


Figure 5.13: Absorbance at wavelength of 298 nm for pH 12 at 27°C

coefficient are reported, the kinetic rate are calculated by the Eq. (5.1) and the σ^2 calculated with the least square method expressed in Eq. (5.2).

It is shown an example of the data collected for every single experiment. First of all, there is a complete table with sampling time, pH, temperature, absorbance at 298 nm, applied current, voltage, calculated kinetic, σ^2 and concentration, derivated by the calibration curve of (5.10). Moreover it is plotted the absorbance spectrum with wavelength in the range 220-500 nm for all the sample time (5.11), the total organic carbon measurement with the relative depicted deviation standards (5.12) and absorbance decay of the peak at 298 nm (5.13).

The complete results for the experiments are reported in Appendix (6).

The absorbance decay is a good index of the degradation of the organic compounds by oxidizing agents, but this does not inform about the mineralization of the organic compounds. Therefore the analyze of the total organic carbon is necessary. The documented decay of TOC analysis is a sure evidence that the oxidation is going on inside the system and the carbon becomes CO_2 . Without the TOC results, it can be argued that the decay of the peak at 298 nm is an index of the generation of new intermediates that absorbe at different wavelengths, but there is no proof of the mineralization process. Introducing the TOC analysis, it can be demonstrated the process leads to the mineralization.

To compare the different experiments, the histograms (5.14) and (5.15) are presented. The values on the columns are the coefficients of the extrapolated curve from the kinetic. It can be observed that the tendency is having a higher degradation rate when one of the two parameters, temperature or pH, is higher.

In particular, the Figure (5.15) shows how the rate constant split in categories in function of the temperature are increasing. The 3 experiments at $27^\circ C$ have higher coefficients (or at least a similar value) than the 3 experiments at $20^\circ C$, that in turn have higher coefficients than the ones at $13^\circ C$. From these histograms, the biggest influence is due to the temperature and consequently the pH.

The experiment with the highest rate constant is the one carried out at pH 12 and $27^\circ C$, instead the one with the lowest rate constant is the one at pH 3 and $13^\circ C$. The influence of the temperature on the oxidative reactions is already described in literature and the experiments confirm the prediction of an increment of the efficiency with the temperature.

About the pH, there are different opinions in the literature. Some authors describe the pH as a parameter with a marginal influence on the system, in some other scientific papers the low pH favors the oxidation and others the high pH is preferable in function of the organic compound to degrate and even in function of the used electrolyte.

It is easily shown for the applied configuration, that the influence of the pH is clear and for a higher pH corresponds a higher kinetic coefficient.

During the sampling a different coloration of the samples has been noticed according with the pH of the experiment. For pH 3, the collected samples had no color, instead for the ones for the experiments carried out at 7 and 12, the tendency of the coloration

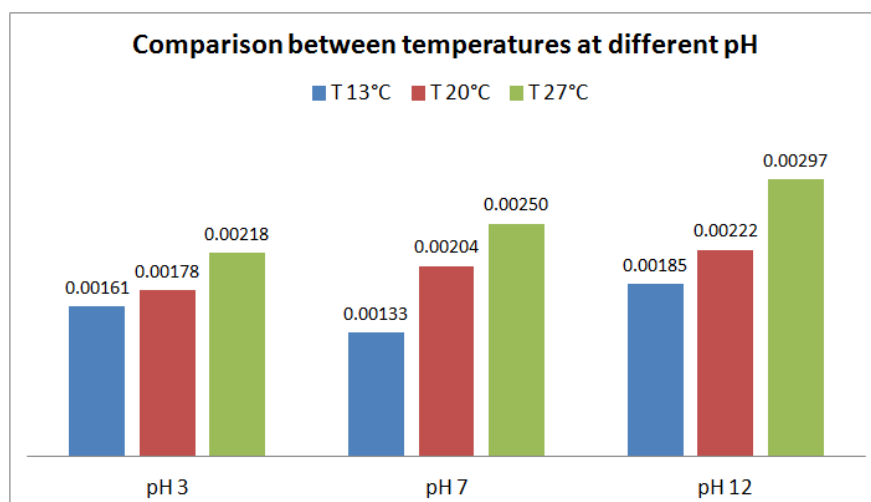


Figure 5.14: Comparison of degradation rate at different pHs at a given temperature with $NaSO_4$ as supporting electrolyte

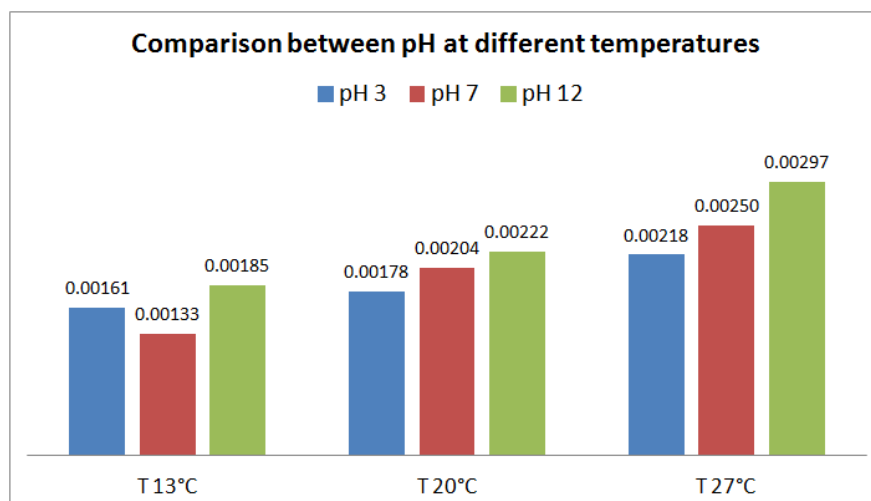


Figure 5.15: Comparison of degradation rate at different temperatures at a given pH with $NaSO_4$ as supporting electrolyte

is to become yellow with the running of time. In the Figure (5.16) an example of the change of samples colour in time for pH 12 is reported.

The natural colour of the sulfur is yellow and some reactions of the $NaSO_4$ at high pH can lead to the formation of derivates of sulfur with its typical coloration.

Despite a different trend in the comparison of the absorbance at 298 nm is visible, for the same experiment the TOC analyze does not show a difference in the oxidation. This means that for the experiments which have a faster decay of the peak of the absorbance spectrum, more intermediates are generated from the system but the mineralization is not enhanced. The salicylic acid is degraded by the radicals in a shorter time, but does not reach complete mineralization because the intermediates are still in the system. This hypothesis is confirmed by the gain of the absorbance at different wavelengths, in particular at 255 nm.

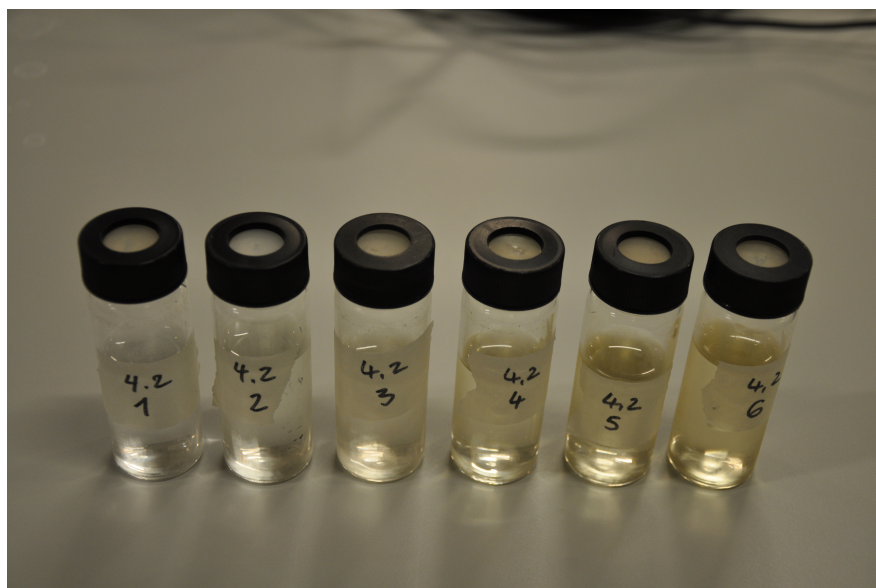


Figure 5.16: Details of the samples for TOC analyze of the experiment at 27°C and pH 12

Two opposite situations can be compared to underline the difference and make them

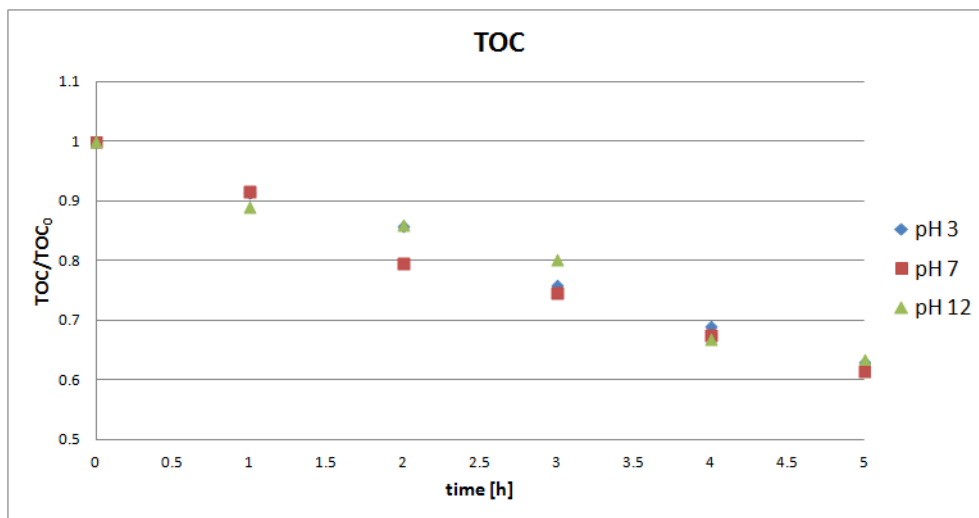


Figure 5.17: TOC measurements at 27°C for different pH

evident.

In the first Figure (5.19), the difference between the first and the last sampling is less wide for the peak at 298 nm, and it basically non existent for the 254 nm where the minimum of the spectrum is recorded. Instead for the second spectrum in Figure (5.20) the distance between the curves is wider in both of the cases and the consequent conclusion is that the investigated compound (salicylic acid) is degraded faster into its intermediates and derivates for the second configuration. These new compounds probably absorb at wavelenghts close to the visible light at 254 nm.

It is important to say that a parallelism between the increment of the minimum at

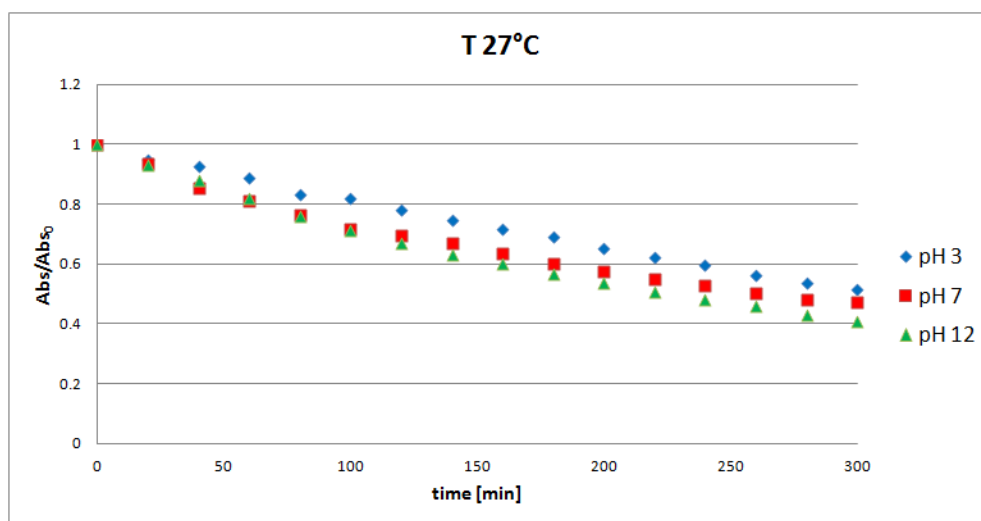


Figure 5.18: Absorbance values at 298 nm at 27°C for different pH

254 nm and the increment of the yellow color can be done. The color arises when a molecule absorbs certain wavelengths of visible light and transmits or reflects others, due to the chromophores, part of a molecule responsible for its color.

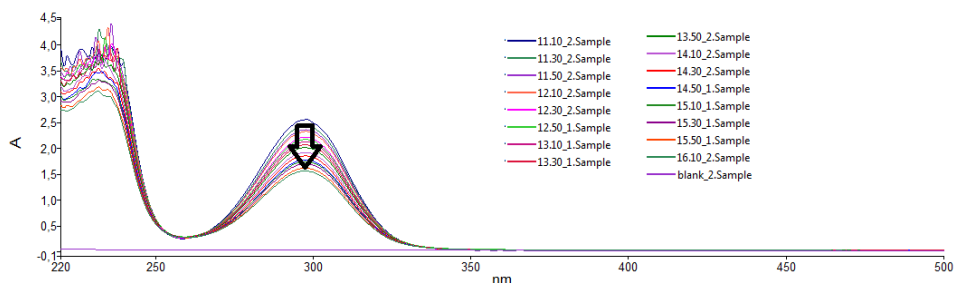


Figure 5.19: Absorbance spectrum for the experiment at 27°C and 3 pH

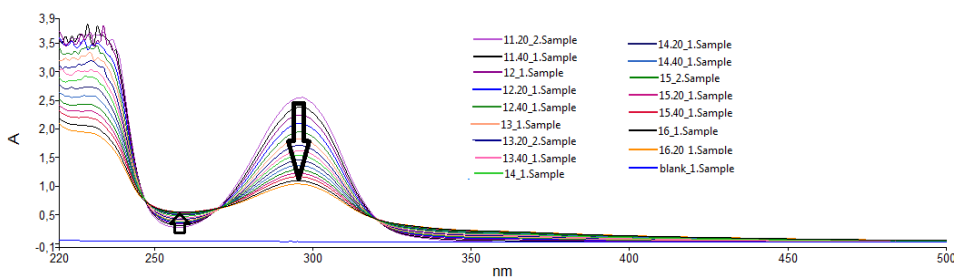


Figure 5.20: Absorbance spectrum for the experiment at 27°C and 12 pH

5.4 Instantaneous Current Efficiency (ICE)

The ICE is a parameter of efficiency and it is calculable by Eq. (5.4), that uses the COD as indicator.

$$ICE = \frac{(COD_t - COD_{t+\Delta t})}{8I\Delta t} FV \quad (5.4)$$

where:

COD_t	chemical oxygen demand for the instant t (mgO_2L^{-1});
$COD_{t+\Delta t}$	chemical oxygen demand for the instant $t + \Delta t$ (mgO_2L^{-1});
I	applied current (A);
F	Faraday's constant ($96487 C eq^{-1}$);
V	volume of the electrolyte (L).

A wide difference of ICE at certain times indicates that the anode material promotes the electro-oxidation and inhibits the side reaction of oxygen evolution. If the hydro-dynamic conditions are not favorable and the organic species are in a small amount in the solution, a slow decay of ICE curve can be obtained because not enough species reach the anodic surface. This is due to the mass transfer coefficient limitation, that is a critical parameter for the determination of the anodic activity, despite of the oxygen evolution reaction [48].

If the anode operates with an applied current higher than the limiting current, its instantaneous current efficiency is lower than its maximum value, this means $ICE_t < 1$. The experiments done are referable to this case.

The $ICE\%$ has been normalized with the maximum value referred to the experiment at pH 12 and temperature $27^\circ C$, in particular at the first sampling time.

The results are summarized in the Figure (5.21) and some aspects have to be commented.

The instantaneous current efficiency is progressively higher with the increment of the temperature. It can be argued that the temperature has an important influence in the efficiency of the electro-oxidation.

The initial trend (the first 60-80 minutes) is not stable as it is shown in Figure (5.21) and for some experiments it has a more oscillative behavior than for the others. It is difficult to give a concrete explanation to this trend, because there are different factors, which can influence it. For instance if the tendency is a flat line, the oscillations could be visible because the ordinate axis is too much zoomed. Another important factor to keep in consideration, is the amount, as well as the adding time, of the buffer solution to maintain the pH stable: for every experiment the addition happens in different times and this can modify the efficiency of the instantaneous degradation.

Analyzing the trend after 80 minutes, the curves with a highest rate are the ones with highest temperature and consequently, the lowest the ones at $13^\circ C$. The only exception is the experiment carried out at pH 3 and temperature $27^\circ C$, that is located in the range of the middle temperature curves with an oscillation range around 0.5. This peculiarity brings to light another interesting behavior shown in Figure (5.22). The trend of the experiments at pH 3 is similar: there is a step in all the 3 cases at 60

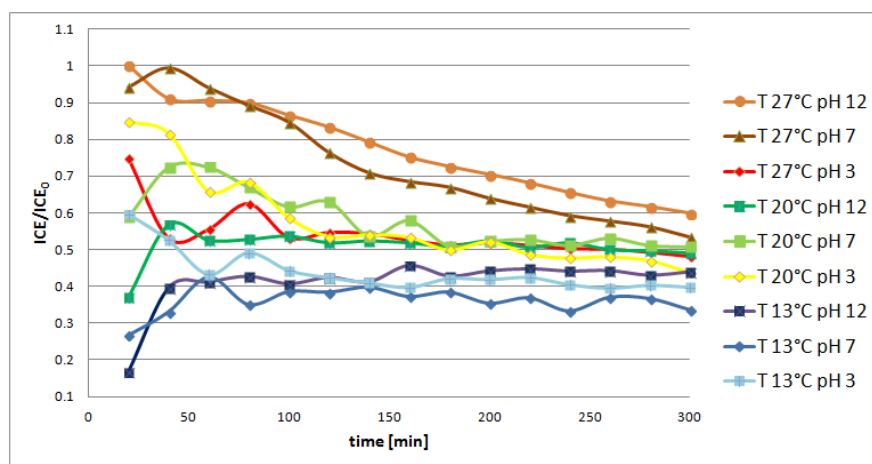


Figure 5.21: Comparison between of the temperature and pH influence on instantaneous current efficiency normalized

and 80 minutes.

This behavior could be explained by the fact that the initial pH of the solution is around 3, that is the natural pH of the acidic solution, being the salicylic acid, an acid. The natural oxidation mechanism expects to stay in the range of low pH and the system leads the lower pH. The experiments carried out at low pH are more close to the natural oxidation process, that involves a rapid degradation of some compounds after 80 minutes. This reactions can be postponed or even taken more time for experiments at higher pH.

To confirm or deny this hypothesis, another technique, capable to distinguish the particular intermediates, has to be applied.

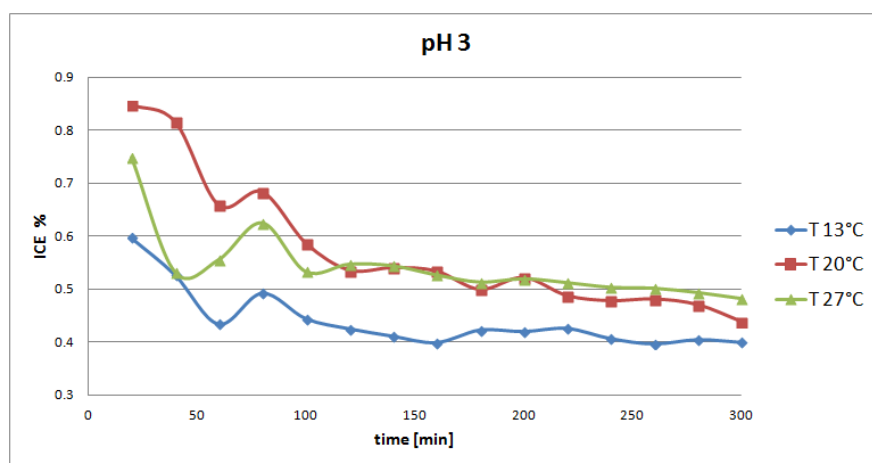


Figure 5.22: Instantaneous current efficiency percentage: comparison for different temperatures at pH 3

Chapter 6

Conclusions and further studies

The present work is part of a major PhD project. The studied topic is very challenging and there are some aspects not completely understood. First of all, not all the reactions are known and in particular it is unpredictable which degradation is attributable to the direct oxidation or other mechanisms. The discussion about the total oxidation rate can be done even without knowing which oxidant agent works on which compound. The complete mechanism that leads mineralization is different, depending on many factors for instance the initial compound concentration, the electrode material, the applied current, the mass transfer coefficient and so on.

Since the used devices have been tested for the first time for this project, an important part of the project is the calibration of the system. The combination gave a positive result for the oxidation of the salicylic acid, which is, as said in the theoretical chapter (3), a radical probe. The fact the degradation takes place consists in an evidence of the radicals reactions. It can be concluded that the system is suitable for organic removal applications even if it can be improved in different ways.

The clear influence of the NaCl as support electrolyte, suggests the application of this one for further experiments to enhance the kinetic of the oxidation. With this aim, it is necessary to develop an isolation around the tank, that connect this last one directly to the hood for a laboratory test.

Moreover the influence of the temperature has been demonstrated, as well as the influence of the pH in the chapter (5). Higher temperature and high pH leads to a faster generation of intermediates, but it not correspond to a more rapid mineralization, as proved by the TOC analyze.

The innovative part of the present work is to test the influence of the parameters, in particular the temperature, with a new setup, created for the disinfection of drinking water, with a special application for the legionella virus, but only in the recent period enlarged to water with a higher pollutant index, as wastewater and leachate treatment. Since the set-up is new, the future works can follow many different ways and investigate several specific aspects.

First of all, there are some pratic aspects to improve. The setup can be optimized creating a new sample port directly after the electrolytic cell, with the aim of measuring the degradation as soon as it happens; a closing valve between the tank and the pump,

for maintaining the aqueous solution inside the pump during the cleaning procedure. As mentioned in the chapter (4.2), the installed pump is a submersible pump and it is mandatory maintaining water inside the system to preserve its lifetime and to make the system running in a short time.

Talking about further possible techniques, the following step can be the evaluation of the hydroxylation of the salicylic acid with a high-performance liquid chromatography (HPLC and LC-MS). With this technique, the identification and quantification of intermediates in the degradation chain is possible and the reaction mechanisms can be better understood. To follow the reactions inside the system and argue which one is the step of the mineralization, this is an important experiment to carry out.

Furthermore, the next step is the evaluation of the degradation of other compounds present inside the leachate for example ammonia (NH_3) or other organic pollutants. The final goal is testing the setup for the real landfill leachate coming from Åremma to evaluate if this process is valide as first treatment. In particular, verify the effective oxidation rate of organic compounds, ammonia and heavy metals and also the real change of BOD_5/COD ratio for low temperatures.

In addition, the influence of some other parameters influencing the degradation of the salicylic acid as the electrode material, the gap between the electrodes and the applied current density, could be investigated.

Bibliography

- [1] Y. Deng and J. D. Englehardt, "Electrochemical oxidation for landfill leachate treatment," *Waste Management*, vol. 27, no. 3, pp. 380 – 388, 2007.
- [2] C. Comminellis, "Electrocatalysis in the electrochemical conversion/combustion of organic pollutants for waste water treatment," *Electrochimica Acta*, vol. 39, no. 11, pp. 1857 – 1862, 1994.
- [3] WaterDiam, "Instructions for follow-up and set up of treatments tests (case of wastewater containing organics)," pp. 1–17, 2015.
- [4] N. Rabaaoui and M. S. Allagui, "Anodic oxidation of salicylic acid on {BDD} electrode: Variable effects and mechanisms of degradation," *Journal of Hazardous Materials*, vol. 243, pp. 187 – 192, 2012.
- [5] M. Panizza and C. A. Martinez-Huitle, "Role of electrode materials for the anodic oxidation of a real landfill leachate – comparison between ti–ru–sn ternary oxide, pbo2 and boron-doped diamond anode," *Chemosphere*, vol. 90, no. 4, pp. 1455 – 1460, 2013.
- [6] <http://www.sigmaaldrich.com/catalog/substance/salicylicacid138126972711?lang=en®ion=NO>.
- [7] <http://www.sigmaaldrich.com/catalog/product/sial/234087?lang=en®ion=NO>.
- [8] https://en.wikipedia.org/wiki/Ultraviolet%E2%80%93visible_spectroscopy.
- [9] Metcalf and Eddy, "Wastewater engineering treatment and reuse," *Mc Graw Hill*, vol. fourth edition, pp. 1196–1202, 2004.
- [10] "Miljødirektoratet norge." www.miljodirektoratet.no/no/Regelverk/Direktiv/Deponidirektivet/, 1999.
- [11] A. Fernandes, M. Pacheco, L. Ciríaco, and A. Lopes, "Review on the electrochemical processes for the treatment of sanitary landfill leachates: Present and future," *Applied Catalysis B: Environmental*, vol. 176–177, pp. 183 – 200, 2015.
- [12] P. Debra R. Reinhart and C. J. Grosh, "Analysis of florida msw landfill leachate quality data," *University of Central Florida Civil and Environmental Engineering Department*, pp. i–xii, March 1997.
- [13] S. M. Raghav, A. M. A. E. Meguid, and H. A. Hegazi, "Treatment of leachate from municipal solid waste landfill," *{HBRC} Journal*, vol. 9, no. 2, pp. 187 – 192, 2013.

- [14] P. Foladori, “Corso di impianti di trattamento delle acque reflue,” *Università degli studi di Trento*, no. 9, pp. 312–317, 2014-2015.
- [15] U. Welander, T. Henrysson, and T. Welander, “Nitrification of landfill leachate using suspended-carrier biofilm technology,” *Water Research*, vol. 31, no. 9, pp. 2351 – 2355, 1997.
- [16] F. Wang, D. W. Smith, and M. G. El-Din, “Application of advanced oxidation methods for landfill leachate treatment – a review,” *Journal of Environmental Engineering and Science*, vol. 2, no. 6, pp. 413–427, 2003.
- [17] A. Amokrane, C. Comel, and J. Veron, “Landfill leachates pretreatment by coagulation-flocculation,” *Water Research*, vol. 31, no. 11, pp. 2775 – 2782, 1997.
- [18] K. Foo and B. Hameed, “An overview of landfill leachate treatment via activated carbon adsorption process,” *Journal of Hazardous Materials*, vol. 171, no. 1–3, pp. 54 – 60, 2009.
- [19] S. Renou, J. Givaudan, S. Poulain, F. Dirassouyan, and P. Moulin, “Landfill leachate treatment: Review and opportunity,” *Journal of Hazardous Materials*, vol. 150, no. 3, pp. 468 – 493, 2008.
- [20] A. Gröhlich, “Evaluation of landfill leachate treatment, considering water quality, legal aspects and site specifics,” *Technical University Hamburg-Harburg*, 2015.
- [21] Harstadt, “Handling and assessment of leachates from municipal solid waste landfills in the northern countries,” *Copenhagen: Nordic Council of Ministers*, 2006.
- [22] C. A. M. Huitle, “Direct and indirect electrochemical oxidation of organic pollutants,” *PhD thesis in Chemical sciences, University of Ferrara*, 2002-2004.
- [23] J. Crittenden, R. Trussel, D. Hand, K. Howe, and G. Tchobanoglous, “Water treatment principles and design,” *MWH*, vol. third edition, pp. 1417–1484, 2012.
- [24] M. M. Benjamin and D. F. Lawler, “Water quality engineering physical/chemical treatment processes,” *WILEY*, pp. 469–486, 2013.
- [25] J. J. Pignatello, E. Oliveros, and A. MacKay, “Advanced oxidation processes for organic contaminant destruction based on the fenton reaction and related chemistry,” *Critical Reviews in Environmental Science and Technology*, vol. 36, no. 1, pp. 1–84, 2006.
- [26] A. Fernandes, D. Santos, M. Pacheco, L. Ciríaco, and A. Lopes, “Electrochemical oxidation of humic acid and sanitary landfill leachate: Influence of anode material, chloride concentration and current density,” *Science of The Total Environment*, vol. 541, pp. 282 – 291, 2016.
- [27] K. Jüttner, U. Galla, and H. Schmieder, “Electrochemical approaches to environmental problems in the process industry,” *Electrochimica Acta*, vol. 45, no. 15–16, pp. 2575 – 2594, 2000.
- [28] A. Rahmani, D. Nematollahi, G. Azarian, K. Godini, and Z. Berizi, “Activated sludge treatment by electro-fenton process: Parameter optimization and degradation mechanism,” *Korean Journal of Chemical Engineering*, vol. 32, no. 8, pp. 1570–1577, 2015.

- [29] C. A. Martínez-Huitle and E. Brillas, “Decontamination of wastewaters containing synthetic organic dyes by electrochemical methods: A general review,” *Applied Catalysis B: Environmental*, vol. 87, no. 3–4, pp. 105 – 145, 2009.
- [30] C. Papastavrou, D. Mantzavinos, and E. Diamadopoulos, “A comparative treatment of stabilized landfill leachate: Coagulation and activated carbon adsorption vs. electrochemical oxidation,” *Environmental Technology*, vol. 30, no. 14, pp. 1547–1553, 2009. PMID: 20183999.
- [31] A. Anglada, A. M. Urtiaga, and I. Ortiz, “Laboratory and pilot plant scale study on the electrochemical oxidation of landfill leachate,” *Journal of Hazardous Materials*, vol. 181, no. 1–3, pp. 729 – 735, 2010.
- [32] A. Anglada, A. Urtiaga, and I. Ortiz, “Contributions of electrochemical oxidation to waste-water treatment: fundamentals and review of applications,” *Journal of Chemical Technology and Biotechnology*, vol. 84, no. 12, pp. 1747–1755, 2009.
- [33] A. Fernandes, P. Spranger, A. Fonseca, M. Pacheco, L. Ciriaco, and A. Lopes, “Effect of electrochemical treatments on the biodegradability of sanitary landfill leachates,” *Applied Catalysis B: Environmental*, vol. 144, pp. 514 – 520, 2014.
- [34] C. Comninellis and G. Chen, “Electrochemistry for the environment,” *Springer Science*, pp. 1–54; 515–551, 2010.
- [35] C. A. Martínez-Huitle, M. A. Quiroz, C. Comninellis, S. Ferro, and A. D. Battisti, “Electrochemical incineration of chloranilic acid using ti/iro2, pb/pbo2 and si/bdd electrodes,” *Electrochimica Acta*, vol. 50, no. 4, pp. 949 – 956, 2004.
- [36] A. Cabeza, A. M. Urtiaga, , and I. Ortiz*, “Electrochemical treatment of landfill leachates using a boron-doped diamond anode,” *Industrial & Engineering Chemistry Research*, vol. 46, no. 5, pp. 1439–1446, 2007.
- [37] A. Anglada, A. Urtiaga, and I. Ortiz, “Pilot scale performance of the electro-oxidation of landfill leachate at boron-doped diamond anodes,” *Environmental Science & Technology*, vol. 43, no. 6, pp. 2035–2040, 2009.
- [38] P. Cañizares, J. García-Gómez, J. Lobato, , and M. A. Rodrigo, “Electrochemical oxidation of aqueous carboxylic acid wastes using diamond thin-film electrodes,” *Industrial and Engineering Chemistry Research*, vol. 42, no. 5, pp. 956–962, 2003.
- [39] E. Brillas, B. Boye, I. Sirès, J. A. Garrido, R. M. Rodríguez, C. Arias, P.-L. Cabot, and C. Comninellis, “Electrochemical destruction of chlorophenoxy herbicides by anodic oxidation and electro-fenton using a boron-doped diamond electrode,” *Electrochimica Acta*, vol. 49, no. 25, pp. 4487–4496, 2004.
- [40] F. Montilla, P. Michaud, E. Morallón, J. Vázquez, and C. Comninellis, “Electrochemical oxidation of benzoic acid at boron-doped diamond electrodes,” *Electrochimica Acta*, vol. 47, no. 21, pp. 3509 – 3513, 2002.
- [41] M. Panizza, P. Michaud, G. Cerisola, and C. Comninellis, “Anodic oxidation of 2-naphthol at boron-doped diamond electrodes,” *Journal of Electroanalytical Chemistry*, vol. 507, no. 1–2, pp. 206 – 214, 2001.

- [42] P. Cañizares, M. Díaz, J. A. Domínguez, J. García-Gómez, and M. A. Rodrigo, “Electrochemical oxidation of aqueous phenol wastes on synthetic diamond thin-film electrodes,” *Industrial and Engineering Chemistry Research*, vol. 41, no. 17, pp. 4187–4194, 2002.
- [43] A. Perret, W. Haenni, N. Skinner, X.-M. Tang, D. Gandini, C. Comninellis, B. Correa, and G. Foti, “Electrochemical behavior of synthetic diamond thin film electrodes,” *Diamond and Related Materials*, vol. 8, no. 2–5, pp. 820 – 823, 1999.
- [44] E. Guinea, C. Arias, P. L. Cabot, J. A. Garrido, R. M. Rodríguez, F. Centellas, and E. Brillas, “Mineralization of salicylic acid in acidic aqueous medium by electrochemical advanced oxidation processes using platinum and boron-doped diamond as anode and cathodically generated hydrogen peroxide,” *Water Research*, vol. 42, no. 1–2, pp. 499 – 511, 2008.
- [45] B. Nanzai, K. Okitsu, N. Takenaka, H. Bandow, and Y. Maeda, “Sonochemical degradation of various monocyclic aromatic compounds: Relation between hydrophobicities of organic compounds and the decomposition rates,” *Ultrasonics Sonochemistry*, vol. 15, no. 4, pp. 478 – 483, 2008.
- [46] K. Azrague, V. Pradines, E. Bonnefille, C. Claparols, M.-T. Maurette, and F. Benoit-Marquié, “Degradation of 2,4-dihydroxibenzoic acid by vacuum {UV} process in aqueous solution: Kinetic, identification of intermediates and reaction pathway,” *Journal of Hazardous Materials*, vol. 237–238, pp. 71 – 78, 2012.
- [47] M. Otero, M. Zabkova, and A. E. Rodrigues, “Comparative study of the adsorption of phenol and salicylic acid from aqueous solution onto nonionic polymeric resins,” *Separation and Purification Technology*, vol. 45, no. 2, pp. 86 – 95, 2005.
- [48] C. Comninellis, M. Doyle, and J. Winnick, “Energy and electrochemical processes for a cleaner environment: Proceedings of the international symposium,” *the Electrochemical society, inc.*, vol. 2001-23, pp. 80–86, 2001.

Ringraziamenti

Sono estremamente grata di aver avuto la possibilità di partecipare al programma Erasmus+ e di aver collaborato con il dipartimento di idraulica ed ingegneria ambientale alla NTNU.

Per primi vorrei ringraziare i miei genitori per avermi sostenuto sia psicologicamente che economicamente per questi ultimi sei mesi e per aver accantonato i loro problemi permettendomi di fare quest'esperienza. Senza di loro non avrei mai potuto permetter-melo!

Ci tengo a ringraziare la mia relatrice in Italia, Paola Foladori, per avermi aiutata con suggerimenti molto utili ed azzeccati in un momento di sconforto, per la sua disponibilità sia nel cercare un contatto alla NTNU, sia durante la mia permanenza all'estero che non era per nulla dovuta. In parallelo, vorrei dire grazie al mio *supervisor* a Trondheim, Thomas Meyn per l'enorme occasione di entrare a far parte di in un ambiente stimolante che mi ha permesso di scoprire le abilità di lavoratrice autonoma.

Un ringraziamento dovuto va a Noëmi Ambauen per i consigli e i lunghi confronti su alcuni aspetti del progetto; per aver sempre mostrato un atteggiamento positivo e per avermi seguito nei primi esperimenti in laboratorio. Inoltre ringrazio Trine e Gøril, dell'*Analitical lab* per l'aiuto con i vari macchinari ma soprattutto per essere il grado di creare un ambiente rilassante e piacevole durante tutto il periodo che vi ho trascorso.

Un enorme Grazie con la G maiuscola va a Kamal Azrague per avermi guidata e sostenuta in un momento di stallo, oltre che essere una bella persona: i suoi consigli e le sue delucidazioni sono stati preziosissimi dovuti alla sua grande esperienza mi hanno aiutato ad ottimizzare i tempi.

Voglio dire grazie ad Anna Gröhlich per il supporto che abbiamo saputo darci in momenti tristi, come solo due persone che hanno imparato a vivere in simbiosi per così a lungo sanno fare, ma anche per tutti i momenti felici condivisi anche con tutti i compagni dell'ufficio del secondo piano: il piccolo ghetto tedesco con Muriel e Thomas, Flora, Peiyao, Carlos, Vladimir e la nostra piccola speciale minoranza italiana con Gigi e Vittò, che si è dimostrata abbastanza numerosa da distruggere la quiete che caratterizzava il dipartimento prima del nostro arrivo.

Ringrazio in più Slaven per la compagnia durante le vacanze di Natale, Raniero per il suo caffè da Moka, Ganesh per le infinite chiacchierate e i miei compagni di uscite serali, di viaggi alla scoperta dei bellissimi angoli della Norvegia e di varie sfaticate alla ricerca delle Koiene (Viki, Martina, Mika, Timo, Daniel, Amrei, Rafael ed Anthony).

Mi mancherete tutti un sacco, così come mi mancherà quel bellissimo paese che è la Norvegia!

Grazie a chi mi ha supportato da casa per tutto il periodo universitario e pure da molto tempo prima. Le mie amiche di sempre: Lety, Marta, Sil, Niki e Ale che hanno condiviso sogni, fantasie, compagnie, pranzi, cene, viaggi, figli e molte più cose che non posso stare qui ad elencare. I miei fantastici coinquilini di Piedicastello con le nostre

cene stravaganti, le partite a calcetto e ping pong, le birre al Picaro e le interminabili sessioni di esami durante le quali ogni superficie veniva ricoperta di libri, quaderni e fogli. Grazie ad HIMYM per avermi insegnato che un gruppo di amici può rimanere tale per sempre e al mio fedele compagno di serie tv, Andrea che nonostante tutte le incomprensioni è stato un punto fisso.

Grazie inoltre a tutti gli amici degli anni di università che terrò nel cuore come uno dei periodi migliori. Ognuno di voi è stato importante per qualche motivo e ci tengo a dirvi grazie!

Appendix

	Substance
1	Arsenic
2	Bisphenol A
3	Brominated flame retardants
4	DEHP
5	DTDMAC, DSD;AC, DHTDMAC
6	1,2-Dichloroethane (EDC)
7	Dioxins and furans
8	Cadmium
8	CABs
10	Chromium
11	Hexachlorobenzene
12	Lead
13	Medium-chain chlorinated paraffins
14	Mercury
15	Musk xylene
16	Nonylphenol and its ethoxylates
17	Octylphenol and its ethoxylates
18	PAHs
19	Pentachlorophenol (PCP)
20	Polychlorinated biphenyls (PCBs)
21	PFOA
22	PFOS
23	Short-chain chlorinated paraffins
24	Siloxane-D4
25	Siloxane-D5
26	TCEP (tris(2-chloroethyl)phosphate)
27	Tetrachloroethene
28	Tributyl tin compounds
29	Trichloroethene
30	Trichloroethene (TRI)
31	Triclosan
32	2.4.6 Tri-tert-butylphenol

Table 6.1: List of Norwegian hazardous substances ([10])

Number	Name of priority substance	CAS number	EU number	Priority category
1)	Alachor	15972-60-8	240-110-8	B
2)	Anthracen	120-12-7	204-371-1	B*
3)	Atrazine	1912-24-9	217-617-8	B*
4)	Benzene	71-43-2	200-753-7	B
5)	Brominated diphenyletheriv	not relevant	not relevant	A
6)	Cadmium and Cadmium compounds	7440-43-9	231-152-8	A
7)	Chloroalkanes, C10-13 iv	85535-84-8	287-467-5	A
8)	Chlorfenvinphos	470-900	207-432-0	B
9)	Chlorpyrifos	2921-88-2	220-864-4	B*
10)	1,2 - Dichloromethane	107-06-2	203-458-1	B
11)	Dichloromethane	75-09-2	200-838-9	B
12)	Di((2-ethylhexyl)phthalate (DEHP)	117-81-7	204-211-0	B*
13)	Diuron	330-54-1	206-354-4	B*
14)	Endosulfan	115-29-7	204-079-4	B*
15)	Fluoranthene	206-44-0	205-912-4	B
16)	Hexachlorobenzene	118-74-1	204-273-9	A
17)	Hexachlorobutadiene	87-68-3	201-765-5	A
18)	Hexachlorocyclohexane (HCH)	608-73-1	210-401-2	A
19)	Isoproturon	34123-59-6	251-835-4	B*
20)	Lead and its compounds	7439-92-1	231-100-4	B*
21)	Mercury and its compounds	7439-97-6	231-106-7	A
22)	Naphtalene	91-20-3	202-049-5	B*
23)	Nickel and its compounds	7440-02-0	231-111-4	B
24)	Nonylphenols (4-nonylphenol)	25154-52-3 104-40-5	246-672-0 203-199-4	A
25)	Octylphenols (4-(1,1',3,3'-tetramethylbutyl)phenol)	1806-26-4 140-66-9	217-302-5 not relevant	B*
26)	Pentachlorobenzene	608-93-5	210-172-5	A
27)	Pentachlorophenol	87-86-5	201-778-6	B*
28)	Polyaromatic hydrocarbons (PAH)	not relevant	not relevant	A
	Benzo(a)pyrene	50-32-8	200-028-5	
	Benzo(b)fluoranthene	205-99-2	205-911-9	
	Benzo(g,h,i)perylene	191-24-2	205-883-8	
	Benzo(k)fluoranthene	207-08-9	205-916-6	
	Indeno(1,2,3-cd)pyrene	193-39-5	205-893-2	
29)	Simazine	122-34-9	204-535-2	B*
30)	Tributyltin (Tributyltin-cation)	688-73-3 36643-28-4	211-704-4 not relevant	A
31)	Trichlorobenzenes	12002-48-1	234-413-4	B*
32)	Trichloromethane (chloroform)	67-66-3	200-663-8	B
33)	Trifluralin	1582-09-8	216-428-8	B*
34)	Dicofol	115-32-2		A
35)	PFOS	1763-23-1		A
36)	Quinoxifen	124495-18-7	not relevant	A
37)	Dioxins and dioxin-like compounds	not relevant	not relevant	A
38)	Aclonifen	74070-46-5	277-704-1	B
39)	Bifenox	42576-02-3	255-984-7	B
40)	Cybutryne	28159-98-0	257-842-9	B
41)	Cypermethrin	52315-07-8	257-842-9	B
42)	Dichlorvos	62-73-7	200-547-7	B
43)	Heabromocyclododecanes (HBCDD)	not relevant	not relevant	B
44)	Heptachlor and heptachlor epoxide	76-44-8	200-962-3	A
45)	Terbutryn	886-50-0	212-950-5	B

Table 6.2: European list of priority substances (European Parliament and of the Council EU 2013)

6.1 Total organic carbon analyze

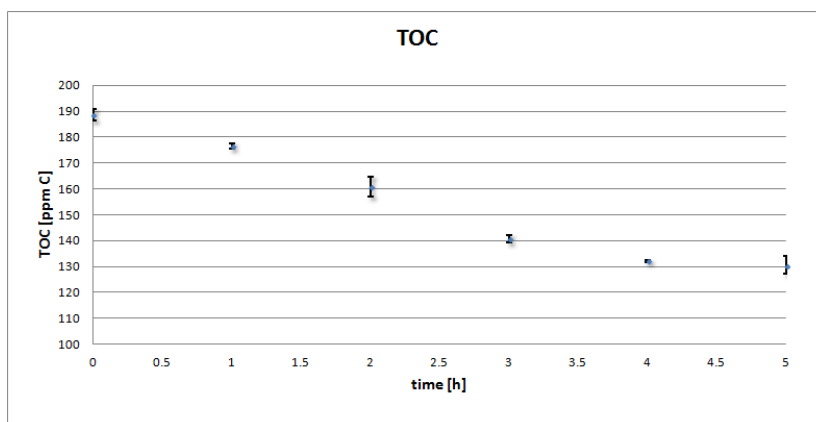


Figure 6.1: Total organic carbon at pH 3 - 13°C

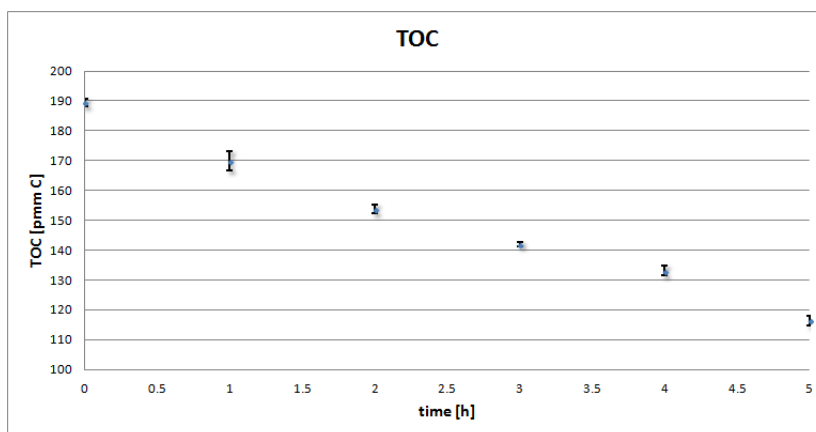


Figure 6.2: Total organic carbon at pH 3 - 20°C

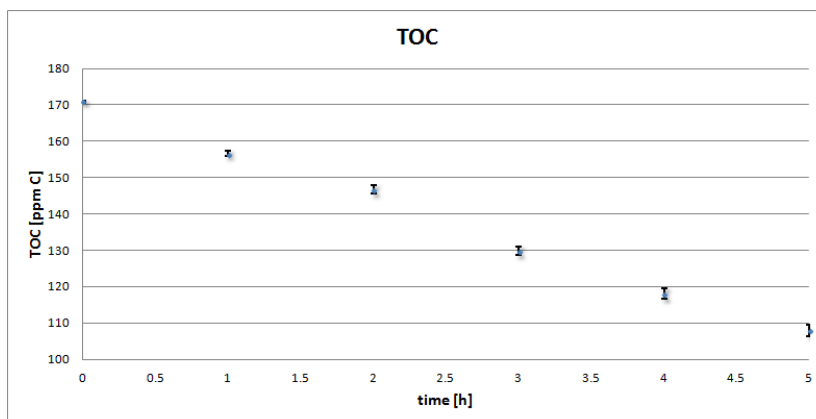


Figure 6.3: Total organic carbon at pH 3 - 27°C

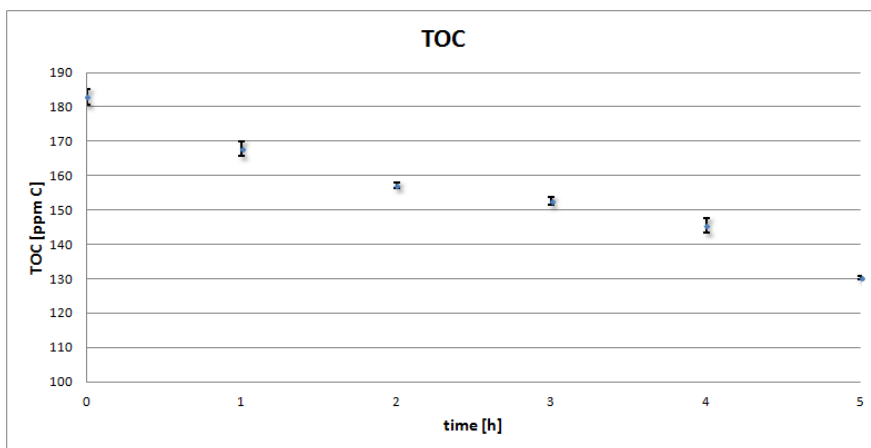


Figure 6.4: Total organic carbon at pH 7 - 13°C

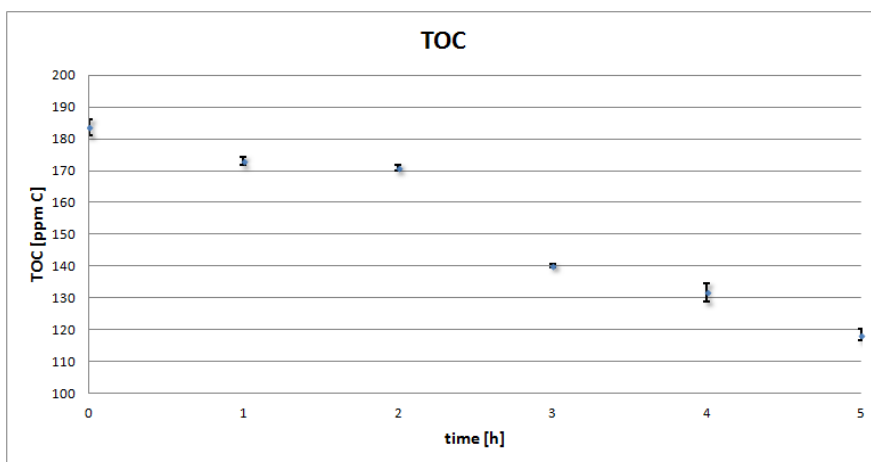


Figure 6.5: Total organic carbon at pH 7 - 20°C

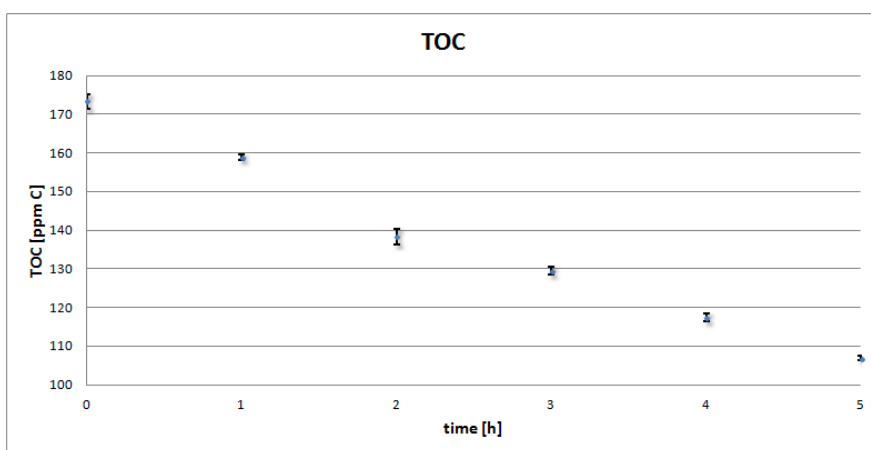


Figure 6.6: Total organic carbon at pH 7 - 27°C

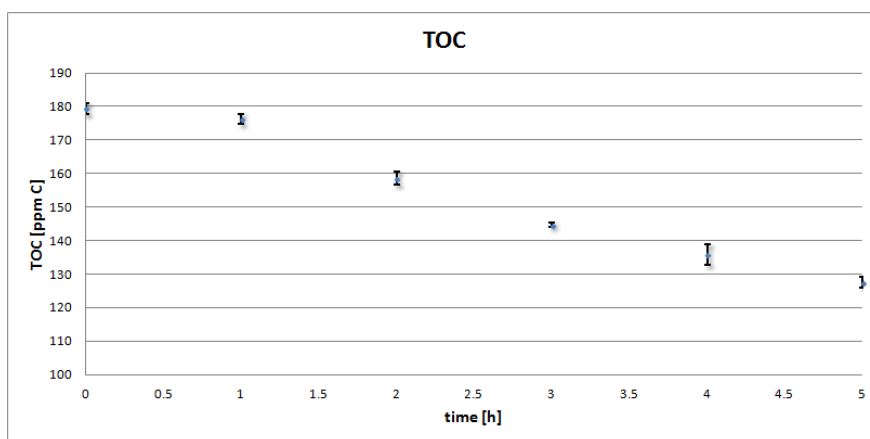


Figure 6.7: Total organic carbon at pH 12 - 13°C

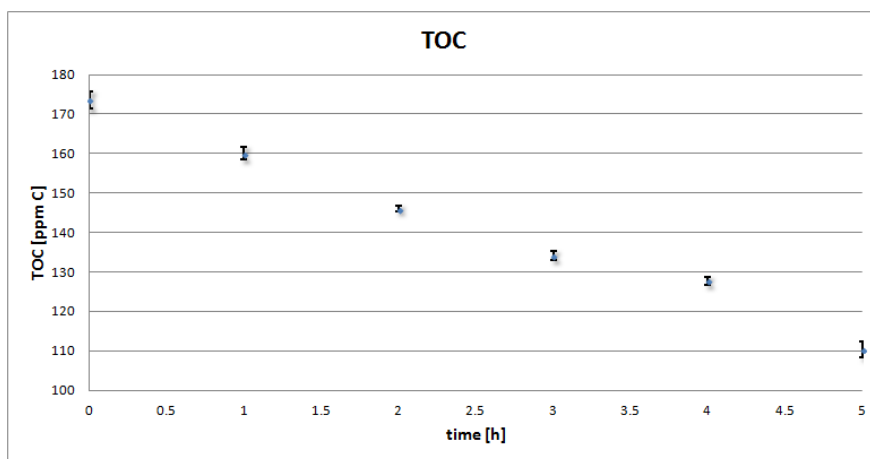


Figure 6.8: Total organic carbon at pH 12 - 20°C

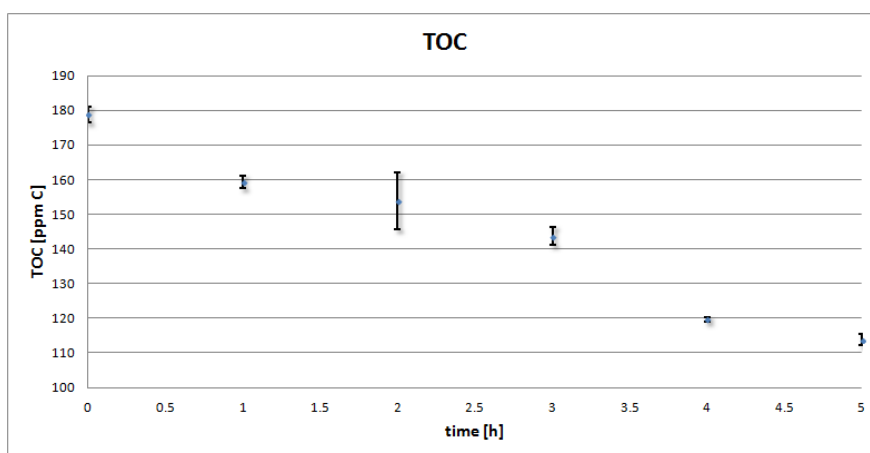


Figure 6.9: Total organic carbon at pH 12 - 27°C

6.2 Absorbance spectrum

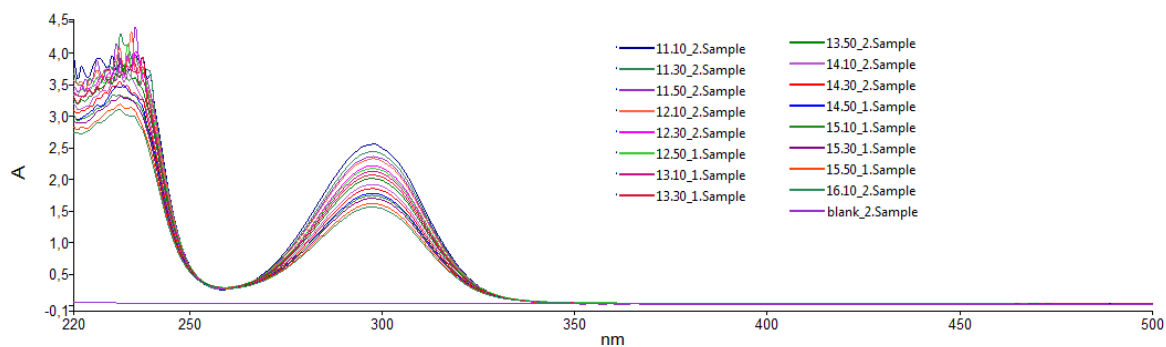


Figure 6.10: Absorbance spectrum at pH 3 - 13°C

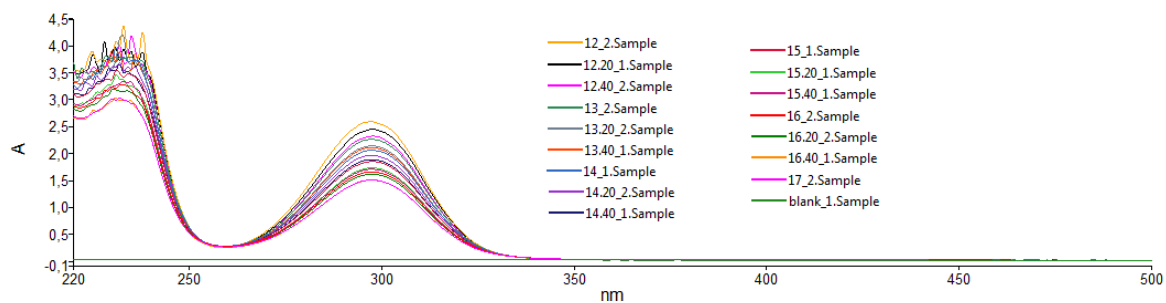


Figure 6.11: Absorbance spectrum at pH 3 - 20°C

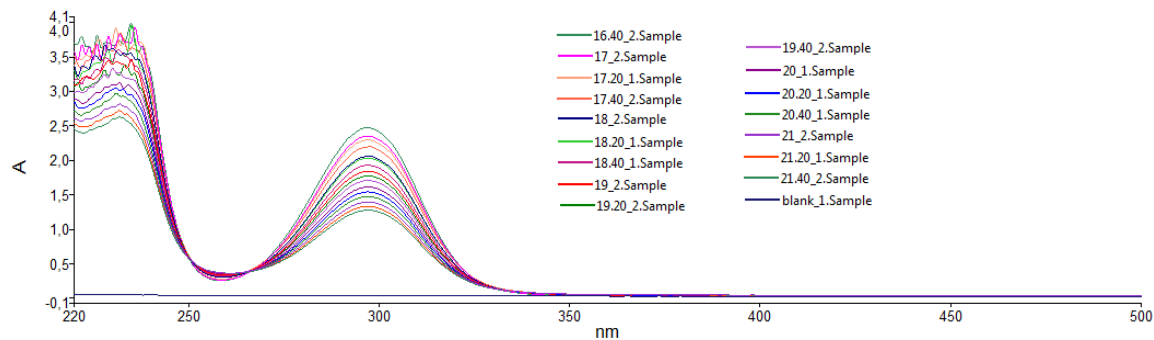


Figure 6.12: Absorbance spectrum at pH 3 - 27°C

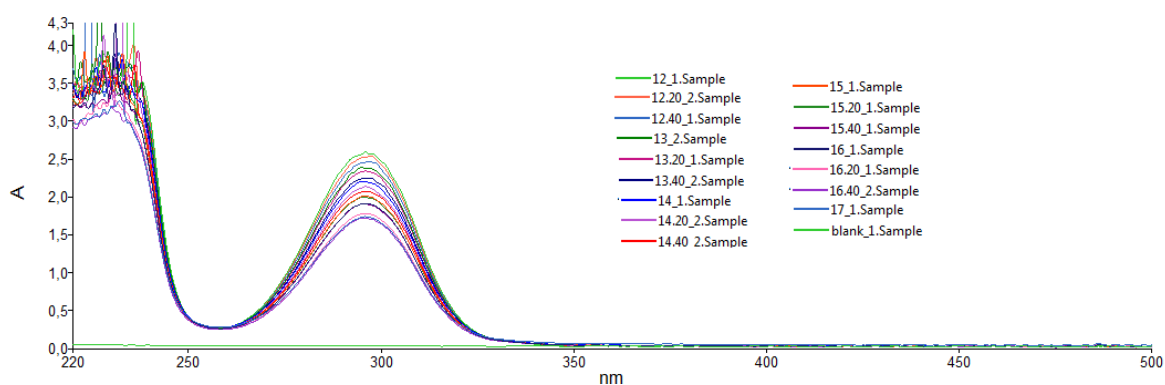


Figure 6.13: Absorbance spectrum at pH 7 - 13°C

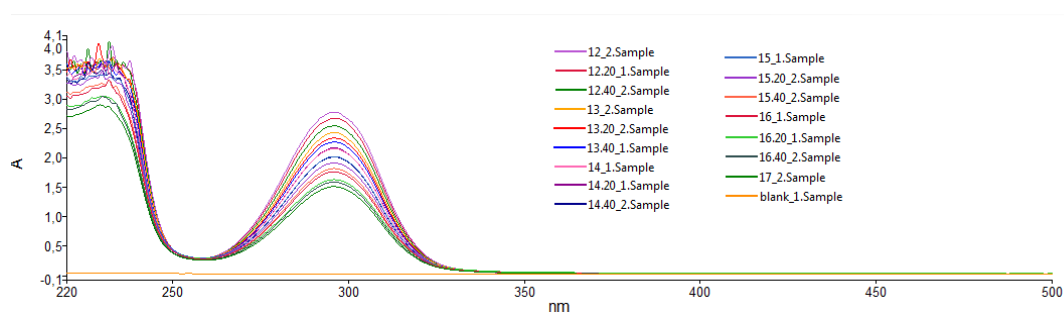


Figure 6.14: Absorbance spectrum at pH 7 - 20°C

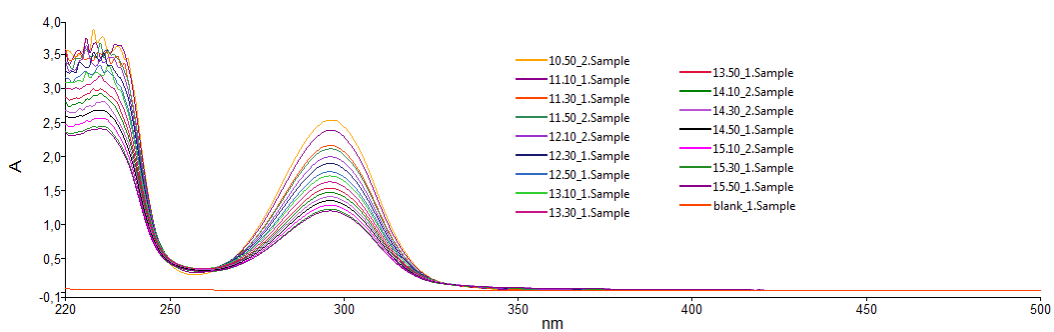


Figure 6.15: Absorbance spectrum at pH 7 - 27°C

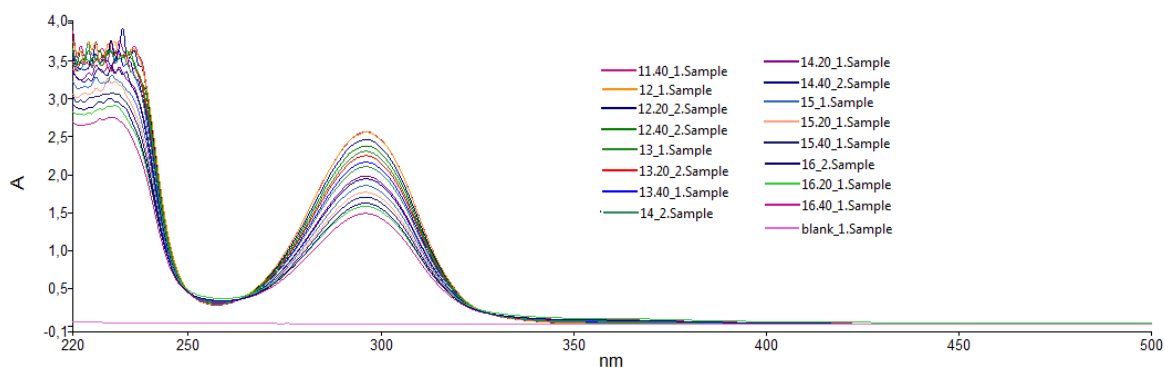


Figure 6.16: Absorbance spectrum at pH 12 - 13°C

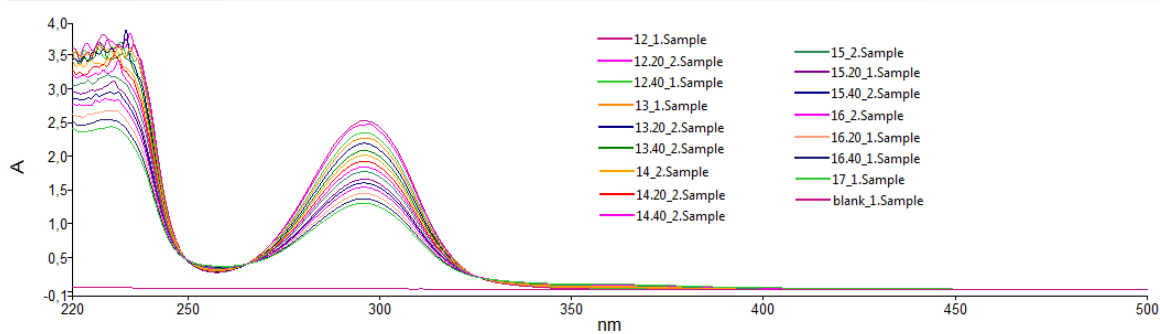


Figure 6.17: Absorbance spectrum at pH 12 - 20°C

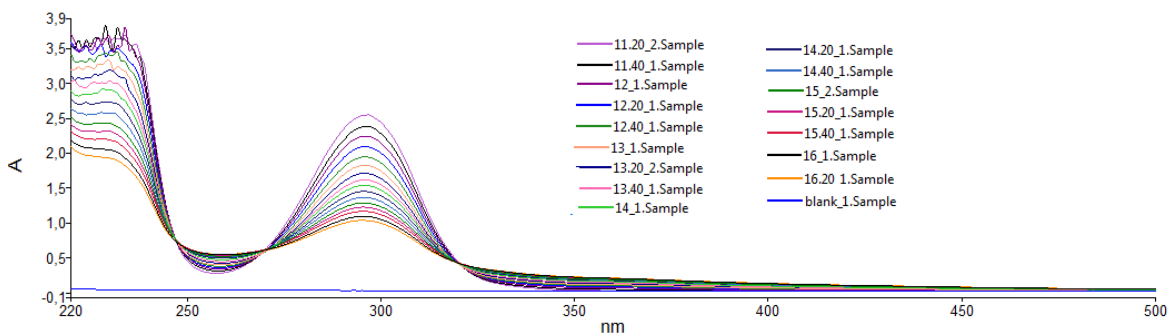


Figure 6.18: Absorbance spectrum at pH 12 - 27°C

6.3 Comparison pH and temperature

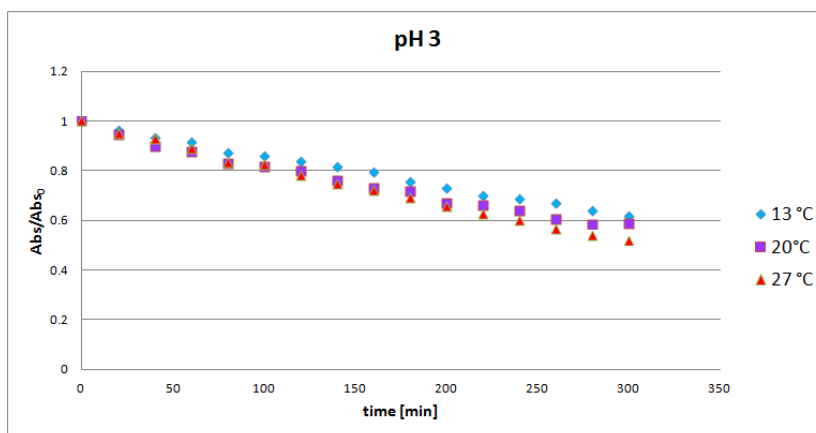


Figure 6.19: Comparison of different temperature at pH 3

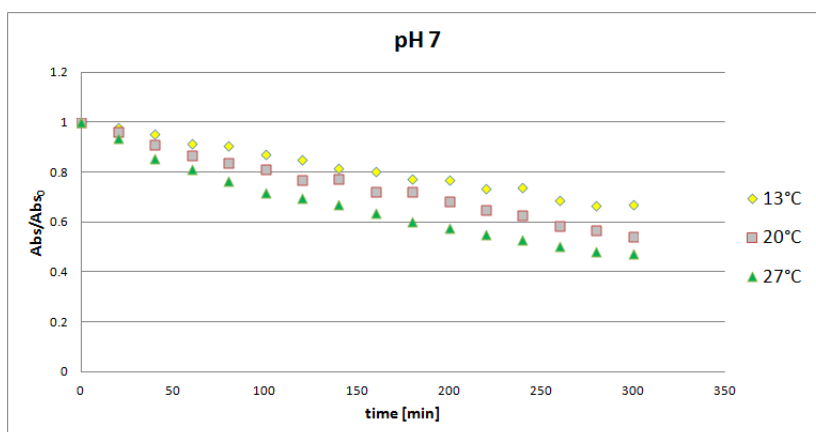


Figure 6.20: Comparison of different temperature at pH 7

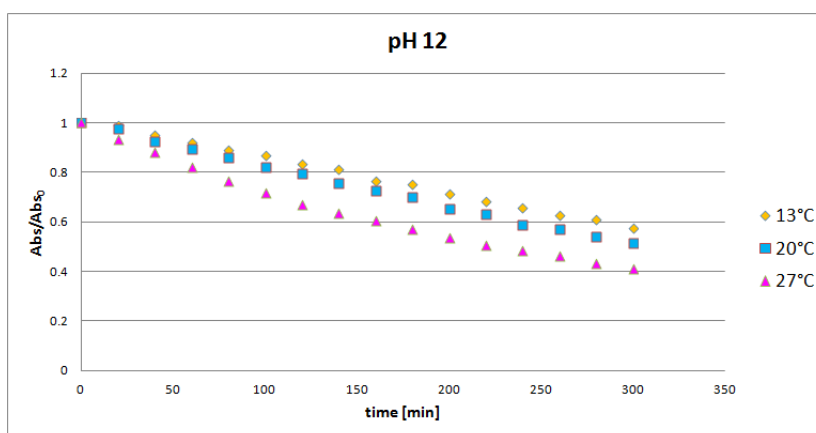


Figure 6.21: Comparison of different temperature at pH 12

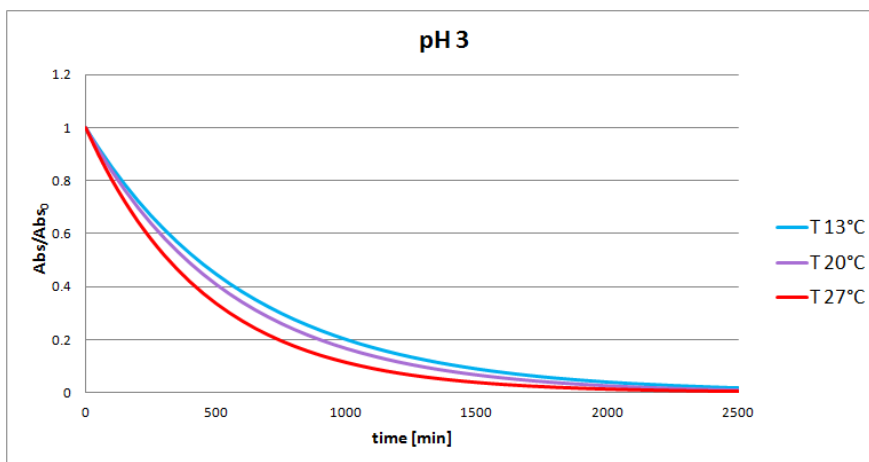


Figure 6.22: Comparison of different temperature at pH 3

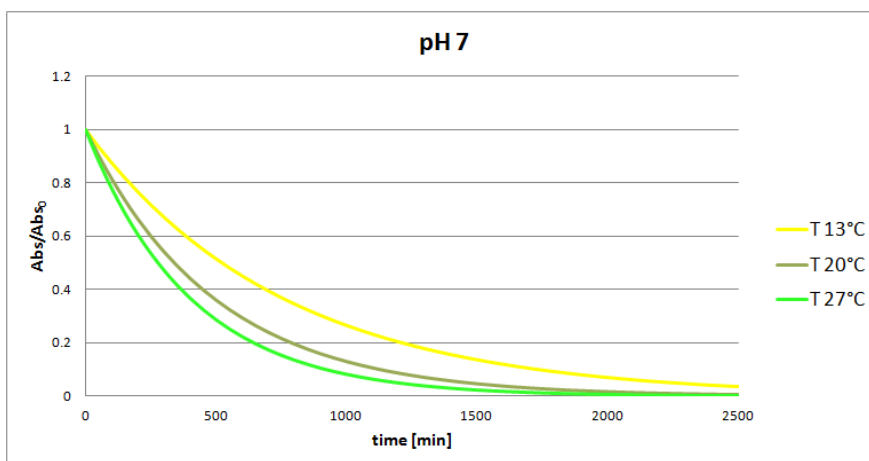


Figure 6.23: Comparison of different temperature at pH 7

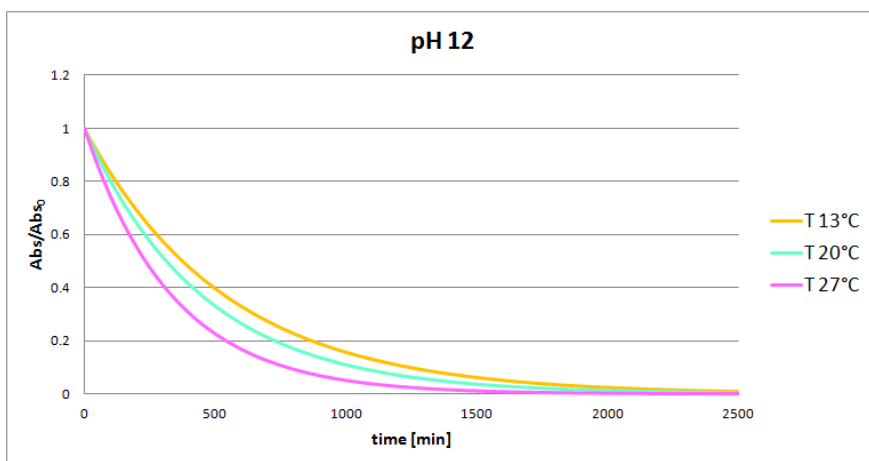


Figure 6.24: Comparison of different temperature at pH 12

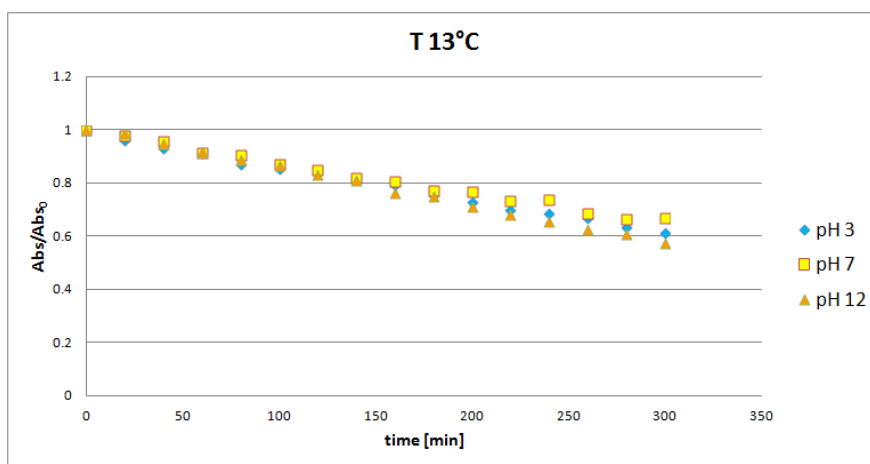


Figure 6.25: Comparison of different pH at 13°C

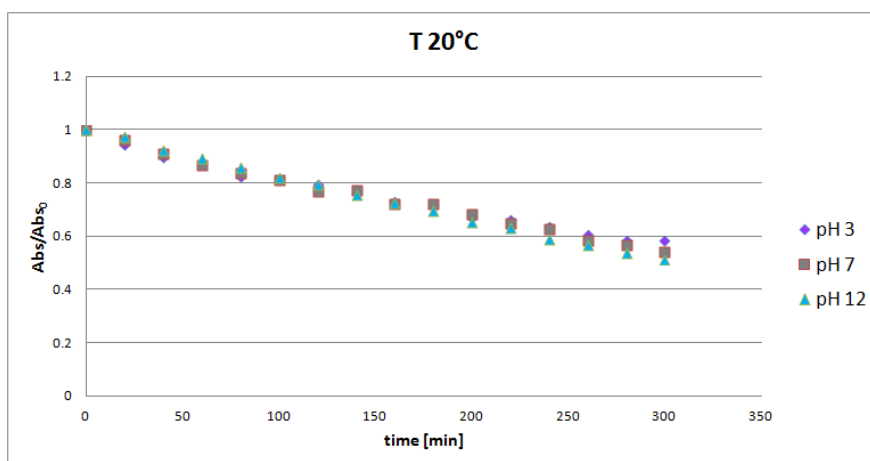


Figure 6.26: Comparison of different pH at 20°C

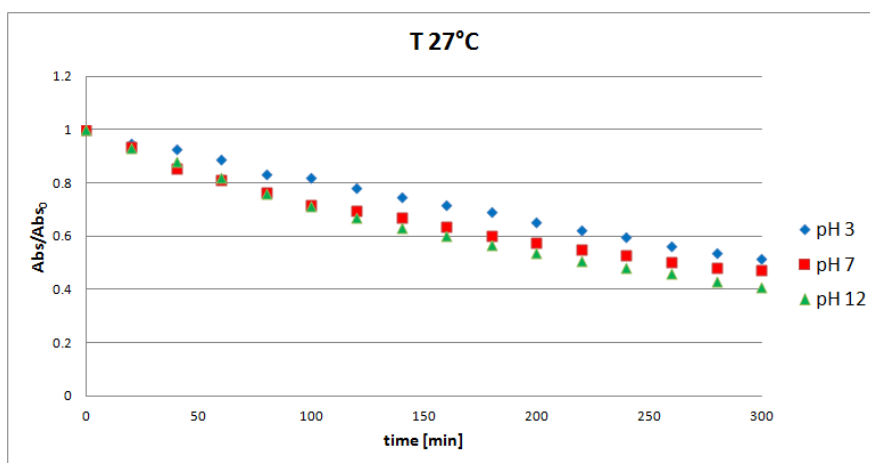


Figure 6.27: Comparison of different pH at 27°C

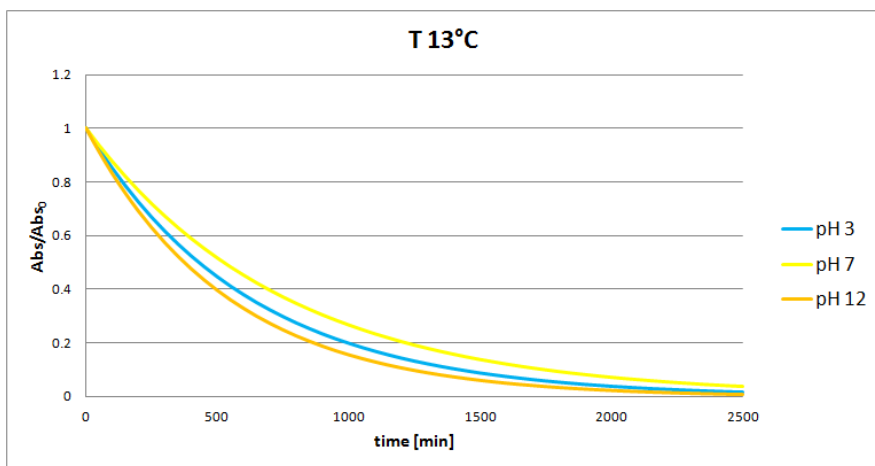


Figure 6.28: Comparison of different pH at 13°C

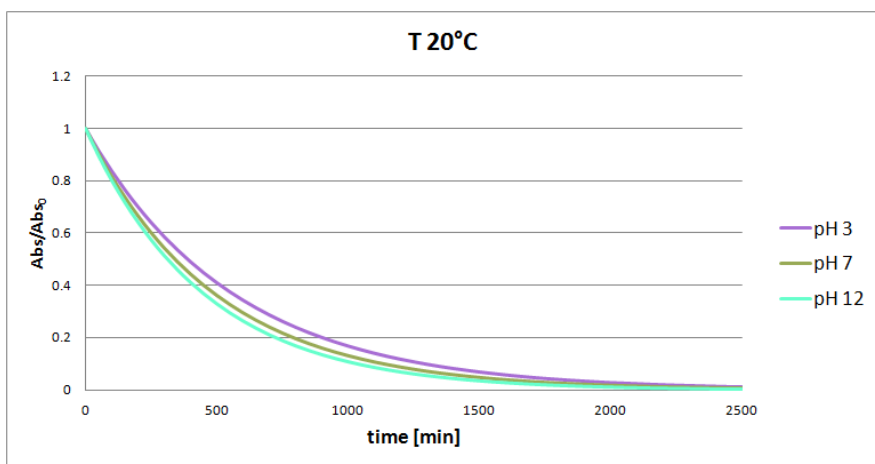


Figure 6.29: Comparison of different pH at 20°C

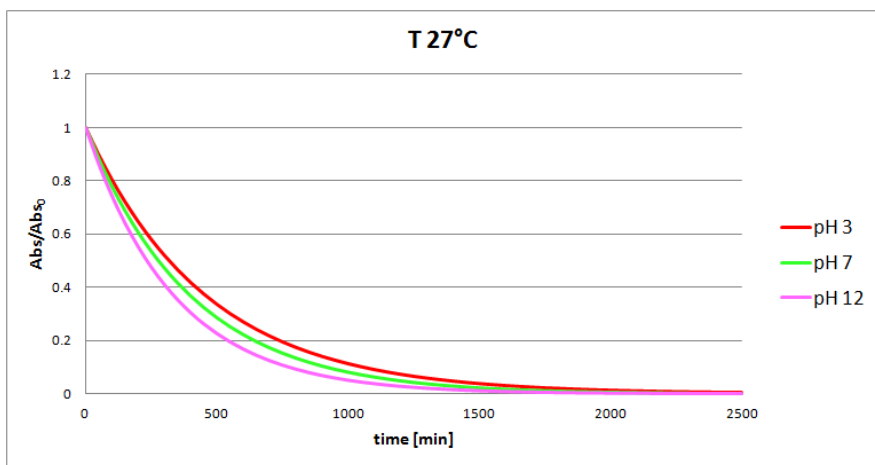


Figure 6.30: Comparison of different pH at 27°C

Day 02.01.2016 Dilution 1:3
 Concentration of salicylic acid 300 mg/L
 Concentration of NaCl 0.1 M
 Volume 10 L

time	T (°C)	pH	Absorbance	conductivity (µS/cm)	current (A)	voltage (V)	time (min)	Abs/abs_0	$k = 1/\Delta t \ln(c_1/c_2)$	$\sigma = \sum (k - k_m)^2$	concentration (mg/L)
11.45	20.08	2.88	8.9986	8.47	7	8.2	0	1	-	-	362.5182
12.05	21.54	3.33	7.8582	7.86	7	8.2	20	0.8733	0.006776	8.3031E-07	316.3482
12.25	22.23	5.95	6.9097	7.63	-6.4	-8.7	40	0.7679	0.006432	1.5756E-06	277.9474
12.45	22.12	6.55	6.1643	7.71	6.9	8.7	60	0.6850	0.005708	3.9173E-06	247.7692
13.05	21.97	6.62	5.5630	7.79	7	8.4	80	0.6182	0.005132	6.5277E-06	223.4251
13.25	21.23	6.46	4.6125	7.86	-6.4	-8.8	100	0.5126	0.009368	2.8277E-06	184.9433
13.45	20.65	6.4	3.9180	7.83	7	8.6	120	0.4354	0.008159	2.234E-07	156.8259
14.05	20.12	6.4	3.4562	7.8	7	8.4	140	0.3841	0.006271	2.0056E-06	138.1296
14.25	19.98	6.4	3.1101	7.85	-6.5	-8.7	160	0.3456	0.005276	5.8131E-06	124.1174
14.45	19.89	6.38	2.4259	7.88	7	8.4	180	0.2696	0.012423	2.2428E-05	96.4170
15.05	20.17	6.46	2.0006	7.8	7	8.2	200	0.2223	0.009638	3.8063E-06	79.1984
15.25	20.21	6.57	1.6357	7.72	-6.4	-8.5	220	0.1818	0.010069	5.6741E-06	64.4251
15.45	19.91	6.58	1.3727	7.68	-6.4	-8.4	240	0.1525	0.008765	1.1616E-06	53.7773
16.05	20.08	6.59	1.1590	7.69	7	8.4	260	0.1288	0.008463	6.0224E-07	45.1239
16.25	20.09	6.58	1.0590	7.71	7	8.2	280	0.1177	0.004511	1.0084E-05	41.0757
16.45	19.95	6.6	0.8968	7.68	-6.4	-8.4	300	0.0997	0.008313	3.9238E-07	34.5085
									Average	Sum	
									0.007687	6.7869E-05	

Day 07.01.2016 Dilution 1:3
 Concentration of salicylic acid 300 mg/L
 Concentration of NaSO₄ 0.05 M
 Volume 10 L

time	T (°C)	pH	Absorbance	conductivity (µS/cm)	current (A)	voltage (V)	time (min)	Abs/abs_0	$k = 1/\Delta t \ln(c_1/c_2)$	$\sigma^2 = \sum (k - k_m)^2$	concentration (mg/L)
11.30	20.98	3.26	7.4951	6.79	7	8.8	0	1.0000	-	-	301.6478
11.50	20.94	3.21	7.3666	6.82	7	8.2	20	0.9829	0.000865	1.07514E-06	296.4453
12.10	20.63	3.22	6.9699	6.76	-6.4	-8.7	40	0.9299	0.002768	7.50339E-07	280.3846
12.30	20.23	3.24	6.8708	6.74	-6.4	-8.6	60	0.9167	0.000716	1.40549E-06	276.3725
12.50	20.09	3.25	6.5845	6.74	7	8.3	80	0.8785	0.002128	5.13289E-08	264.7814
13.10	20.06	3.29	6.5835	6.72	-6.4	-8.6	100	0.8784	0.000008	3.58706E-06	264.7409
13.30	19.96	3.26	6.2629	6.69	-6.4	-8.6	120	0.8356	0.002496	3.53562E-07	251.7611
13.50	19.95	3.27	5.9309	6.72	7	8.3	140	0.7913	0.002723	6.75388E-07	238.3198
14.10	20.04	3.27	5.5619	6.66	-6.4	-8.3	160	0.7421	0.003212	1.71678E-06	223.3806
14.30	20.07	3.29	5.3404	6.7	-6.4	-8.4	180	0.7125	0.002032	1.70074E-08	214.4130
14.50	20	3.3	5.2545	6.79	7	8.2	200	0.7011	0.000811	1.18976E-06	210.9352
15.10	20.03	3.31	5.1098	6.67	-6.4	-8.6	220	0.6818	0.001396	2.55347E-07	205.0769
15.30	19.97	3.31	4.7993	6.75	-6.4	-8.5	240	0.6403	0.003135	1.52019E-06	192.5061
15.50	19.97	3.33	4.6210	6.71	7	8.2	260	0.6165	0.001893	7.39844E-11	185.2874
16.10	20.06	3.34	4.5074	6.67	-6.4	-8.6	280	0.6014	0.001245	4.31671E-07	180.6883
16.30	19.98	3.36	4.2507	6.66	-6.4	-8.5	300	0.5671	0.002932	1.0615E-06	170.2955
16.50	19.99	3.36	4.2922	6.69	7	8.1	320	0.5727	-0.000486	5.69937E-06	171.9757
17.10	20.03	3.37	3.9264	6.86	-6.4	-8.5	340	0.5239	0.004454	6.5141E-06	157.1660
Average											
									Sum		
									0.001902		2.63041E-05

Day 08.01.2016 Dilution 1:3
 Concentration of salicylic acid 300 mg/L
 Concentration of NaCl 0.05 M
 Volume 10 L

time	T (°C)	pH	Absorbance	conductivity (µS/cm)	current (A)	voltage (V)	time (min)	Abs/abs_0	k	$\sigma^2 = \sum (k - k_m)^2$	concentration (mg/L)
12.10	20.03	2.93	7.4753	4.74	7	9.3	0	1.0000	-	-	300.8462
12.30	20.68	3.27	7.0274	4.68	7	9.2	20	0.9401	0.003089	3.9146E-06	282.7126
12.50	20.66	4.05	6.2738	4.36	-6.4	-9.7	40	0.8393	0.005672	3.6459E-07	252.2024
13.10	20.42	6	5.7701	4.29	7	9.5	60	0.7719	0.004185	7.8017E-07	231.8097
13.30	20.16	6.21	5.3368	4.3	7	9.4	80	0.7139	0.003903	1.3567E-06	214.2672
13.50	20.04	6.22	4.8492	4.33	-6.4	-9.8	100	0.6487	0.004791	7.6889E-08	194.5263
14.10	20.02	6.23	4.2886	4.43	6.9	9.6	120	0.5737	0.006143	1.1551E-06	171.8300
14.30	19.92	6.27	3.8799	4.31	7	9.5	140	0.5190	0.005008	3.6439E-09	155.2834
14.50	19.96	6.31	3.5255	4.3	-6.4	-9.8	160	0.4716	0.004789	7.7594E-08	140.9352
15.10	20.03	6.33	3.0601	4.42	7	9.6	180	0.4094	0.007079	4.0434E-06	122.0931
15.30	19.85	6.41	2.8273	4.3	7	9.5	200	0.3782	0.003956	1.2357E-06	112.6680
15.50	19.98	6.44	2.6416	4.35	-6.4	-9.8	220	0.3534	0.003397	2.7924E-06	105.1498
16.10	20.11	6.48	2.2437	4.31	7	9.7	240	0.3001	0.008163	9.5791E-06	89.0405
16.30	20.04	6.48	2.0016	4.33	7	9.6	260	0.2678	0.005709	4.1096E-07	79.2389
Average									0.005068	Sum	2.5791E-05

Day 09.01.2016 Dilution 1:3
 Concentration of salicylic acid 300 mg/L
 Concentration of NaCl 0.05 M
 Volume 10 L

time	T (°C)	pH	Absorbance	conductivity (µS/cm)	current (A)	voltage (V)	time (min)	Abs/abs_0	k	$\sigma^2 = \sum(k - k_m)^2$	concentration (mg/L)
12.50	21.20	2.98	7.5997	4.87	7	9.7	0	1.0000	-	-	305.8826
13.10	21.10	3.38	6.8364	4.46	7	9.5	20	0.8996	0.005292	4.5137E-07	274.9798
13.30	20.52	5.63	6.1930	4.37	7	9.5	40	0.8149	0.004942	1.0447E-06	248.9312
13.50	20.13	6.26	5.7597	4.38	7	9.6	60	0.7579	0.003627	5.4639E-06	231.3887
14.10	20.08	6.34	5.2517	4.3	7	9.6	80	0.6910	0.004617	1.8158E-06	210.8219
14.30	20.04	6.29	4.4580	4.28	7	9.6	100	0.5866	0.008193	4.9656E-06	178.6883
14.50	19.87	6.31	4.1001	4.32	7	9.6	120	0.5395	0.004184	3.1676E-06	164.1984
15.10	19.91	6.33	3.7064	4.28	7	9.5	140	0.4877	0.005048	8.4033E-07	148.2591
15.30	19.89	6.36	3.2388	4.27	7	9.5	160	0.4262	0.006743	6.0637E-07	129.3279
15.50	20.01	6.38	2.8811	4.28	7	9.5	180	0.3791	0.005852	1.2696E-08	114.8462
16.10	19.85	6.42	2.4993	4.32	7	9.5	200	0.3289	0.007108	1.3084E-06	99.3887
16.30	19.93	6.45	2.2187	4.3	7	9.5	220	0.2919	0.005954	9.5052E-11	88.0283
16.50	19.94	6.51	1.9265	4.27	7	9.5	240	0.2535	0.007061	1.2026E-06	76.1984
17.10	20.05	6.47	1.6119	4.23	7	9.5	260	0.2121	0.008915	8.7046E-06	63.4615
Average									0.005964212	Sum	2.9584E-05

Day 11.01.2016 Dilution 1:3
 Concentration of salicylic acid 300 mg/L
 Concentration of NaSO₄ 0.05 M
 Volume 10 L

time	T (°C)	pH	Absorbance	conductivity (µS/cm)	current (A)	voltage (V)	time (min)	Abs/abs_0	k = 1/Δt · ln(c1/c2)	$\sigma^2 = \sum(k - k_m)^2$	concentration (mg/L)
13.20	20.72	3.15	7.4478	7.2	7	8.7	0	1.0000	-	-	299.7328
13.40	20.87	3.18	7.2515	6.91	7	8.6	20	0.9736	0.001336	2.9317E-07	291.7854
14.00	20.5	3.19	6.9084	6.97	7	8.6	40	0.9276	0.002424	2.9871E-07	277.8947
14.20	20.32	3.21	6.7232	6.9	7	8.5	60	0.9027	0.001359	2.6861E-07	270.3968
14.40	20.2	3.22	6.4576	6.94	7	8.5	80	0.8670	0.002015	1.9143E-08	259.6437
15.00	19.99	3.24	6.2490	6.78	7	8.5	100	0.8390	0.001642	5.5297E-08	251.1984
15.20	20.01	3.25	5.9610	6.77	7	8.4	120	0.8004	0.002359	2.3251E-07	239.5385
15.40	20.01	3.27	5.8193	7.09	7	8.3	140	0.7813	0.001203	4.5435E-07	233.8016
16.00	20.04	3.3	5.4664	6.94	7	8.3	160	0.7340	0.003128	1.565E-06	219.5142
16.20	19.93	3.31	5.3257	6.78	7	8.3	180	0.7151	0.001304	3.2852E-07	213.8178
16.40	19.94	3.33	5.0617	6.82	7	8.2	200	0.6796	0.002542	4.4238E-07	203.1296
17.00	19.99	3.34	4.8370	6.9	7	8.2	220	0.6495	0.002270	1.5478E-07	194.0324
17.20	19.95	3.36	4.6612	6.86	7	8.2	240	0.6258	0.001851	6.6975E-10	186.9150
17.40	20.02	3.39	4.5718	6.9	7	8.2	260	0.6138	0.000968	8.2568E-07	183.2955
Average									0.001876968	Sum	
									0.001876968	4.9389E-06	

Day 15.01.2016 Dilution 1:3
 Concentration of salicylic acid 300 mg/L
 Concentration of NaSO₄ 0.1 M
 Volume 10 L

time	T (°C)	pH	Absorbance	conductivity (µS/cm)	current (A)	voltage (V)	time (min)	Abs/abs_0	$k=1/\Delta t \ln(c1/c2)$	$\sigma^2=\sum(k-k_m)^2$	concentration (mg/L)
11.30	22.60	3.60	7.3695	15.32	7.00	7.80	0	1	-	-	296.5628
11.50	22.20	3.79	7.1660	17.29	7.00	7.60	20	0.9724	0.001400	1.3872E-07	288.3219
12.10	21.08	3.82	6.6734	17.33	-6.40	-7.80	40	0.9055	0.003561	3.197E-06	268.3785
12.30	20.40	3.85	6.7827	16.83	7.00	7.70	60	0.9204	-0.000813	6.6852E-06	272.8057
12.50	20.27	3.91	6.2423	17.14	7.00	7.60	80	0.8470	0.004152	5.6587E-06	250.9251
13.10	20.07	3.94	6.2667	16.20	-6.50	-7.80	100	0.8504	-0.000195	3.8745E-06	251.9150
13.30	20.16	3.91	5.8595	16.60	7.00	7.60	120	0.7951	0.003360	2.5179E-06	235.4271
13.50	20.02	3.94	5.9183	17.18	7.00	7.30	140	0.8031	-0.000499	5.1627E-06	237.8077
14.10	19.97	3.91	5.4434	17.32	-6.40	-7.60	160	0.7386	0.004182	5.8052E-06	218.5810
14.30	19.99	3.98	5.3262	16.61	7.00	7.80	180	0.7227	0.001088	4.6934E-07	213.8381
14.50	20.03	4.02	5.2778	16.86	7.00	7.70	200	0.7162	0.000457	1.7319E-06	211.8765
15.10	19.96	4.08	4.9193	16.48	-6.40	-7.50	220	0.6675	0.003517	3.0425E-06	197.3623
15.30	19.92	4.13	4.5995	16.83	7.00	7.70	240	0.6241	0.003361	2.5219E-06	184.4150
15.50	20.06	4.14	4.6733	18.20	7.00	7.60	260	0.6341	-0.000796	6.5988E-06	187.4028
16.10	19.87	4.23	4.3779	16.38	-6.40	-7.70	280	0.5941	0.003264	2.2242E-06	175.4453
16.30	20.08	4.28	4.3296	16.64	7.00	8.10	300	0.5875	0.000555	1.484E-06	173.4899
									Average	0.001773	5.1113E-05
									Sum		

Day 18.01.2016 Dilution 1:3
 Concentration of salicylic acid 300 mg/L
 Concentration of NaSO₄ 0.05 M
 Volume 10 L

time	T (°C)	pH	Absorbance	conductivity (µS/cm)	current (A)	voltage (V)	time (min)	Abs/abs_0	k	$\sigma^2 = \sum(k - k_m)^2$	concentration (mg/L)
12.10	20.14	3.27	7.7423	10.50	1.00	5.60	0	1.0000	-	-	311.6538
12.30	20.35	3.27	7.3548	10.69	1.00	5.10	20	0.9500	0.002567	6.5893E-06	295.9676
12.50	19.83	3.27	7.2303	10.31	-0.80	-5.00	40	0.9339	0.000854	7.2869E-07	290.9271
13.10	19.97	3.27	7.0569	10.36	1.00	5.40	60	0.9115	0.001214	1.4731E-06	283.9069
13.30	19.89	3.27	6.9311	10.31	1.00	5.00	80	0.8952	0.000900	8.0951E-07	278.8117
13.50	19.80	3.27	6.7775	10.52	-0.80	-5.00	100	0.8754	0.001121	1.2556E-06	272.5931
14.10	19.93	3.27	6.5363	10.39	1.00	5.20	120	0.8442	0.001812	3.2829E-06	262.8279
14.30	20.01	3.27	6.5166	10.28	1.00	5.10	140	0.8417	0.000151	2.2663E-08	262.0324
14.50	19.89	3.27	6.3899	10.10	-0.80	-5.10	160	0.8253	0.000982	9.6452E-07	256.9008
15.10	19.95	3.28	6.2432	10.30	1.00	5.20	180	0.8064	0.001161	1.3486E-06	250.9615
15.30	20.03	3.28	5.8392	10.51	1.00	5.00	200	0.7542	0.003345	1.1186E-05	234.6073
15.50	19.96	3.28	5.8140	10.21	-0.80	-5.00	220	0.7509	0.000216	4.6764E-08	233.5870
16.10	19.93	3.28	5.6589	10.21	1.00	5.10	240	0.7309	0.001352	1.8278E-06	227.3077
16.30	19.92	3.28	5.4276	10.15	1.00	5.00	260	0.7010	0.002087	4.354E-06	217.9433
16.50	20.10	3.28	5.3985	10.14	-0.80	-5.00	280	0.6973	0.000269	7.2251E-08	216.7652
17.10	20.02	3.28	5.0700	10.00	1.00	5.10	300	0.6548	0.003139	9.8534E-06	203.4656
Average									0.001411	Sum	
									0.001411	4.3815E-05	

Day 22.01.2016 Dilution 1:3
 Concentration of salicylic acid 300 mg/L
 Concentration of NaSO₄ 0.05 M
 Volume 10 L

time	T (°C)	pH	Absorbance	conductivity (µS/cm)	current (A)	voltage (V)	time (min)	Abs/abs_0	k	$\sigma^2 = \sum(k - k_m)^2$	concentration (mg/L)
13.25	20.23	3.27	8.0817	9.75	3.50	6.60	0	1.0000	-	-	325.3968
13.45	20.30	3.27	7.8843	9.73	3.50	6.40	20	0.9756	0.001236	2.24392E-07	317.4049
14.05	20.09	3.28	7.2920	9.51	-3.10	-5.90	40	0.9023	0.003905	4.81794E-06	293.4231
14.25	20.03	3.29	6.9668	9.79	3.50	7.00	60	0.8620	0.002281	3.26004E-07	280.2571
14.45	19.97	3.29	6.8946	9.76	3.50	6.70	80	0.8531	0.000521	1.4152E-06	277.3360
15.05	19.94	3.29	6.7398	9.92	-3.10	-6.00	100	0.8340	0.001135	3.30313E-07	271.0688
15.25	20.03	3.29	6.4950	9.58	3.50	6.70	120	0.8037	0.001850	1.95271E-08	261.1579
15.45	20.20	3.29	6.5369	9.58	3.50	6.60	140	0.8088	-0.000321	4.12609E-06	262.8522
16.05	20.10	3.29	6.0893	9.77	-3.10	-6.00	160	0.7535	0.003547	3.3723E-06	244.7308
16.25	19.96	3.29	5.8341	9.62	3.50	6.70	180	0.7219	0.002140	1.8499E-07	234.4008
16.45	19.97	3.29	5.6966	9.57	3.50	6.60	200	0.7049	0.001193	2.67471E-07	228.8320
17.05	20.04	3.29	5.5803	9.54	-3.10	-5.90	220	0.6905	0.001031	4.61355E-07	224.1255
17.25	19.98	3.29	5.4080	9.54	3.50	6.70	240	0.6692	0.001569	2.00275E-08	217.1478
17.45	20.03	3.30	5.1822	9.55	3.50	6.60	260	0.6412	0.002132	1.77983E-07	208.0081
18.05	20.08	3.30	5.0947	9.74	-3.10	-6.60	280	0.6304	0.000851	7.37359E-07	204.4656
18.25	19.96	3.30	4.8657	9.56	3.50	6.50	300	0.6021	0.002300	3.47356E-07	195.1943
10.55	19.95	3.33	4.6749	9.72	3.50	7.10	320	0.5785	0.002000	8.41002E-08	187.4696
11.15	19.98	3.33	4.4663	9.7	3.50	6.50	340	0.5526	0.002283	3.2809E-07	179.0223
11.35	20.04	3.34	4.3194	9.38	-3.10	-5.90	360	0.5345	0.001672	1.48297E-09	173.0769
11.55	20.02	3.34	4.2525	9.6	3.50	6.70	380	0.5262	0.000780	8.64282E-07	170.3684
12.15	20.06	3.34	4.1459	9.68	3.50	6.50	400	0.5130	0.001270	1.93758E-07	166.0506
12.35	20	3.38	3.9926	9.9	-3.10	-5.90	420	0.4940	0.001884	3.01873E-08	159.8441
12.55	20.02	3.39	3.8358	9.86	3.50	6.60	440	0.4746	0.002003	8.55356E-08	153.4980
13.15	20.07	3.39	3.7064	9.98	3.50	6.60	460	0.4586	0.001717	4.07301E-11	148.2571
13.35	20.01	3.4	3.5564	9.84	-3.10	-5.90	480	0.4400	0.002066	1.26381E-07	142.1842
Average									0.001710	Sum	
										1.85422E-05	

Day 29.01.2016 Dilution 1:3
 Concentration of salicylic acid 300 mg/L
 Concentration of NaSO₄ 0.05 M
 Volume 10 L

time	T (°C)	pH	Absorbance	conductivity (µS/cm)	current (A)	voltage (V)	time (min)	Abs/abs_0	k	$\sigma^2 = \sum(k - k_m)^2$	concentration (mg/L)	
12.00	19.89	6.87	8.0372	9.96	7.00	9.10	0	1	-	-	323.5931	
12.20	20.56	6.78	7.7529	9.91	7.00	8.60	20	0.9646	0.001800	5.6931E-08	312.0850	
12.40	20.06	6.80	7.3371	9.62	-6.50	-7.90	40	0.9129	0.002756	5.1435E-07	295.2510	
13.00	19.97	6.64	6.9866	9.58	7.00	8.70	60	0.8693	0.002448	1.6717E-07	281.0587	
13.20	20.00	6.78	6.7421	9.75	7.00	8.70	80	0.8389	0.001781	6.6481E-08	271.1599	
13.40	19.95	7.05	6.5468	9.81	-6.50	-7.90	100	0.8146	0.001470	3.2401E-07	263.2530	
14.00	20.06	6.93	6.2079	9.84	7.00	8.60	120	0.7724	0.002657	3.8232E-07	249.5344	
14.20	19.93	6.95	6.2231	9.78	7.00	8.70	140	0.7743	-0.000122	4.6693E-06	250.1478	
14.40	20.04	7.25	5.7996	9.87	-6.50	-7.90	160	0.7216	0.003524	2.204E-06	233.0040	
15.00	19.94	7.19	5.8209	9.77	7.00	8.60	180	0.7242	-0.000183	4.9385E-06	233.8664	
15.20	20.00	7.27	5.5116	9.64	7.00	8.70	200	0.6858	0.002730	4.775E-07	221.3441	
15.40	20.03	7.36	5.2359	9.80	-6.50	-7.90	220	0.6515	0.002566	2.7755E-07	210.1822	
16.00	19.94	7.15	5.0732	9.61	7.00	8.70	240	0.6312	0.001579	2.1173E-07	203.5931	
16.20	19.98	7.15	4.7001	9.79	7.00	8.60	260	0.5848	0.003819	3.1681E-06	188.4899	
16.40	20.00	7.09	4.5794	9.84	-6.50	-8.00	280	0.5698	0.001301	5.4412E-07	183.6012	
17.00	20.04	7.25	4.3596	9.86	7.00	8.60	300	0.5424	0.002459	1.7628E-07	174.7045	
									Average			
									0.002039	Sum		
										1.8178E-05		

Day 30.01.2016 Dilution 1:3
 Concentration of salicylic acid 300 mg/L
 Concentration of NaSO₄ 0.05 M
 Volume 10 L

time	T (°C)	pH	Absorbance	conductivity (µS/cm)	current (A)	voltage (V)	time (min)	Abs/abs_0	k	$\sigma^2 = \sum (k - k_m)^2$	concentration (mg/L)
12.00	19.78	3.13	7.6731	10.25	7.00	9.40	0	1			x=40.48y-1.797
12.20	20.21	3.04	7.2636	9.70	7.00	8.60	20	0.9466	0.002742	9.1904E-07	308.8543
12.40	19.89	3.05	6.8847	9.76	-6.40	-7.80	40	0.8973	0.002679	8.0122E-07	292.2753
13.00	19.94	3.06	6.7190	9.77	7.00	8.70	60	0.8756	0.001218	3.1935E-07	276.9352
13.20	19.84	3.06	6.3525	9.76	7.00	8.60	80	0.8279	0.002804	1.0416E-06	270.2247
13.40	19.96	3.07	6.2558	9.70	-6.50	-7.80	100	0.8153	0.000767	1.0327E-06	255.3887
14.00	20.14	3.02	6.1206	9.78	7.00	8.90	120	0.7977	0.001092	4.7824E-07	251.4717
14.20	20.08	3.03	5.8461	9.78	7.00	8.70	140	0.7619	0.002294	2.6079E-07	246.0000
14.40	20.00	3.04	5.6096	9.68	-6.40	-7.90	160	0.7311	0.002065	7.9311E-08	234.8866
15.00	19.94	3.03	5.5028	9.81	7.00	8.90	180	0.7171	0.000961	6.7645E-07	225.3097
15.20	20.06	3.03	5.1531	9.85	7.00	8.80	200	0.6716	0.003282	2.2466E-06	220.9858
15.40	19.99	3.03	5.0825	9.75	-6.40	-7.90	220	0.6624	0.000690	1.1954E-06	206.8300
16.00	20.06	3.03	4.9028	9.81	7.00	8.90	240	0.6390	0.001799	2.4824E-10	203.9696
16.20	19.96	3.03	4.6515	9.77	7.00	8.70	260	0.6062	0.002631	7.1782E-07	196.6964
16.40	20.04	3.04	4.4913	9.88	-6.40	-7.80	280	0.5853	0.001752	9.7434E-10	186.5223
17.00	20.00	3.04	4.4936	9.89	7.00	8.90	300	0.5856	-0.000025	3.2712E-06	180.0364
									Average	0.001784	180.1275
									Sum	1.3041E-05	

Day 01.02.2016 Dilution 1:3
 Concentration of salicylic acid 300 mg/L
 Concentration of NaSO₄ 0.05 M
 Volume 10 L

time	T (°C)	pH	Absorbance	conductivity (µS/cm)	current (A)	voltage (V)	time (min)	Abs/abs_0	$k = 1/\Delta t \ln(c1/c2)$	$\sigma^2 = \sum(k - k_m)^2$	concentration (mg/L)
12.00	12.86	6.86	7.4396	9.19	7.00	9.50	0	1	-	-	299.3988
12.20	13.50	6.59	7.3103	9.44	7.00	8.90	20	0.9826	0.000877	2.0139E-07	294.1640
12.40	13.76	6.67	7.1198	9.41	-6.40	7.90	40	0.9570	0.001320	2.668E-11	286.4514
13.00	13.54	6.80	6.8241	9.41	7.00	9.20	60	0.9173	0.002121	6.3234E-07	274.4818
13.20	13.27	6.89	6.7616	9.47	7.00	8.90	80	0.9089	0.000460	7.4821E-07	271.9494
13.40	13.20	6.73	6.5085	9.53	-6.50	8.00	100	0.8749	0.001907	3.3843E-07	261.7045
14.00	13.25	6.88	6.3261	9.51	7.00	9.10	120	0.8503	0.001421	9.1864E-09	254.3198
14.20	13.20	6.90	6.0956	9.55	7.00	8.90	140	0.8193	0.001856	2.8179E-07	244.9858
14.40	13.56	6.88	5.9996	9.54	-6.40	7.90	160	0.8064	0.000794	2.8269E-07	241.0992
15.00	13.46	6.95	5.7684	9.55	7.00	8.90	180	0.7754	0.001964	4.0842E-07	231.7409
15.20	13.70	6.90	5.7279	9.50	7.00	9.00	200	0.7699	0.000352	9.4696E-07	230.1012
15.40	13.88	7.00	5.4800	9.59	-6.40	7.90	220	0.7366	0.002213	7.872E-07	220.0628
16.00	13.65	6.89	5.5061	9.57	7.00	9.00	240	0.7401	-0.000238	2.4429E-06	221.1194
16.20	13.43	6.82	5.1144	9.58	7.00	8.80	260	0.6875	0.003689	5.5883E-06	205.2632
16.40	13.78	6.93	4.9581	9.53	-6.40	7.90	280	0.6665	0.001552	5.1287E-08	198.9352
17.00	13.80	7.02	4.9988	9.56	7.00	8.90	300	0.6719	-0.000408	3.0056E-06	200.5810
Average									0.001325	Sum	1.5725E-05

Day 02.02.2016 Dilution 1:3
 Concentration of salicylic acid 300 mg/L
 Concentration of NaSO₄ 0.05 M
 Volume 10 L

time	T (°C)	pH	Absorbance	conductivity (µS/cm)	current (A)	voltage (V)	time (min)	Abs/abs_0	k	$\sigma^2 = \sum(k-k_m)^2$	concentration (mg/L)
11.10	12.89	3.08	7.5332	9.67	7.00	9.40	0	1	-	-	303.1883
11.30	13.74	3.06	7.2452	9.86	7.00	8.90	20	0.9618	0.001949	1.14748E-07	291.5283
11.50	13.68	3.06	7.0248	9.67	-6.50	-8.00	40	0.9325	0.001544	4.3597E-09	282.6073
12.10	14.02	3.07	6.9059	9.73	7.00	9.30	60	0.9167	0.000854	5.72158E-07	277.7915
12.30	13.89	3.07	6.5835	9.66	7.00	8.90	80	0.8739	0.002390	6.08109E-07	264.7409
12.50	13.25	3.06	6.4623	9.70	-6.50	-7.90	100	0.8578	0.000929	4.64093E-07	259.8340
13.10	13.12	3.07	6.3042	9.62	7.00	9.10	120	0.8369	0.001238	1.38268E-07	253.4332
13.30	13.20	3.07	6.1467	9.90	7.00	8.90	140	0.8160	0.001265	1.1921E-07	247.0567
13.50	13.13	3.07	5.9957	9.65	-6.50	-7.90	160	0.7959	0.001244	1.34137E-07	240.9413
14.10	13.05	3.07	5.7002	9.62	7.00	8.90	180	0.7567	0.002527	8.40487E-07	228.9777
14.30	13.31	3.08	5.5098	9.64	7.00	8.70	200	0.7314	0.001698	7.72703E-09	221.2713
14.50	13.22	3.07	5.2763	9.65	-6.50	-7.90	220	0.7004	0.002166	3.08392E-07	211.8158
15.10	13.51	3.08	5.1833	9.63	7.00	9.10	240	0.6881	0.000889	5.20039E-07	208.0506
15.30	13.43	3.08	5.0501	9.62	7.00	8.90	260	0.6704	0.001302	9.52329E-08	202.6579
15.50	13.26	3.08	4.8051	9.68	-6.50	-7.90	280	0.6379	0.002486	7.66868E-07	192.7409
16.10	13.16	3.08	4.6470	9.69	7.00	9.20	300	0.6169	0.001673	3.90568E-09	186.3401
									Average	Sum	
									0.001610	4.69774E-06	

Day 03.02.2016 Dilution 1:3
 Concentration of salicylic acid 300 mg/L
 Concentration of NaSO₄ 0.05 M
 Volume 10 L

time	T (°C)	pH	Absorbance	conductivity (µS/cm)	current (A)	voltage (V)	time (min)	Abs/abs_0	$k = 1/\Delta t \ln(c_1/c_2)$	$\sigma^2 = \sum (k - k_m)^2$	concentration (mg/L)
11.40	13.08	12.03	7.4702	10.27	7.00	9.40	0	1	-	-	300.6377
12.00	13.66	11.97	7.3899	10.32	7.00	8.80	20	0.9893	0.000540	1.71E-06	297.3887
12.20	13.51	11.88	7.0881	10.29	-6.40	-7.90	40	0.9489	0.002085	5.62314E-08	285.1700
12.40	13.25	11.86	6.8742	10.49	7.00	9.30	60	0.9202	0.001532	9.96096E-08	276.5101
13.00	13.22	11.94	6.6455	10.47	7.00	8.80	80	0.8896	0.001692	2.42018E-08	267.2490
13.20	13.16	11.87	6.4890	10.50	-6.50	-7.90	100	0.8687	0.001191	4.3101E-07	260.9150
13.40	13.47	11.91	6.2423	10.82	7.00	9.40	120	0.8356	0.001938	8.2219E-09	250.9251
14.00	13.34	11.88	6.0785	10.76	7.00	8.90	140	0.8137	0.001330	2.68494E-07	244.2935
14.20	13.22	11.87	5.7077	10.74	-6.50	-8.00	160	0.7641	0.003147	1.68845E-06	229.2814
14.40	13.51	11.89	5.6117	11.07	7.00	9.30	180	0.7512	0.000848	9.99166E-07	225.3947
15.00	13.27	11.85	5.3387	10.95	7.00	8.90	200	0.7147	0.002494	4.1717E-07	214.3421
15.20	13.69	11.83	5.0943	11.07	-6.50	-7.90	220	0.6820	0.002343	2.44842E-07	204.4494
15.40	13.54	11.82	4.9151	10.95	7.00	9.40	240	0.6580	0.001791	3.21436E-09	197.1923
16.00	13.66	11.85	4.6937	11.33	7.00	8.90	260	0.6283	0.002305	2.08719E-07	188.2287
16.20	13.29	11.87	4.5647	11.23	-6.50	-8.00	280	0.6111	0.001393	2.06966E-07	183.0085
16.40	13.22	11.87	4.2914	11.09	7.00	9.30	300	0.5745	0.003088	1.53752E-06	171.9413
Average									0.001848	Sum	7.90382E-06

Day 04.02.2016 Dilution 1:3
 Concentration of salicylic acid 300 mg/L
 Concentration of NaSO₄ 0.05 M
 Volume 10 L

time	T (°C)	pH	Absorbance	conductivity (µS/cm)	current (A)	voltage (V)	time (min)	Abs/abs_0	k	$\sigma^2 = \sum(k - k_m)^2$	concentration (mg/L)
11.20	27.34	11.88	7.3523	10.79	7.00	9.40	0	1	-	-	295.8644
11.40	26.85	11.85	6.8690	11.16	7.00	8.50	20	0.9343	0.003400	1.8296E-07	276.2976
12.00	27.03	11.82	6.4725	11.19	-6.40	-7.70	40	0.8803	0.002972	1.7856E-13	260.2470
12.20	26.88	11.78	6.0407	11.24	7.00	8.80	60	0.8216	0.003453	2.309E-07	242.7632
12.40	27.04	11.80	5.6156	11.71	7.00	8.50	80	0.7638	0.003649	4.5777E-07	225.5526
13.00	27.10	11.74	5.2623	11.68	-6.40	-7.70	100	0.7157	0.003249	7.6479E-08	211.2510
13.20	26.98	11.85	4.9376	12.63	7.00	8.90	120	0.6716	0.003185	4.5338E-08	198.1032
13.40	26.94	11.86	4.6730	12.70	7.00	8.50	140	0.6356	0.002754	4.7561E-08	187.3907
14.00	27.25	11.85	4.4475	12.56	-6.40	-7.70	160	0.6049	0.002472	2.496E-07	178.2632
14.20	26.87	11.84	4.1967	12.25	7.00	8.80	180	0.5708	0.002902	4.8772E-09	168.1093
14.40	27.04	11.87	3.9498	13.07	7.00	8.50	200	0.5372	0.003032	3.5592E-09	158.1134
15.00	27.01	11.81	3.7317	13.32	-6.40	-7.70	220	0.5076	0.002840	1.7415E-08	149.2834
15.20	26.94	11.80	3.5559	13.46	7.00	8.80	240	0.4836	0.002413	3.1274E-07	142.1660
15.40	27.02	11.86	3.3848	13.32	7.00	8.50	260	0.4604	0.002466	2.5564E-07	135.2368
16.00	27.06	11.81	3.1824	13.26	-6.40	-7.70	280	0.4328	0.003082	1.2145E-08	127.0445
16.20	26.97	11.84	3.0144	13.17	7.00	8.80	300	0.4100	0.002712	6.7744E-08	120.2429
Average									0.002972	Sum	1.9647E-06

Day 05.02.2016 Dilution 1:3
 Concentration of salicylic acid 300 mg/L
 Concentration of NaSO₄ 0.05 M
 Volume 10 L

time	T (°C)	pH	Absorbance	conductivity (µS/cm)	current (A)	voltage (V)	time (min)	Abs/abs_0	k	$\sigma^2 = \sum(k-k_m)^2$	concentration (mg/L)
10.50	27.13	6.85	7.3389	9.61	7.00	9.20	0	1	-	-	295.3239
11.10	27.24	6.88	6.8837	9.57	7.00	8.80	20	0.9380	0.003202	4.9726E-07	276.8927
11.30	27.15	6.75	6.2928	9.71	-6.50	-7.80	40	0.8575	0.004487	3.9614E-06	252.9717
11.50	26.94	6.84	5.9757	9.62	7.00	8.90	60	0.8143	0.002585	7.7728E-09	240.1348
12.10	27.05	6.88	5.6141	9.71	7.00	8.50	80	0.7650	0.003122	3.9046E-07	225.4919
12.30	27.02	6.94	5.2935	9.73	-6.50	-7.70	100	0.7213	0.002940	1.9608E-07	212.5142
12.50	27.06	6.78	5.1231	9.73	7.00	8.90	120	0.6981	0.001636	7.4103E-07	205.6154
13.10	26.97	6.79	4.9418	9.58	7.00	8.50	140	0.6734	0.001802	4.8277E-07	198.2733
13.30	27.06	6.88	4.6905	9.65	-6.50	-7.70	160	0.6391	0.002609	1.2586E-08	188.1012
13.50	26.96	6.79	4.4259	9.68	7.00	8.80	180	0.6031	0.002903	1.652E-07	177.3887
14.10	27.04	6.85	4.2483	9.71	7.00	8.50	200	0.5789	0.002048	2.0168E-07	170.1984
14.30	26.89	6.84	4.0668	9.77	-6.50	-7.70	220	0.5541	0.002183	9.8412E-08	162.8502
14.50	27.05	6.78	3.9042	9.75	7.00	8.70	240	0.5320	0.002040	2.0853E-07	156.2672
15.10	26.99	6.97	3.7118	9.85	7.00	8.50	260	0.5058	0.002527	9.3896E-10	148.4757
15.30	27.00	6.91	3.5379	9.79	-6.50	-7.70	280	0.4821	0.002399	9.6673E-09	141.4372
15.50	27.02	6.88	3.4700	9.68	7.00	8.80	300	0.4728	0.000970	2.3323E-06	138.6862
Average									0.002497	Sum	9.306E-06

Day 05.02.2016 Dilution 1:3
 Concentration of salicylic acid 300 mg/L
 Concentration of NaSO₄ 0.05 M
 Volume 10 L

time	T (°C)	pH	Absorbance	conductivity (µS/cm)	current (A)	voltage (V)	time (min)	Abs/abs_0	k=1/Δt ln(c1/c2)	$\sigma^2 = \sum (k - k_m)^2$	x=40.48y-1.797
									k	σ	concentration (mg/L)
16.40	27.84	3.10	7.2776	9.78	7.00	9.20	0	1	-	-	292.8401
17.00	27.75	3.11	6.9161	9.76	7.00	8.80	20	0.9503	0.002547	1.33401E-07	278.2045
17.20	27.10	3.10	6.7635	9.76	-6.40	-7.80	40	0.9294	0.001115	1.13853E-06	272.0283
17.40	27.35	3.11	6.4725	9.57	7.00	8.80	60	0.8894	0.002199	2.77953E-10	260.2470
18.00	27.17	3.12	6.0699	9.62	7.00	8.60	80	0.8341	0.003211	1.0584E-06	243.9474
18.20	26.94	3.11	5.9898	9.80	-6.50	-7.80	100	0.8231	0.000664	2.3044E-06	240.7045
18.40	27.04	3.11	5.6916	9.79	7.00	8.80	120	0.7821	0.002553	1.37715E-07	228.6316
19.00	27.05	3.12	5.4377	9.64	7.00	8.50	140	0.7472	0.002282	9.99785E-09	218.3502
19.20	26.99	3.12	5.2415	9.89	-6.40	-7.80	160	0.7202	0.001837	1.18881E-07	210.4069
19.40	27.03	3.13	5.0451	9.83	7.00	8.80	180	0.6932	0.001909	7.46364E-08	202.4575
20.00	27.09	3.11	4.7673	9.87	7.00	8.50	200	0.6551	0.002832	4.22028E-07	191.2105
20.20	26.92	3.12	4.5549	9.79	-6.40	-7.80	220	0.6259	0.002279	9.33054E-09	182.6113
20.40	27.00	3.13	4.3580	9.80	7.00	8.80	240	0.5988	0.002210	7.76116E-10	174.6377
21.00	27.03	3.12	4.1259	9.88	7.00	8.50	260	0.5669	0.002736	3.06526E-07	165.2429
21.20	27.04	3.12	3.9378	10.02	-6.40	-7.80	280	0.5411	0.002333	2.2761E-08	157.6275
21.40	26.97	3.11	3.7815	9.86	7.00	8.80	300	0.5196	0.002025	2.47617E-08	151.3002
									Average	Sum	
									0.002182	5.76242E-06	

Day 06.02.2016 Dilution 1:3
 Concentration of salicylic acid 300 mg/L
 Concentration of NaSO₄ 0.05 M
 Volume 10 L

time	T (°C)	pH	Absorbance	conductivity (µS/cm)	current (A)	voltage (V)	time (min)	Abs/abs_0	k=1/Dt ln(c1/c2)	$\sigma^2 = \sum (k - k_m)^2$	concentration (mg/L)
12.10	20.18	11.97	7.3344	10.27	7.000	9.00	0	1	-	-	295.1417
12.30	20.07	11.93	7.1558	10.35	7.000	8.50	20	0.9756	0.001233	9.6764E-07	287.9089
12.50	19.98	11.89	6.7853	10.38	-6.400	-7.70	40	0.9251	0.002658	1.9501E-07	272.9089
13.10	20.01	11.85	6.5711	10.42	7.000	8.70	60	0.8959	0.001604	3.755E-07	264.2368
13.30	20.06	11.81	6.3129	10.46	7.000	8.50	80	0.8607	0.002004	4.5255E-08	253.7854
13.50	19.94	11.89	6.0357	10.92	-6.400	-7.70	100	0.8229	0.002245	8.1283E-10	242.5628
14.10	20.04	11.86	5.8284	10.71	7.000	8.70	120	0.7947	0.001747	2.2014E-07	234.1700
14.30	19.96	11.83	5.5611	10.61	7.000	8.40	140	0.7582	0.002347	1.7076E-08	223.3482
14.50	20.07	11.94	5.3265	10.97	-6.400	-7.70	160	0.7262	0.002155	3.7918E-09	213.8502
15.10	20.01	11.79	5.1212	10.80	7.000	8.80	180	0.6982	0.001966	6.2945E-08	205.5364
15.30	20.03	11.84	4.7997	11.04	7.000	8.50	200	0.6544	0.003241	1.0499E-06	192.5223
15.50	19.97	11.87	4.6394	11.09	-6.400	-7.70	220	0.6325	0.001699	2.6801E-07	186.0304
16.10	20.01	11.84	4.3242	11.25	7.000	8.70	240	0.5896	0.003517	1.6918E-06	173.2713
16.30	20.00	11.79	4.1880	11.17	7.000	8.50	260	0.5710	0.001600	3.8003E-07	167.7571
16.50	20.10	11.78	3.9698	11.12	-6.400	-7.80	280	0.5413	0.002676	2.11E-07	158.9211
17.10	20.03	11.86	3.7719	11.06	7.000	8.80	300	0.5143	0.002556	1.153E-07	150.9109
Average									0.002217	Sum	
									0.002217	5.6042E-06	